ANL/OEPM-79-12

ANL/OEPM-79-12

ANNUAL REPORT FOR 1979 ON RESEARCH, DEVELOPMENT AND DEMONSTRATION OF NICKEL-ZINC BATTERIES FOR ELECTRIC VEHICLE PROPULSION

Contract No. 31-109-38-4448

by

Exide Management and
Technology Company

ARGONNE NATIONAL LABORATORY, ARGONNE, ILLINOIS

Operated for the U. S. DEPARTMENT OF ENERGY
under Contract W-31-109-Eng-38

DISCLAIMER

Printed in the United States of America
Available from
National Technical Information Service
U. S. Department of Commerce
5285 Port Royal Road
Springfield, VA 22161

NTIS price codes
Printed copy: A06
Microfiche copy: A01

Distribution Category:
Energy Storage--Electrochemical--
Near-Term Batteries (UC-94ca)

ANL/OEPM-79-12

Annual Report for 1979 on

RESEARCH, DEVELOPMENT AND DEMONSTRATION OF NICKEL-ZINC BATTERIES FOR ELECTRIC VEHICLE PROPULSION

Prepared for

The Office for Electrochemical Project Management
Argonne National Laboratory
Under Contract No. 31-109-38-4448

by

Exide Management and Technology Company
Yardley, Pennsylvania

June 1980

TABLE OF CONTENTS

ACKNOWLEDGEMENTS

This Annual Report was prepared by the VIBROCEL™ Program Team at the ESB Technology Company, Yardley, Pa. The work reported herein was performed by:

Mr. V. J. Spera

Dr. M. Knaster

Mr. S. J. Thornell

Mr. J. Consolloy

Mr. K. Jeffries

Mr. M. Manning

Mr. I. Williams

Ms. L. Rodriguez

In addition, the work of our associates at INCO Research and Development Laboratories at Sterling Forest, N. Y. and Birmingham, England is gratefully acknowledged. Daily efforts of support personnel in areas such as design, prototype fabrication, analytical chemistry and quality assurance are an integral part of the program and of great help in accomplishing the goals of the program.

LIST OF TABLES

LIST OF FIGURES

LIST OF FIGURES (cont'd)

LIST OF FIGURES (cont'd)

1.0 INTRODUCTION

The goals of the present R&D program are to develop a Nickel/Zinc Battery for electric vehicle propulsion having the performance characteristics given below:

1.	Battery Capacity[a] (kW-hr)	20-30
2.	Battery Dimension (cm H x cm W x cm L)	to be determined
3.	Volume (L)	to be determined
4.	Weight (kg)	to be determined
5.	Installation Voltage[b]	to be determined
6.	Volumetric Energy[a] (W-hr/L)	>120
7.	Specific Energy[a] (W-hr/kg)	> 70
8.	Specific Power (W/kg)	
	Peak Battery[c] - 5 sec. avg.	>125
	Sustained[f]	> 45
9.	Duty Cycle	
	Charge (hrs)	4-8
	Discharge (hrs)	2-4
10.	Lifetime	
	Deep Discharges[d]	>400
	Wet Life (years)	> 2
11.	Price/Energy[e] ($/kW-hr)	< 75
12.	Energy Efficiency (%)	> 60

---

[a] C/3 rate discharge; 8 hour charge; rated at 100% discharge

[b] For compact passenger car.

[c] At 80% discharged state.

[d] 80% depth-of-discharge from rated capacity

[e] Price delivered to auto manufacturer for production of 10,000 units/year

[f] 20 minute sustained power drain after 50% DOD at C/3.

In order to accomplish these goals, a Program Management Plan was written detailing the major technical tasks to be accomplished in order to achieve these goals. Five major tasks were delineated, and a Milestone Schedule and Status Report prepared to show the scheduled progress of these tasks, and an up-to-date report of the status of each task. The Program Management Plan was submitted on 15 May 1979 and listed these five major technical tasks:

ESB No. 6050 - Battery Design and Development

ESB No. 6051 - Nickel Cathode Study

ESB No. 6052 - Basic Electrochemistry

ESB No. 6053 - Reporting

ESB No. 8345 - Four Cell Monobloc Mold Procurement.

2.0 TECHNICAL PROGRESS IN REPORTING PERIOD

2.1 Battery Design and Development

A) Cells being tested during the ESB Development Program were continued on test to logical conclusion. Experimental Cell S/N-001 was the first cell constructed in a plastic jar, and was tested to determine the feasibility of the plastic jar construction as well as the suitability of brass anode substrates. The cell was not optimized for energy density. The design specificatons sheet for this cell is shown in Table 1. Test data for the cell is presented in Figure 1.

Testing of S/N-001 was terminated after 86 cycles because of the unusually high frequency and amplitude of voltage excursions during charge. Examination of the cell revealed damage to the plastic netting on the nickel electrodes, especially along the bottom edges. These areas of heat distorted plastic matched dense, hard, zinc projections on the opposing anodes. (Figure 2). Apparently, the interelectrode gap was bridged, resulting in periodic short-circuiting, which caused enough heat to soften and distort the plastic netting. It should be noted that the cell was operating in spite of this condition. Further investigation will be made to find a way to avoid zinc "shape change" and its consequent adverse effect on cell performance.

The following general conclusions have been derived from an analysis of the data:

1) There is initially a relatively rapid decrease in capacity with cycling, reaching a level of about 75-80 percent of the initial value in 10 cycles or less.

2) Cell capacity can be recovered by utilizing a two-stage charge. This is a charge interrupted by an open circuit period, followed by a resumption of charge; the open circuit period being about 16 hours (overnight).

3) Extended charge input, about two to three times normal also appears to result in improved capacity.

4) Additions of zinc oxide during cycling appear to have a beneficial effect on capacity retention, especially when the cell appears to be zinc-limited on discharge. Once the cell becomes positive-limited, no further additon of zinc oxide is needed.

5) For charged stand intervals up to four days, the rate of loss of charge retentions has been about 8 percent a day. It should be noted that this performance was obtained with cadmium-plated brass anode substrate s.

TABLE 1

Experimental Cell - Design Specification Sheet

Cell S/N 001

Type Ni-Zn VIBROCEL™

Positive Electrodes

Type	No. Used	Dimensions	Wt (gm)
Matsushita Sintered	2 (one double riveted)	9.2" H x 4.95" W x .065" T	180 each
Jungner Pocket	2 outside	9.2" H x 4.95" W x .160" T	330 each

Capacity: Each electrode 15 Ah @ C/5 - Cell 60 Ah

Positive Insulator:

Type - Polypropylene Netting 12" x 12" x .025" T

Negative Substrate

Type	No. Used	Dimensions	Wt (gm)
Brass sheet perforated .024" T Screen 24 x 24 mesh welded Cadmium plated	2	4.85" W x 8.8" H x .082" T	190 each

Negative Active Material: ZnO - 110 gm

Interelectrode Spacing: 0.1" approx.

Electrolyte: 6M KOH + 10 g/l LiOH · H_2O - 700 ml

Cell Dimensions Overall: 12.0" H x 5.7" W x 2.0" T

Cell Weight: 3629 gm

Cell Jar Material: Polysulfone sheet - cemented

Vibration Mechanism: Eccentric shaft - yoke fitting

PERFORMANCE OF A NICKEL-ZINC VIBROCEL™ OF 5-PLATE (60 Ah NOM) DESIGN

CELL JAR: SLOTTED PLASTIC (POLYSULFONE)
ANODES: CADMIUM-PLATED BRASS SUBSTRATES (2 PER CELL)
CATHODES: COMPOSITE OF ONE THIN MATSUSHITA SINTERED CATHODE IN CENTER, 2 OUTSIDE JUNGNER POCKET CATHODES. TOTAL THEOR. CAPACITY 60 Ah

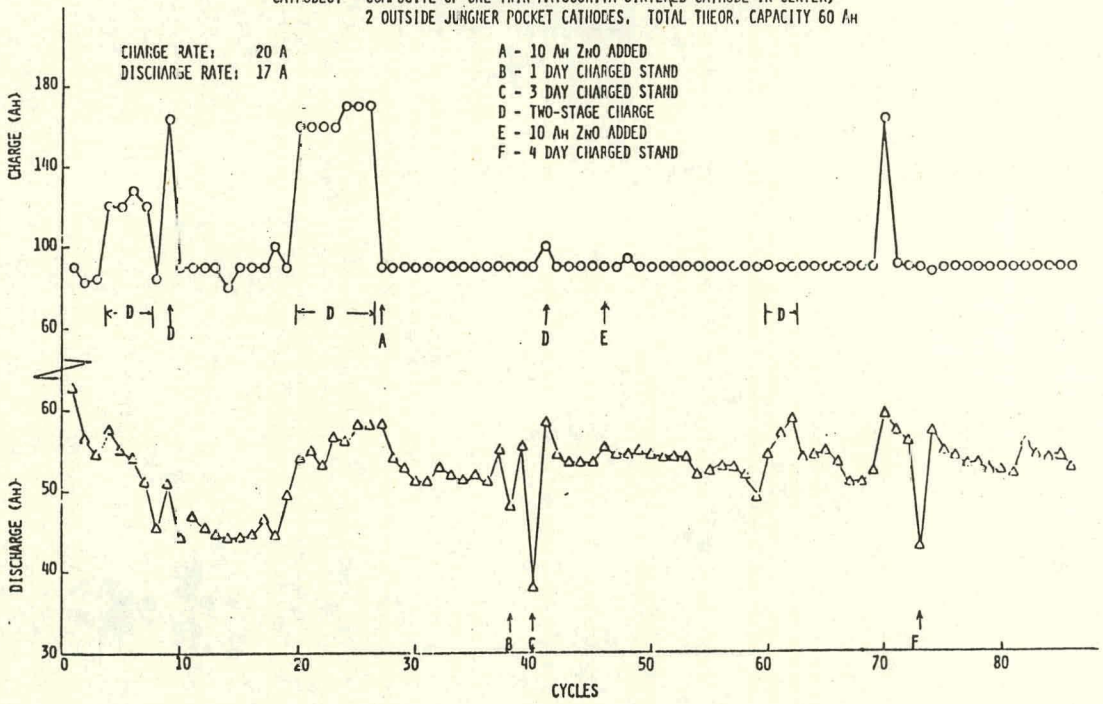

FIGURE 1

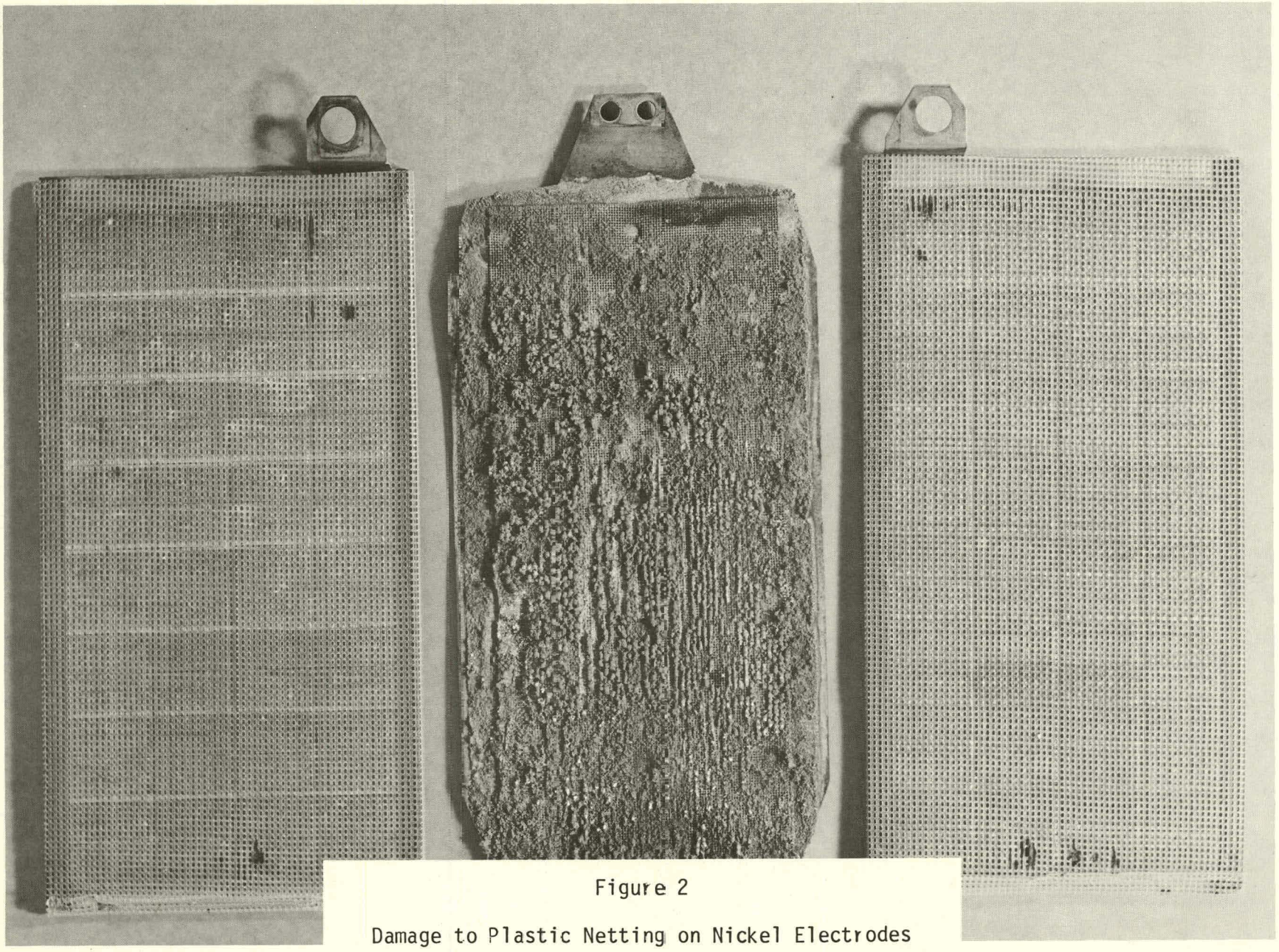

Figure 2

Damage to Plastic Netting on Nickel Electrodes

B) Experimental Cell S/N-002 (Design Specification Sheet shown as Table 2) was one of the earlier models in a steel jar. It included seven (7) electrodes, four (4) positives and three (3) negatives), and had a nominal capacity of 72 Ah based on the nickel electrodes. This experiment was run in order to get a general picture of the capacity maintenance of VIBROCEL™ when deep cycled. The test data for this cell are presented in Fig. 3.

VIBROCEL™ S/N-002 continues on test after 165 cycles. Capacity is about 52 Ah or 90 percent of the original value, and the cell appears to be positive-limited. Testing of the cell will be terminated in the near future to make the test facility available for new cells. It is believed that very little remains to be learned from this cell and VIBROCEL™ development will be expedited by the evaluation of other parameters.

C) A new experimental test cell has been designed which incorporates improvements over earlier designs. Details of construction of the new test cell are shown in the photographs of Figures 4-7 and detailed drawings in Appendix A. Also included is the design of the test stations in which each cell can be easily accommodated for testing.

The new design eliminates expensive ball bearings, and minimizes the difficulty in aligning the activator and eccentric shaft. (DWG. 6050-0107, Rev. A, Appendix A - VIBROCEL™ Activator Assembly). Also, a bellows seal (DWG. 6050-1000, Item 8, Appendix A) has been used to prevent electrolyte leakage. A carbon block (DWG. 6050-0111, Appendix A, Zinc Filter for VIBROCEL™) replaces the sheet nickel previously used to react galvanically with the zinc sediment. It is much more reactive with zinc, does not passivate, and will keep the bottom of the cell relatively free of unreacted zinc sediment.

The basic experimental test cell is of 7-plate construction and will be used for the evaluation of various VIBROCEL™ parameters. It incorporates four (4) nickel electrodes and three (3) zinc anode substrates. Initially, the nickel electrodes utilized were Matsushita impregnated sintered nickel each having a nominal capacity of 22 Ah. The first study involving the 7-plate test cell will be concerned with an evaluation of the effect of interelectrode spacing on performance. This spacing was set at 1.5, 2.5 and 3.5 mm, with one cell used to test only one spacing. All other parameters will remain the same. These cells have been built and testing has been initiated. The Design Specification Sheets for the respective cells are shown in Tables 3, 4 and 5.

Test data to date for Test Cells S/N-003,-004 and -005 are shown in Table 6. The nominal capacity of the cells was 132 Ah and the charge input was generally regulated at 135 percent of this value. The amount of zinc oxide was based on an efficiency value of 85 percent, yielding 155 Ah or 232 grams of zinc oxide. The anode vibration frequency was 20-21 Hz. Charge and discharge were at 40 A

TABLE 2

Experimental Cell - Design Specification Sheet

Cell S/N 002

Type Ni-Zn VIBROCEL™

Positive Electrodes

Type	No. Used	Dimensions	Wt (gm)
Matsushita Sintered	4 (2 doubles) riveted inside	9.0" H x 4.9" W x .068"T	196 each
Matsushita Pocket	2 outside	9.1" H x 4.9" W x .190"T	294 each

Capacity (Ah): 72 Ah @ C/3 based on formed Positive Capacity.

Positive Insulator

Type - Polypropylene Netting 12" x 12" x .025" T

Negative Substrate

Type	No. Used	Dimensions	Wt (gm)
Mild Sheet Steel	3	8.8" H x 4.8"W	185 each
30 x 30 x .012 Wire Screen Welded - Cd Plated		x .096" T	

Negative Active Material: ZnO - 123 gm

Interelectrode Spacing: 0.1" approx.

Electrolyte: 6M KOH + 10 g/l LiOH · H_2O - 1000 ml

Cell Dimensions Overall: 12.4" H x 5.9" W x 2.0" T

Cell Weight: 4587 gm

Cell Jar Material: Mild Steel-Ni Plated

Vibration Mechanism: Eccentric shaft-yoke Fitting

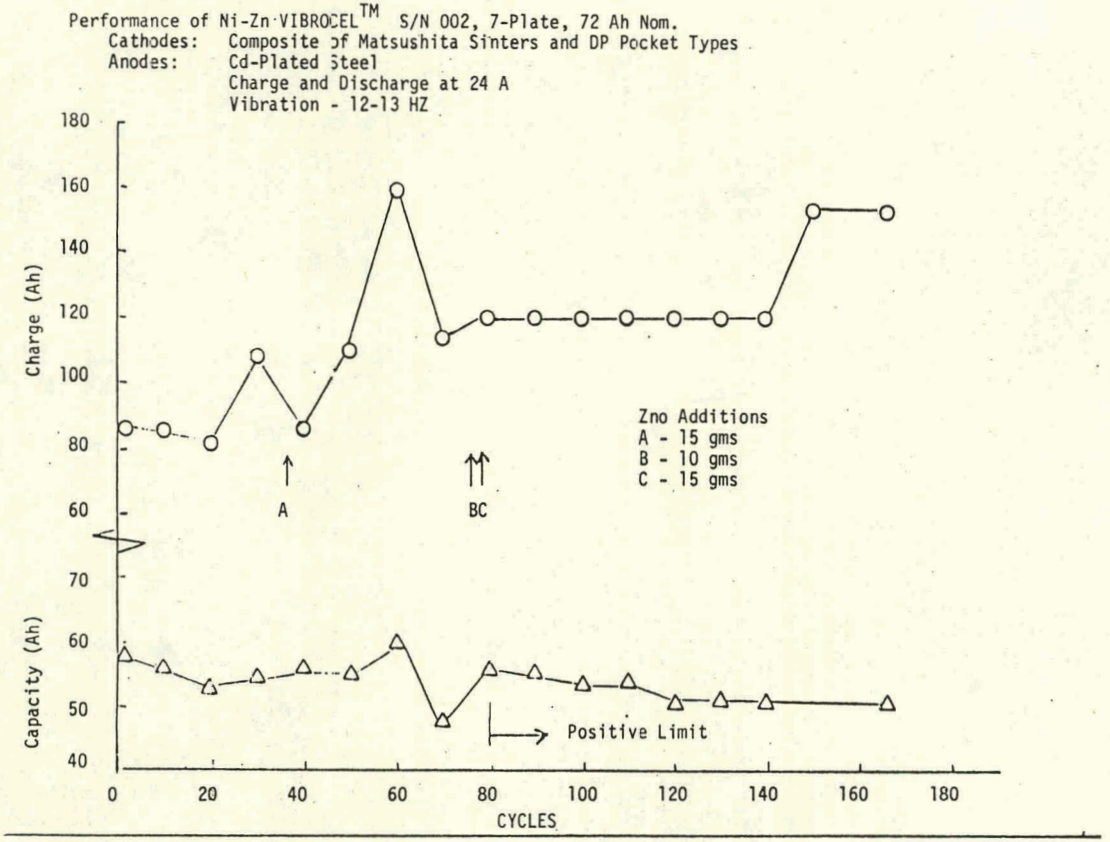
Performance of Ni-Zn VIBROCEL™ S/N 002, 7-Plate, 72 Ah Nom.
Cathodes: Composite of Matsushita Sinters and DP Pocket Types
Anodes: Cd-Plated Steel
Charge and Discharge at 24 A
Vibration - 12-13 HZ
Charge (Ah)
Capacity (Ah)
CYCLES
Zno Additions
A - 15 gms
B - 10 gms
C - 15 gms
A
BC
Positive Limit

Figure 3

Nickel-Zinc VIBROCEL™ (Anode and Cathode Group)

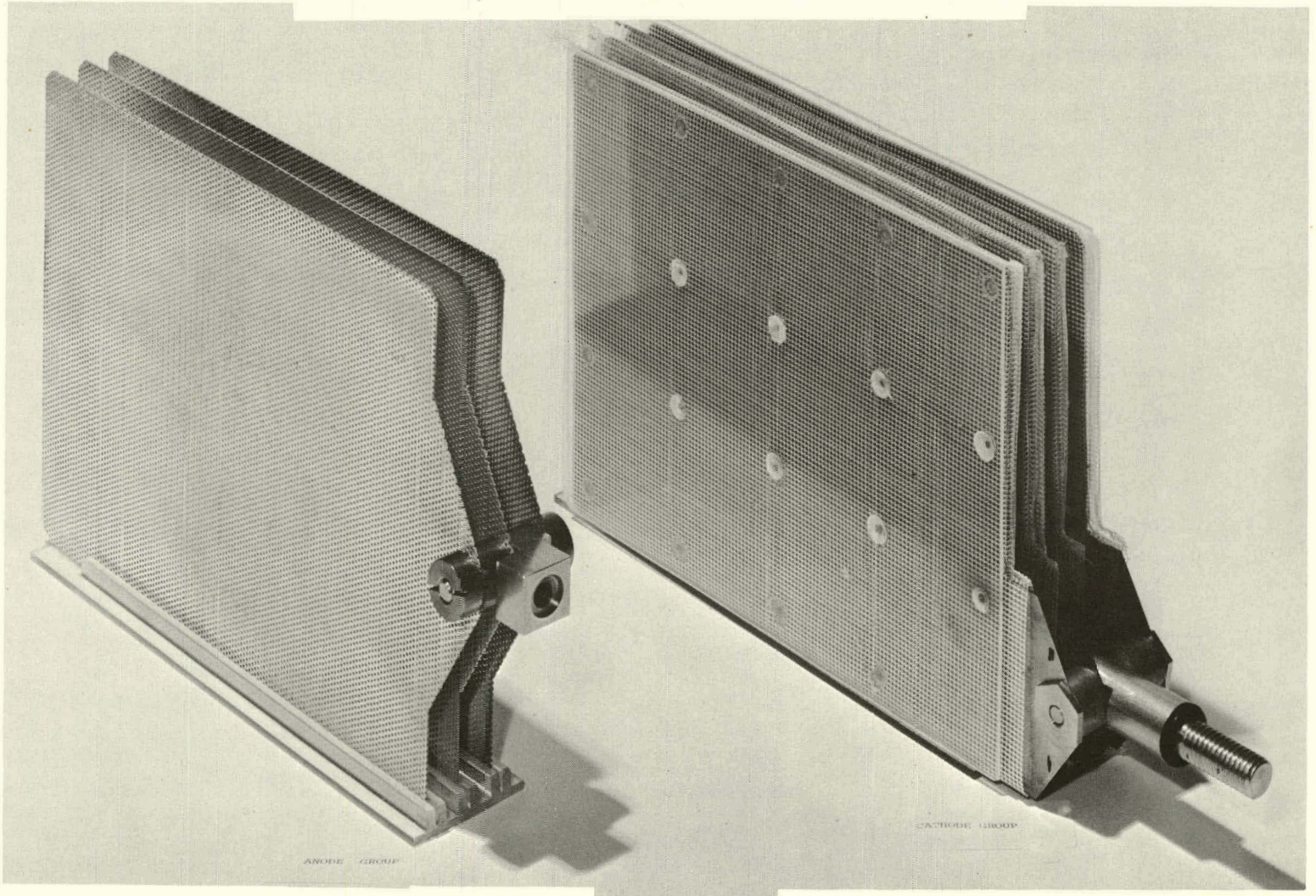

Figure 4

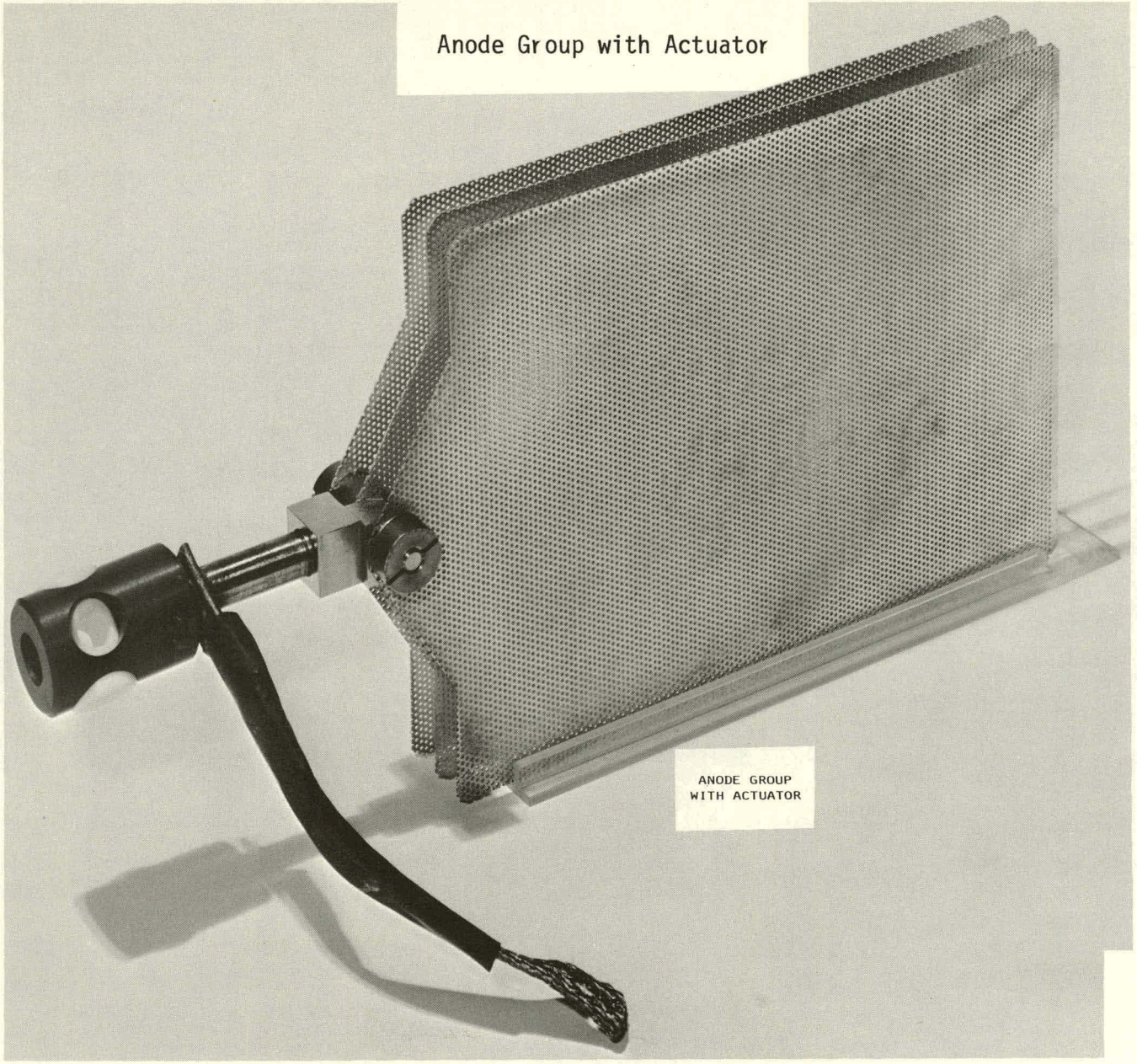

Figure 5

Nickel-Zinc VIBROCEL™

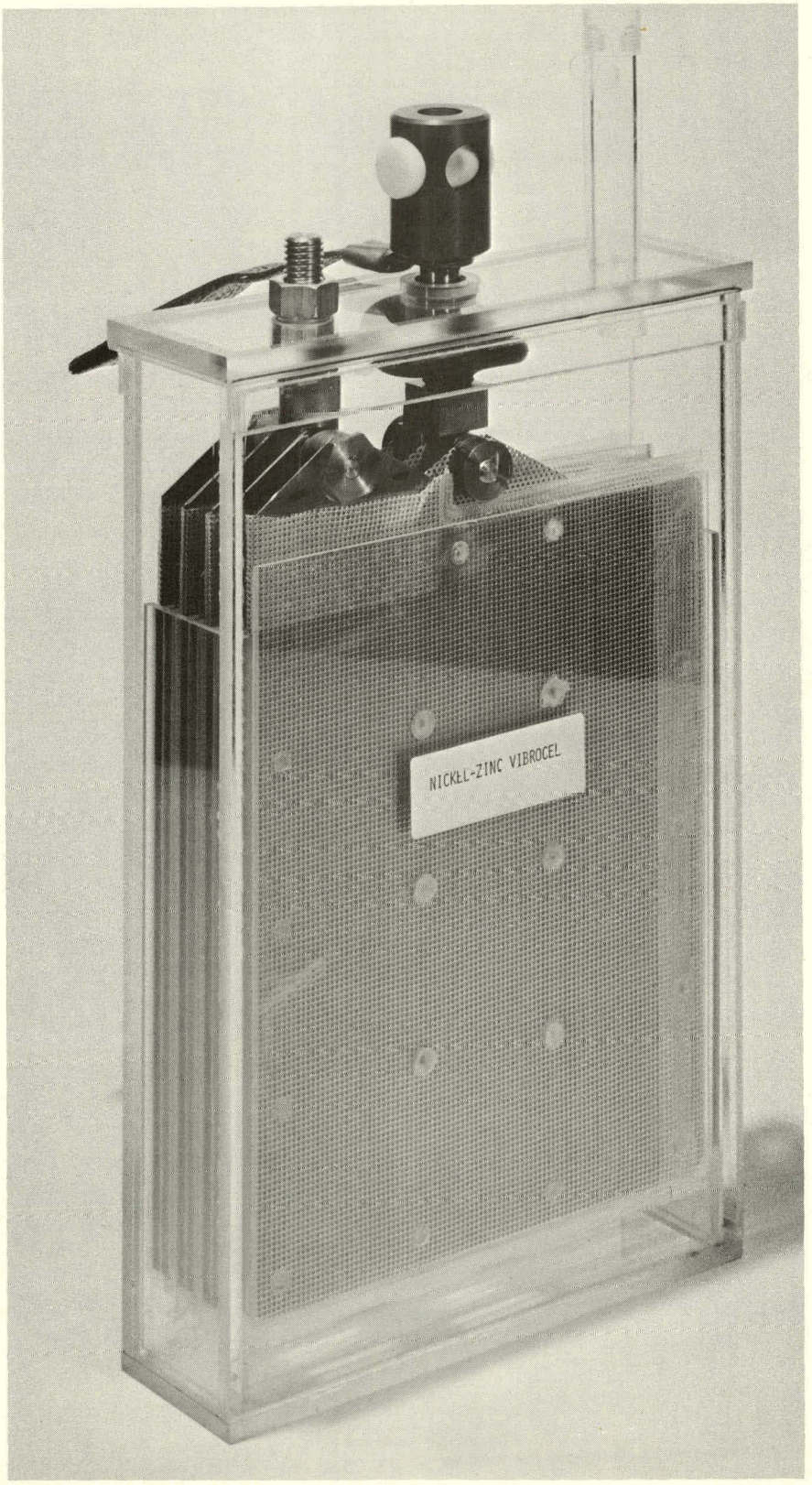

Figure 6

Nickel-Zinc VIBROCEL™ and Test Station

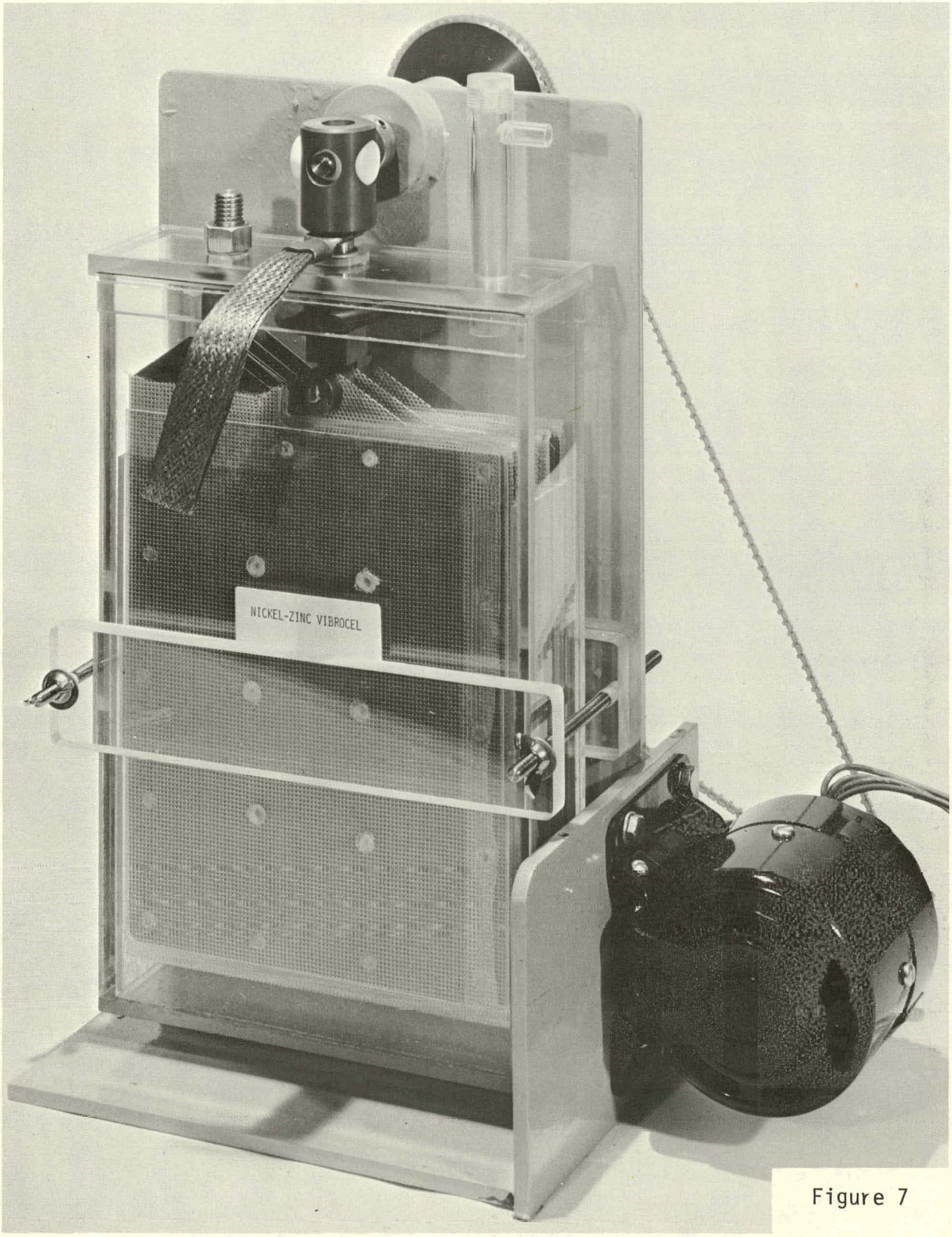

Figure 7

TABLE 3

Experimental Cell - Design Specification Sheet

Cell S/N 003, 7-Plate. Electrode Spacing Test; 1.5mm

Type: Ni-Zn VIBROCEL™ 132 Ah Nom.

Positive Electrodes	Negative Substrate
Type: Matsushita Sinters	Type: Perforated Steel, Cd-Plated
No. per Cell: 6 *	No. per Cell: 3
W 6.89 ≠ .040 in.	W 6.875 + .03 - .00 in.
H 8.937 ≠ .040 in.	H 9.00 + .00 - .03 in.
T 0.064 - 0.067 in.	T 0.024 in.
Wt: 234 ≠ 2 gm. each	Wt: 454 gm. (Total)
Dwg: 6050-0104 6050-0113	Dwg: 6050-0101

Positive Insulator:

Type: Vexar Netting, Polypropylene, 596V 360 PA NL, 11 x 11 mesh, 34-37 mils. Applied as per Dwgs 6050-0104 and 6050-0113.

Negative Active Material: ZnO - 232 gm.

Interelectrode Spacing: 1.5 mm

Electrolyte: 6M KOH + 10 g/l LiOH · H_2O

Cell Dimensions Overall: 16.0" H x 7.80" W x 1.81" T

Cell Weight: Dry - 3940 gm; Filled (Electrolyte & Zno) - 5367 gm

Cell Jar Material: Plexiglas

Vibration Mechanism: Actuator Body - Lucite; Shuttle-Delrin
Total Amplitude - 0.090 in. Frequency - 21 HZ

*The cathode element consisted of two single outer electrodes and two double inner electrodes (4 total)

TABLE 4

Experimental Cell - Design Specification Sheet

Cell S/N 004, 7-Plate. Electrode Spacing Test; 2.5mm

Type: Ni-Zn VIBROCEL™ 132 Ah Nom.

Positive Electrodes		Negative Substrate	
Type:	Matsushita Sinters	Type:	Perforated Steel, Cd Plated
No. per Cell:	6 *	No. per Cell:	3
W	6.89 ≠ .040 in.	W	6.875 + .03 - .00 in.
H	8.937 ≠ .040 in.	H	9.00 + .00 - .03 in.
T	0.064-0.067 in.	T	0.024 in.
Wt:	234 ≠ 2 gm. each	Wt:	501 gm.
Dwg:	6050-0104 6050-0113	Dwg:	6050-0101

Positive Insulator:

Type: Vexar Netting, Polypropylene, 596V 360 PA NL, 11 x 11 mesh, 34-37 mils. Applied as per Dwgs 6050-0104 and 6050-0113.

Negative Active Material:	ZnO - 232 gm.
Interelectrode Spacing:	2.5 mm
Electrolyte:	6M KOH + 10 g/l $LiOH \cdot H_2O$
Cell Dimensions Overall:	16.0" H x 7.80" W x 2.05" T
Cell Weight:	Dry - 4125 gm; Filled (Electrolyte & Zno) - 5857 gm
Cell Jar Material:	Plexiglas
Vibration Mechanism:	Actuator Body - Lucite; Shuttle-Rulon Total Amplitude - 0.090 in. Frequency - 21 HZ

*The cathode element consisted of two single outer electrodes and two double inner electrodes (4 total)

TABLE 5

Experimental Cell - Design Specification Sheet

Cell S/N 005, 7-Plate. Electrode Spacing Test; 3.5mm

Type: Ni-Zn VIBROCEL™ 132 Ah Nom.

Positive Electrodes	Negative Substrate
Type: Matsushita Sinters	Type: Perforated Steel, Cd-Plated
No. per Cell: 6 *	No. per Cell: 3
W 6.89 ≠ .04 in.	W 6.875 + .03 in. .00 in.
H 8.937 ≠ .04 in.	H 9.00 + .00 in. - .03 in.
T 0.064-.067 in.	T 0.024 in.
Wt: 234 ≠ 2 gm. each	Wt: 532 gm. (Total)
Dwg: 6050-0104 6050-0113	Dwg: 6050-0101

Positive Insulator:

Type: Vexar Netting, Polypropylene, 596V 360 PA NL, 11 x 11 mesh, 34-37 mils. Applied as per Dwgs 6050-0104 and 6050-0113.

Negative Active Material: ZnO -232 gm.

Interelectrode Spacing: 3.5 mm

Electrolyte: 6M KOH + 10 g/l $LiOH \cdot H_2O$

Cell Dimensions Overall: 16.0" H x 7.80" W x 2.285" T

Cell Weight: Dry - 4270 gm; Filled (Electrolyte & Zno) - 6274 gm

Cell Jar Material: Plexiglas

Vibration Mechanism: Actuator Body - Lucite; Shuttle-Nylon GS
Total Amplitude - .090 in. Frequency - 21 HZ.

*The cathode element consisted of two single outer electrodes and two double inner electrodes (4 total)

TABLE 6

EFFECT OF INTERELECTRODE SPACING ON VIBROCEL™ PERFORMANCE

CHARGE AND DISCHARGE AT 40A

Cycle	S/N-003		S/N-004		S/N-005	
	Charge (Ah)	Discharge (Ah)	Charge (Ah)	Discharge (Ah)	Charge (Ah)	Discharge (Ah)
1	180	125(1)	180	125	180	130
2			180	97.4	180	104
3			180	90	180	96
4			200	90	200	99
5			180(2)	95	180(2)	106
6			180(3)	94	180(3)	94
7			180(4)	88	180(4)	-
8			220(5)	98	220(5)	94.6

Remarks

(1) Cell S/N-003 failed after Cycle 1. Outside cathodes buckled, contacted anodes and prevented vibration of the negative groups.

(2)-(4) The pre-charge frequency was changed from 1300 RPM (21 Hz) on Cycle 5 to 1000 RPM on Cycle 6 and then to 875 RPM on Cycle 7. Samples of electrolyte were removed from the top and bottom of cells at intervals of 0, 15, 30 and 60 minutes during each pre-charge test.

(5) Two-day charge conducted at 875 RPM. Charge was interrupted overnight (open circuit).

S/N-003 failed after the first cycle. The anode group was found to be incapable of being vibrated. An examination of the cell revealed that the outside nickel electrodes had become distorted, contracting the adjacent anodes, thereby preventing independent movement of the anode group. A new method of supporting the outside (single) cathodes has been found and is effective in minimizing buckling or distortion of the cathode. Testing was discontinued after 8 cycles because the same condition existed in the other cells. It was not so catastrophic as in Cell S/N-003 but still precluded a reliable evaluation of the effect of interelectrode spacing on VIBROCEL™ performance. The cells will be rebuilt using properly supported outside nickel electrodes.

Samples of electrolyte were taken from the top and bottom of Cells S/N-004 and S/N-005 on Cycles 5, 6 and 7 (see REMARKS, Table 6). The aim was to determine the vibration period required at various frequencies to minimize zincate concentration gradients developed during discharge. Cell S/N-005, having the widest spacing, required no vibration to equalize zincate concentration. However, Cell S/N-004 required from 15 to 60 minutes of pre-charge vibrations, the time increasing as the frequency decreased in the range 1300 to 875 RPM (Figure 8). The purpose of the study is to find a way to reduce vibration frequency, thereby increasing the operating life of the actuators and other vibration hardware.

It is postulated that the concentration gradient must be minimized to avoid zinc "shape" change during charge. Therefore, pre-charge vibration for the prescribed interval should be effective in minimizing or eliminating shape change during cycling. The other requirement for vibration is to break dendrites that would result in short-circuiting during charge. It has been found in previous tests that a frequency of 500 RPM or lower is completely effective. However, pre-charge vibration time is too long for practical purposes. A frequency of 875 RPM appears to be a good compromise, and will be utilized when testing is resumed.

D) In addition to the 7-plate test cells, an increase in length "L", as shown in Container Drawing 6050-0102, Appendix A, will allow use of the test station to test a full size (15-plate, 300 Ahr) cell. Parts for a 300 Ahr cell have been received, and the cell will be fabricated in the near future. This first cell will utilize Matsushita impregnated, sintered nickel electrodes. It will be tested to determine the state-of-the-art specific energy, peak power and sustained power capabilities.

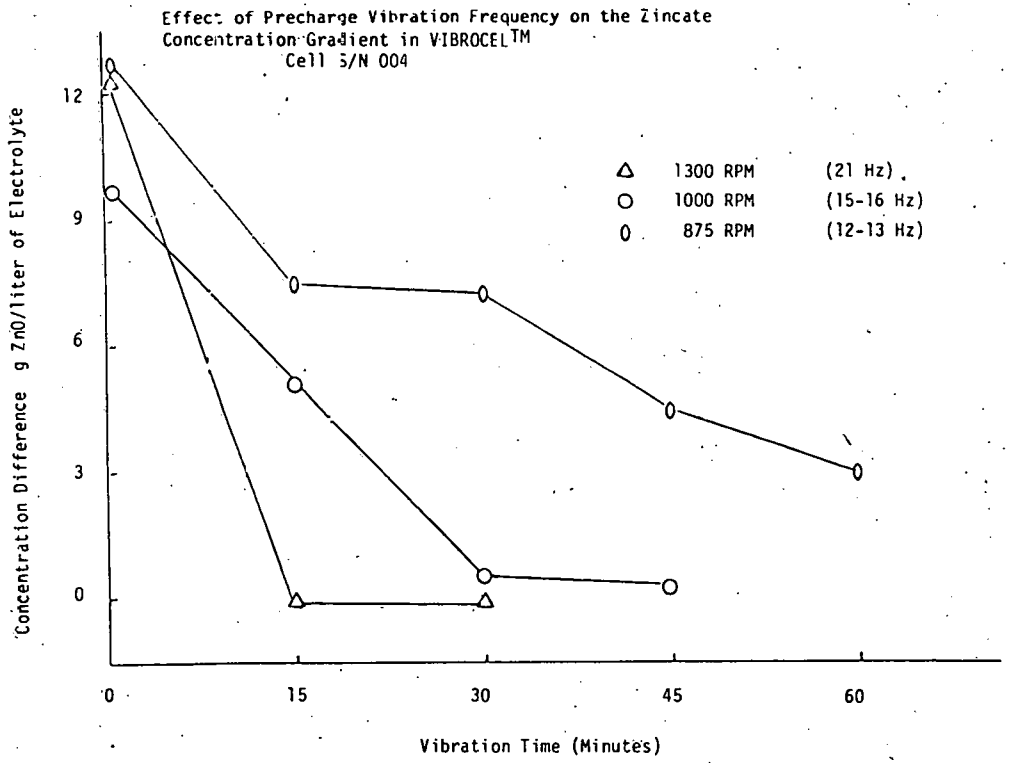
Effect of Precharge Vibration Frequency on the Zincate Concentration Gradient in VIBROCEL™ Cell S/N 004
Concentration Difference g ZnO/liter of Electrolyte
12
9
6
3
0
△ 1300 RPM (21 Hz)
○ 1000 RPM (15-16 Hz)
0 875 RPM (12-13 Hz)
0
15
30
45
60
Vibration Time (Minutes)

Figure 8

E) One of the problems encountered in the design of the nickel-zinc VIBROCEL™ has been the transmission of high currents to and from the vibrating zinc anode in this system. At present, a woven metal strap is employed which has a number of disadvantages. First, each individual strand has a high surface area to volume ratio. Hence, the woven metal strap is very susceptible to corrosion damage. Second, the woven metal strand wire may act as a wick for any electrolyte that may creep past the battery's static post and sliding pushrod seals. Third, each individual strand of the woven metal cell interconnector straps must be plated in a pore-free manner with nickel in order to prevent corrosion.

Because of these shortcomings, a flexible leaf type of intercell connector has been designed. In this interconnector system, the conductive medium which is typically a copper alloy, or copper-metal oxide dispersion, has been arranged so that it is divided into individually sliding members only in a plane normal to the geometry axis of flexure. In this the surface area of the flexible connector is minimized thus reducing the possibility of this cell strap's failure via electrolyte attack to an absolute minimum.

It is a common practice in those applications which utilize copper in a flexing mode to employ alloying or hardening agents to maximize cycle time to failure. Such techniques are common throughout the motor and relay industries. With this in mind, we selected several alloys for evaluation in this application. These are listed in Table 7 along with their chemical composition, flexure strength and conductivity.

TABLE 7

ALLOYS USED FOR FLEXIBLE CONNECTOR

Name	Chemical Composition	Fatigue Str. (psi)	Elect. Cond. % I.C.A.C.
Mallory-3	Cr .4-1.2%; rem. Cu.	32,000	78-85
Berylco 10	Be .4-.7%; Co 2.4-2.7%; rem. Cu.	45,000	48
Berylco 25	Be 1.8-2.0%;, Co + Ni .2% min.; Fe .4% Max; rem. Cu	60,000	22
BeNi 440	Be 1.95%; Ti .5%; rem. Ni	140,000	7
GLIDCOP 20	Al_2O_3 .4%; Cu 99.6%	20,000	89

With the exception of GLIDCOP 20, all of these alloys were heat treated to maximize hardness and conductivity and then electroplated with nickel to avoid corrosion due to alkaline electrolyte creepage. The electroless process was chosen in preference to conventional electroplating in order to minimize hydrogen enbrittlement of the strap samples under consideration.

At present, a test jig (Fig. 9) is being constructed which will allow cycle life or fatigue testing of these straps to take place in a controlled environment. Conductivity measurements will be made before and after fatigue testing to determind if work hardening has an adverse effect on sample conductivity.

2.2 Nickel Cathode SStudy

A) Candidates - Presently, the following companies'nickel electrodes are being evaluated:

Manufacturer	Electrode Construction
INCO	CMG-Controlled Microgeometry- Layered Nickel Foil-Slurry Coated with Active Material.
MATSUSHITA	Sintered Nickel Powder (Impregnated)
JUNGNER (NIFE)	Pocket Type
DAUG (MERCEDES)	Sintered Nickel Wool (Impregnated)
ESB	Plastic Bonded.

B) Preliminary Evaluation of CMG Electrodes

Initial testing of the CMG electrode was in vented nickel cadmium cells having the following basic design:

Cell Design

- Positive Plates - 1/Cell

  Theoretical Capacity - 36.5 Ahr

  Dimensions - 5.8" x 12" x .085"-.090"

  Weight - Electrode No. 40-1 (209);
  Electrode No. 40-2 (222.5 gm)

  Number of Foils/Electrode - 40

  Active Material - Slurry Coated on Nickel Foil

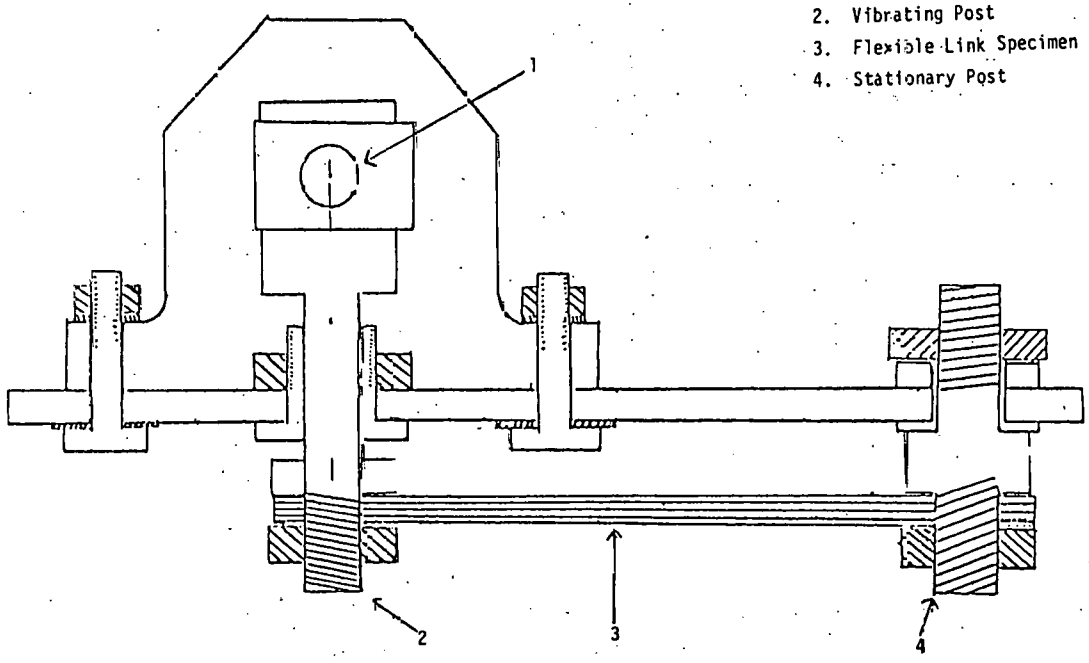

Fatigue Test Jig

Figure 9

- Negative Plates - 2/Cell (Plastic-bonded Calcium)
- Separator - GAF 10,010 (Polypropylene Felt) + VEXAR (Plastic Mesh)
- Electrolyte - 30% KOH + 10 g/l $LiOH \cdot H_2O$

Two (2) test cells were assembled in oversize cell jars with excess electrolyte. One variation in the cell design was in the type of restraint used to support the cell core assembly. These were:

- Shimmed - usual NiCd cell configuration with plexiglas shims added to insure tightness of cell core assembly.
- Bolted - the cell core assembly was bolt (8) restrained between two pieces of plexiglas (.5" T) and placed in a cell jar.

After sufficient formation cycling to develop full capacity of the nickel electrodes, the following regime was run:

Test Regime - the cells were tested at three temperatures - R.T. (-18°C/-0.4°F); -30°C/-22°F).

-Room Temperature-

Charge - 12 Amps for 6 hours

Discharge - C/5, C/3, C/2 and C/1 rates to 0 Volts vs Hg/Hgo ref.

-Low Temperature-

Charge - With cell stabilized at room temperature - 12 Amps for 6 hours or 150% of capacity removed on previous discharge. Temperature Stabilization - The cells were stored at temperatures for a minimum of 16 hours.

Discharge - C/5, C/3, C/2 and C/1 rates to 0 Volts vs Hg/HgO ref.

Test Results

- Room Temperature

  Figure 10 - the bolted restrained electrode (40-2) yielded 211.6 Ah/kg at the C/5 rate. At the C/1 rate, the electrode yielded 184 Ah/kg (87% of the C/5 rate).

- Figure 11 - the shimmed restrained electrode (40-1) performance was somewhat less than the bolted restrained construction.

Evaluation of Slurry-Coated CMG Nickel Cathodes - Room Temperature

Electrode 40-2 (40 Foil)

Assembled vs Cd Anodes - Bolted Restraint

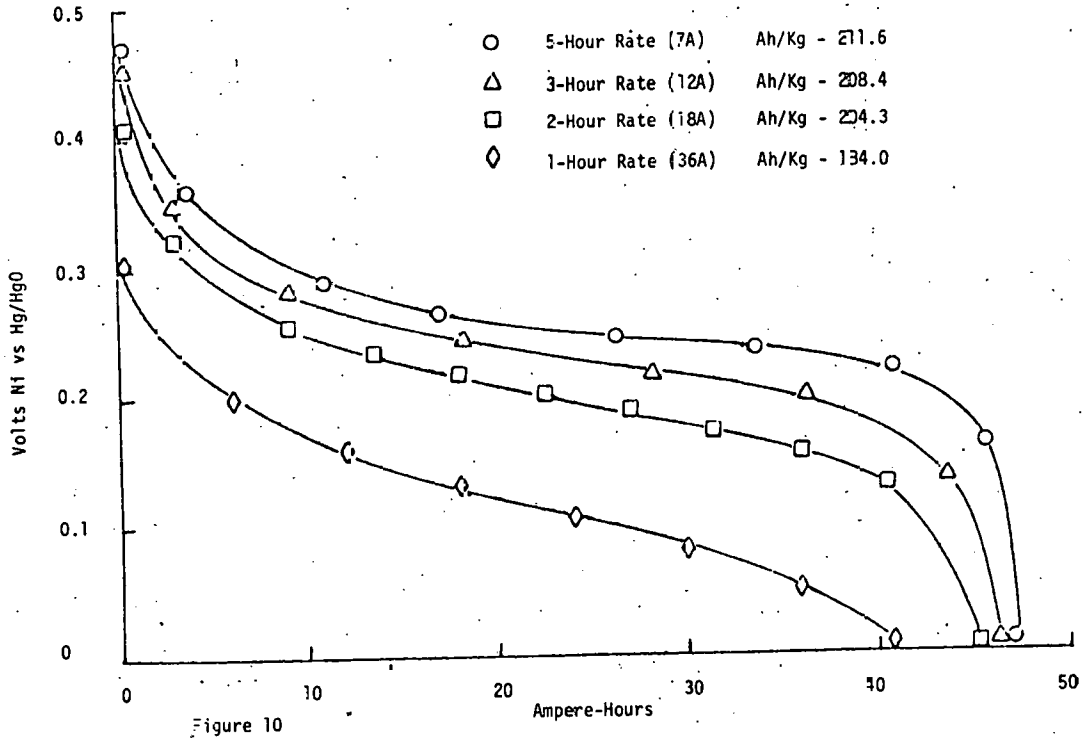

Figure 10

Evaluation of Slurry Coated CMG Nickel Cathodes - Room Temperature

Electrode 40-1 (40 Foil)

Assembled vs Cadmium Anodes in Normal (Shim) Restraint

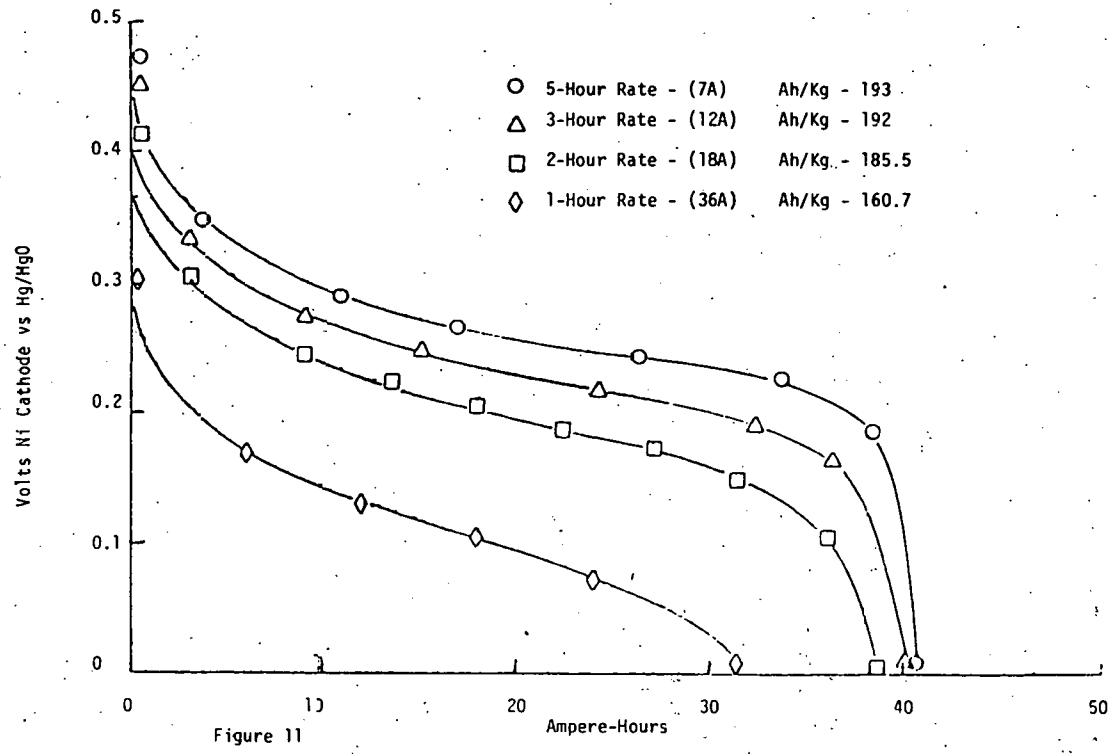

Figure 11

- Low Temperature

-18°C/-0.4°F:

The test results are shown in Figures 12 and 13. Again, the test results at low temperatures were encouraging at the C/5 and C/3 discharge rates. As expected, the high rate discharges C/2 and C were derated appreciably at this lower temperature. As at room temperature, the bolted restraint construction outperformed the normal shim restraint.

-30°C/-22°F:

The test results are shown in Figures 14 and 15. There was a marked decrease in the voltage performance of the cell with the normal shim restraint. The bolted restraint gave acceptable performance up to the C/1 rate. At the C/1 rate, both cells were below the 0 Volt cut-off at the start of the discharge.

These initial results on the CMG electrodes were encouraging, particularly the bolted restraint design. The Ah/kg figures were good and the electrodes delivered a narrow range of capacities, up to and including the C/3 discharge rate.

C) Evaluation of CMG Electrodes - in VIBROCEL™ Configuration

CMG electrodes were evaluated in the "free standing" or VIBROCEL™ type configuration. We were aware of some problems in cycling this type of electrode unsupported, namely, warping and delamination of the layers. Several design changes were made to improve these characteristics . Two constructions were made to give some physical support to these electrodes in the free-standing condition. these were:

- Riveted - The electrodes were bagged in a non-woven absorber (polyamide felt). They were then overlaid with a heat shrinkable P.V.C. netting. The layers of foil were then fastened thru pre-punched holes with nickel rivets (Figure 16). Average electrode weight was 196 gms and electrode dimensions were 5.0 in. W x 9.46 in. H x .20 in. T.

- Stitched - The bagging and overlaying with P.V.C. was similar to the riveted design. The layers of foil were fastened by stitching thru the electrode structure with polypropylene thread on half-inch centers (Figure 16). The average electrode weight was 185 gms, and dimensions were 4.96 in. W x 9.42 in. H x .19 in. T.

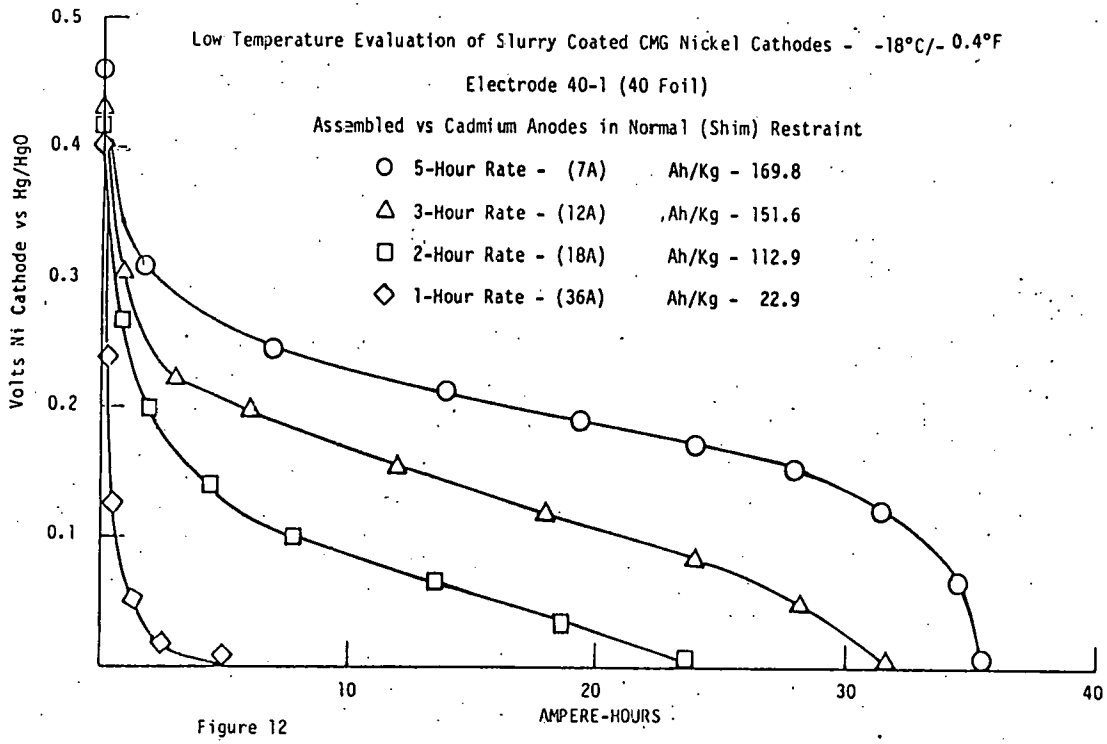
Low Temperature Evaluation of Slurry Coated CMG Nickel Cathodes - -18°C/- 0.4°F
Electrode 40-1 (40 Foil)
Assembled vs Cadmium Anodes in Normal (Shim) Restraint
5-Hour Rate - (7A) Ah/Kg - 169.8
3-Hour Rate - (12A) Ah/Kg - 151.6
2-Hour Rate - (18A) Ah/Kg - 112.9
1-Hour Rate - (36A) Ah/Kg - 22.9
Volts Ni Cathode vs Hg/HgO
0.5
0.4
0.3
0.2
0.1
10
20
30
40
AMPERE-HOURS

Figure 12

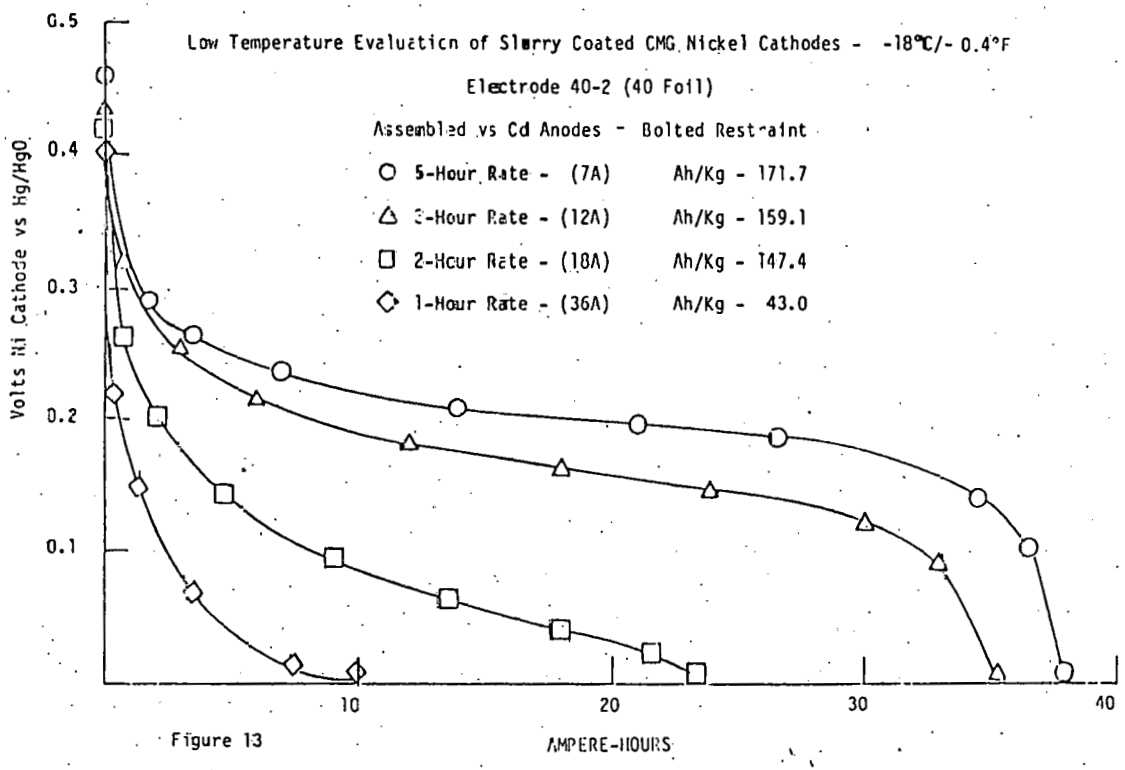
Low Temperature Evaluation of Slurry Coated CMG Nickel Cathodes - -18°C/- 0.4°F
Electrode 40-2 (40 Foil)
Assembled vs Cd Anodes - Bolted Restraint
5-Hour Rate - (7A) Ah/Kg - 171.7
3-Hour Rate - (12A) Ah/Kg - 159.1
2-Hour Rate - (18A) Ah/Kg - 147.4
1-Hour Rate - (36A) Ah/Kg - 43.0
Volts Ni Cathode vs Hg/HgO
0.5
0.4
0.3
0.2
0.1
10
20
30
40
AMPERE-HOURS

Figure 13

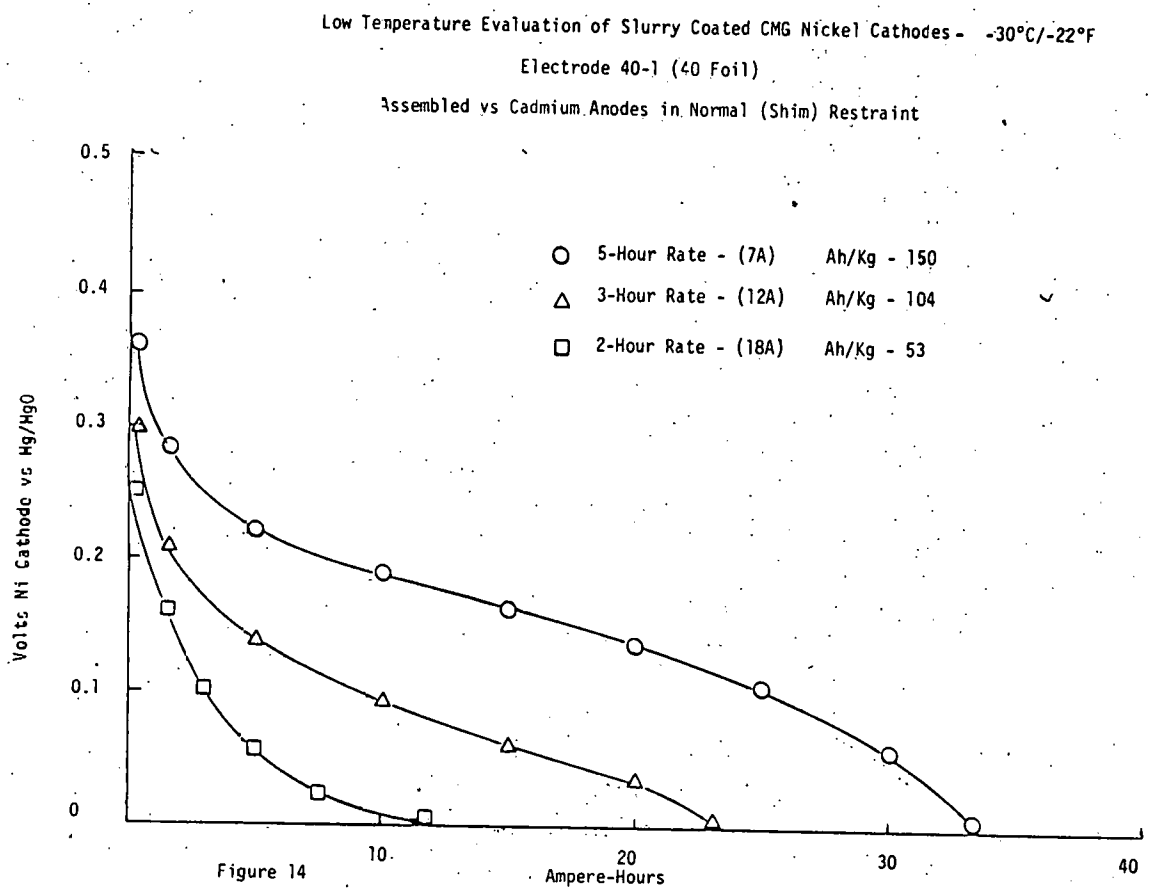
Low Temperature Evaluation of Slurry Coated CMG Nickel Cathodes - -30°C/-22°F
Electrode 40-1 (40 Foil)
Assembled vs Cadmium Anodes in Normal (Shim) Restraint
5-Hour Rate - (7A) Ah/Kg - 150
3-Hour Rate - (12A) Ah/Kg - 104
2-Hour Rate - (18A) Ah/Kg - 53
Volts Ni Cathode vs Hg/HgO
0.5
0.4
0.3
0.2
0.1
0
10
20
30
40
Ampere-Hours

Figure 14

Low Temperature Evaluation of Slurry Coated CMG Nickel Cathodes - -30°C/-22°F

Electrode 40-2 (40 Foil)

Assembled vs Cd Anodes - Bolted Restraint

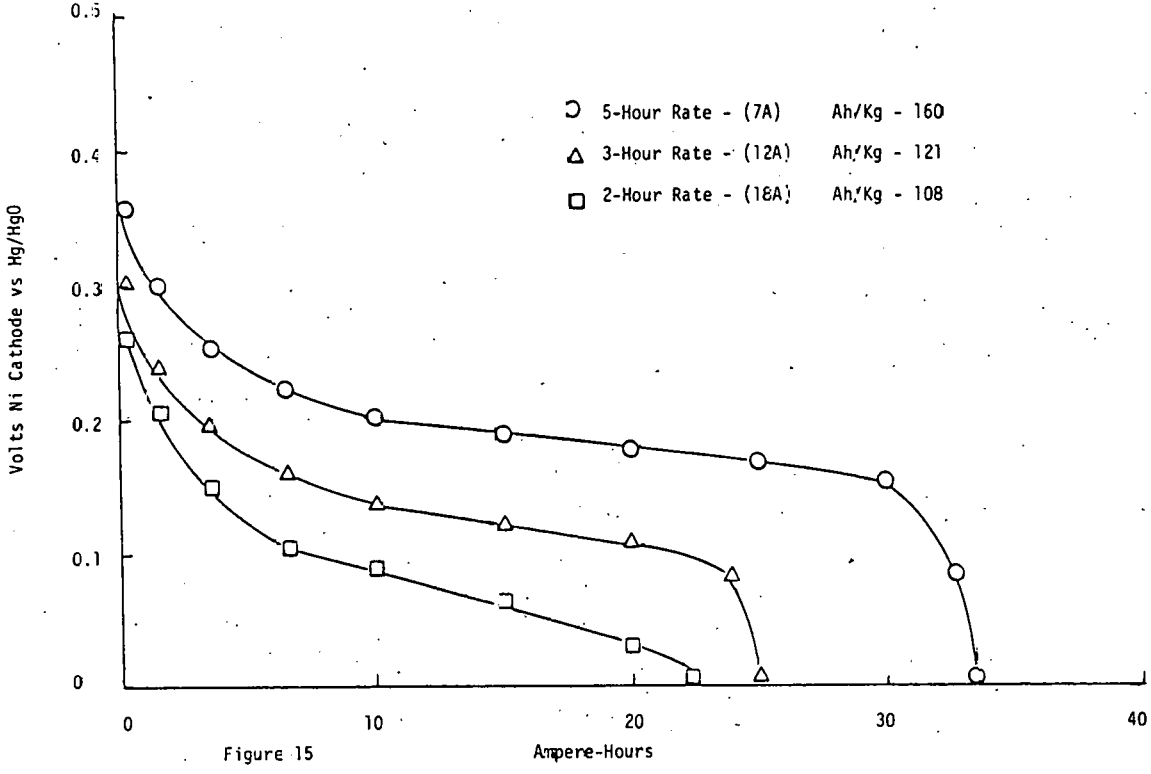

Figure 15

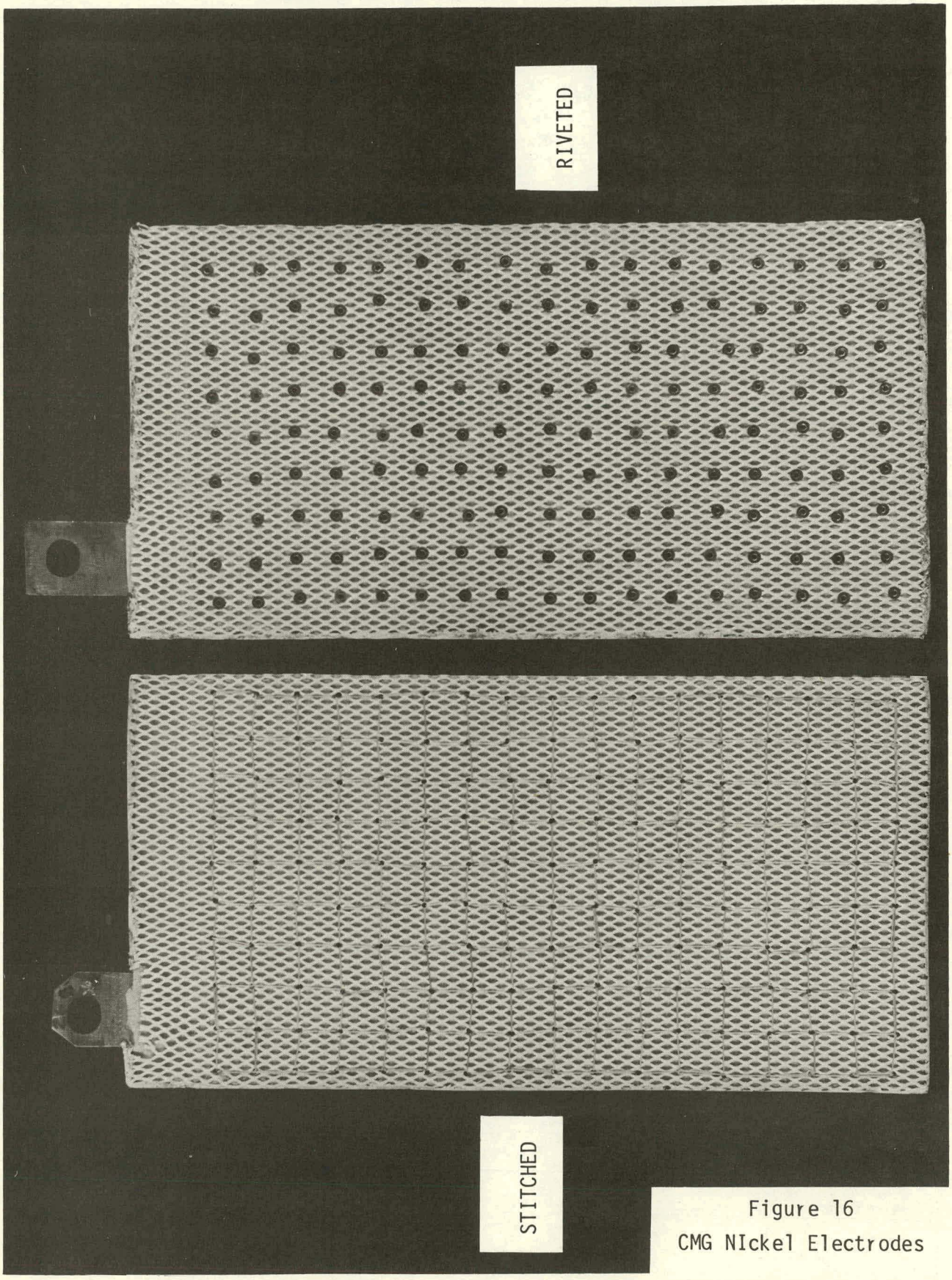

Figure 16
CMG NIckel Electrodes

Test Results

Two 3-plate cells were assembled using the nickel sheet counter electrodes for each cell. The cycling regime was:

Charge - 14 Amps - 10 hrs.

Discharge - Various rates to 0 Volts vs Hg/HgO ref.

Test results for the cell containing CMG electrodes VSM 13, 14 and 15 (Riveted) are given in Figure 17 and Table 8 and for the cell containing CMG electrodes VSM 25, 26 and 27, (Stitched), are shown in Figure 18 and Table 9 . The results clearly indicate the superiority of the stitched version. Capacity densities in the range of 145 Ah/kg were obtained with a good V-I relationship. No degradation was observed over an 18-cycle test regime. The riveted version on the other hand, never reached nominal capacity, capacity deteriorated as testing progressed and showed a poor V-I relationship. Some loss of active material from these electrodes was seen as black particulate material which settled at the bottom of the cell. Considering these results, the stitched construction has been selected for use in the prototype VIBROCEL™ designs.

D) Matsushita Sintered Nickel Electrodes

Sintered nickel electrodes supplied by Matsushita measured 6.9 in. W x 8.95 in. H x .065 in. T. and had a nominal capacity of 23 Ah. The electrodes were tank-formed and after five formation cycles, delivered an average of 22 Ah or 100 percent of the rated capacity. Following formation, the plates were washed in deionized water and dried. In order to use the Matsushita electrodes in the VIBROCEL™ configurations, a "double thickness" plate was required. This was accomplished by riveting two plates (.065" each) back-to-back for a final thickness of .130" and a nominal capacity of 46 Ah at C/5.

As required for VIBROCEL™ operation, the free-standing electrode was insulated with Conwed 5340 polypropylene netting having 15 x 15 strands/inch and a weight of 50-60 pounds per 1000 sq.ft. The test regime (in triplicate) using two nickel sheet anodes, and zinc-free electrolyte, was as follows:

Charge - 9 amps for 10 hrs (100% overcharge at the 5-hr rate)

Stand - 1/4 hour

Discharge - C/5, C/3, C/2 and C/1 rates to 0 Volts vs Hg/HgO reference

Evaluation of CMG Nickel Electrode for VIBROCEL™ Application
Performance of 3-Plate Groups of Stitched and Riveted Electrodes

Nom. Three-Plate Capacity - 72 Ah
Stitched-VSM 25-27
Riveted-VSM 13-15

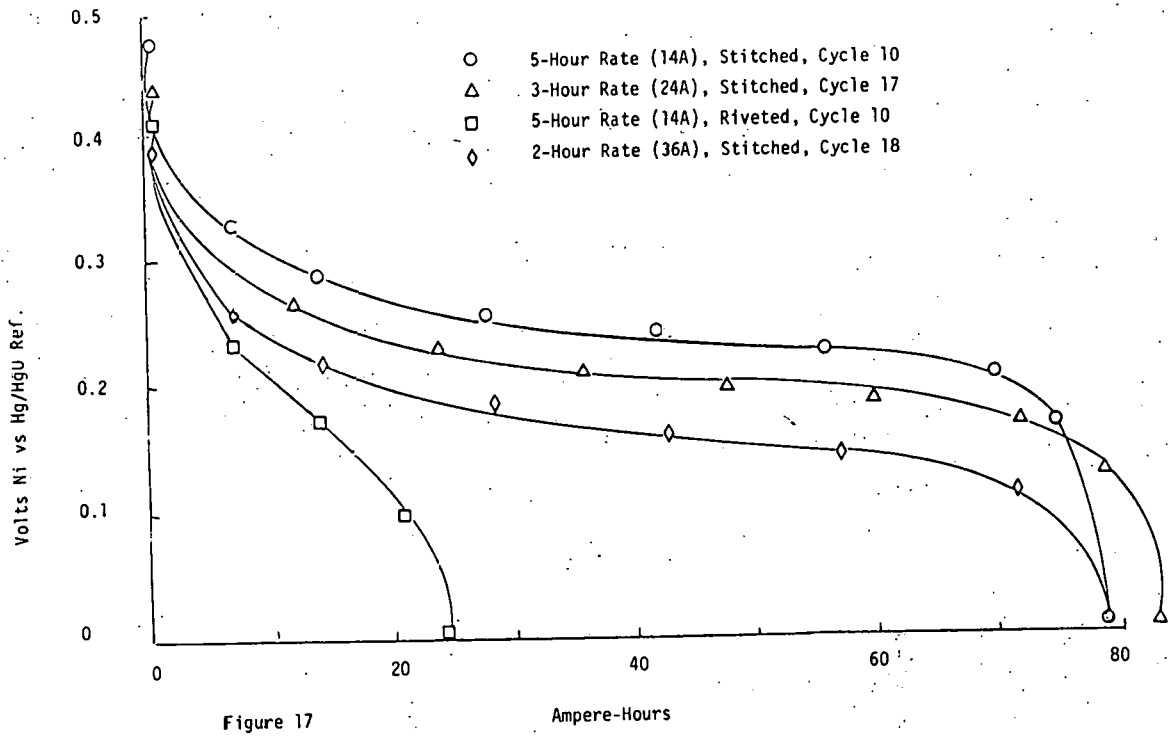

Figure 17

Table 8

Performance of CMG Nickel Electrodes Prepared

For VIBROCEL™ Application

Three-Electrode Group VSM 13-15 [Riveted]

All Charging at 14A, 10 Hours

Cycle	Discharge Rate (A)	Group Capacity (Ah)	Ah/Kg (3-Plate Group) Bare CMG Electrodes	Complete CMG Electrodes
1	14	36.5	89.4	61.8
2	14	54.0	132.3	91.5
3	14	49.3	120.8	83.5
4	14	43.2	105.8	73.2
5	14	41.1	100.7	69.6
6	14	41.2	101	69.8
7	14	35.1	86	59.5
8	14	31.2	76.4	52.8
9	14	27.0	66.1	45.7
10	14	24.7	60.5	41.8
11	24	16.8	41.1	28.4
12	24	14.8	36.2	25.0

Table 9

Performance of CMG Nickel Electrodes Prepared For VIBROCEL™ Application

Three-Electrode Group VSM-25-27 [Stitched]

All Charging - 14A, 10 Hours

Cycle	Discharge Rate (A)	Group Capacity (Ah)	Ah/Kg (3-Plate Group) Bare CMG Electrodes	Complete CMG Electrodes
1	14	41.5	103.2	74.5
2	14	65.2	162.1	117.1
3	14	68.6	170.6	123.2
4	14	69.5	172.9	124.8
5	14	74.0	184.0	132.9
6	14	72.0	180.0	130.0
7	14	76.0	189.0	136.5
8	14	79.0	196.5	141.9
9	14	76.1	189.3	136.7
10	14	79.0	196.5	141.9
11	24	76.8	191.0	137.9
12	24	76.8	191.0	137.9
13	24	79.9	198.7	143.5
14	24	80.1	199.2	143.9
15	24	80.6	200.5	144.8
16	24	82.3	204.7	147.8
17	24	83.2	206.9	149.4
18	36	78.9	196.2	141.7

Performance with CONWED 5340

The test results with the netting are shown in Figure 18. The capacity was marginal at the C/5 and C/3 rates and the voltage level was depressed somewhat. The higher rates, particularly the C/1 rate, were exceptionally poor. By a process of elimination, it was determined that CONWED 5340 netting open area was not sufficient and could be affecting the performance of the electrode. Following Cycle 7, the netting was removed from Electrode #1 and the 40 amp discharge repeated. The results with and without the netting at 40 amps are shown in Figure 19. The performance was improved markedly. There was about a 0.3 V improvement in the discharge voltage.

Performance without Netting

The netting was removed from all electrodes and the test regime repeated. The results are shown in Figure 20. The improved performance without the netting can be easily seen, especially at the high discharge rates.

The use of netting as a positive insulator without a sufficiently open structure to permit adequate circulation of electrolyte can effect the performance of positive (nickel) electrodes. this effect is likely to be more pronounced in a stationary test cell (non-vibrating) such as these, however, it is obvious that candidate insulating netting material will have to be tested in the future to find materials having the least adverse effect in electrode performance.

Two candidate nettings selected for testing were:

- VEXAR-V360 PANL - polypropylene
- CONWED-XN 3230 - polypropylene

Electrode Performance with VEXAR Netting

The test results and the various discharge rates are shown in Figure 22. The capacities and voltage levels were all acceptable and the VEXAR is a suitable netting for use in the VIBROCEL™.

Electrode Performance with CONWED XN-3230 Netting

Again, the test results at various discharge rates are shown in Figure 21. The capacities and voltage levels were slightly better than the electrode with the VEXAR netting. These slight differences may be due to variations in the electrodes themselves. In either case, both nettings are suitable for VIBROCEL™ application.

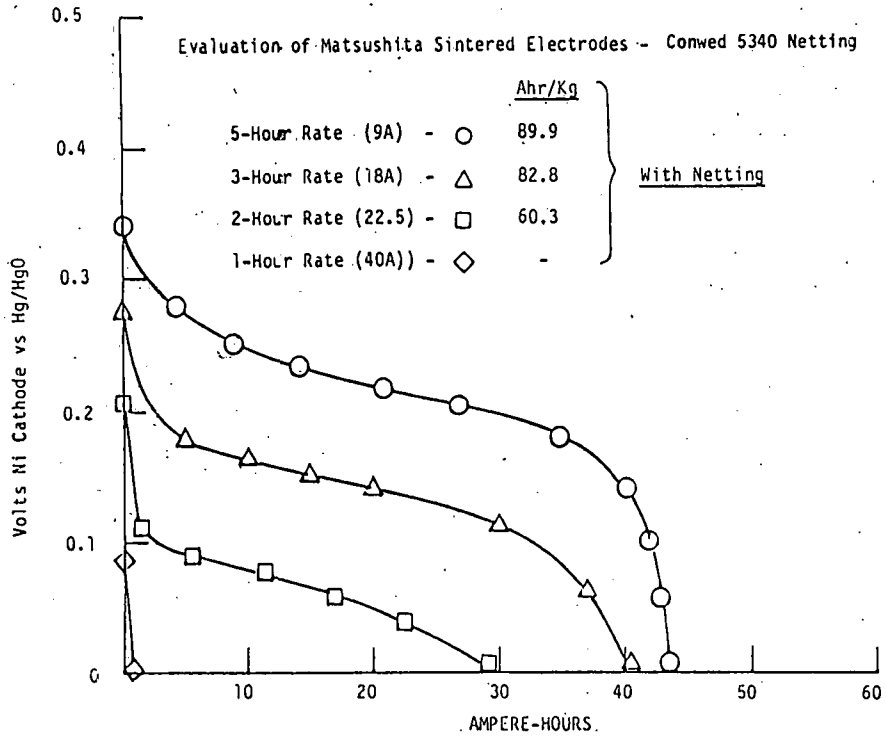
Evaluation of Matsushita Sintered Electrodes - Conwed 5340 Netting
Ahr/Kg
5-Hour Rate (9A) - ○ 89.9
3-Hour Rate (18A) - △ 82.8
2-Hour Rate (22.5) - □ 60.3
1-Hour Rate (40A)) - ◇ -
With Netting
Volts Ni Cathode vs Hg/HgO
0.5
0.4
0.3
0.2
0.1
0
10
20
30
40
50
60
AMPERE-HOURS

Figure 18

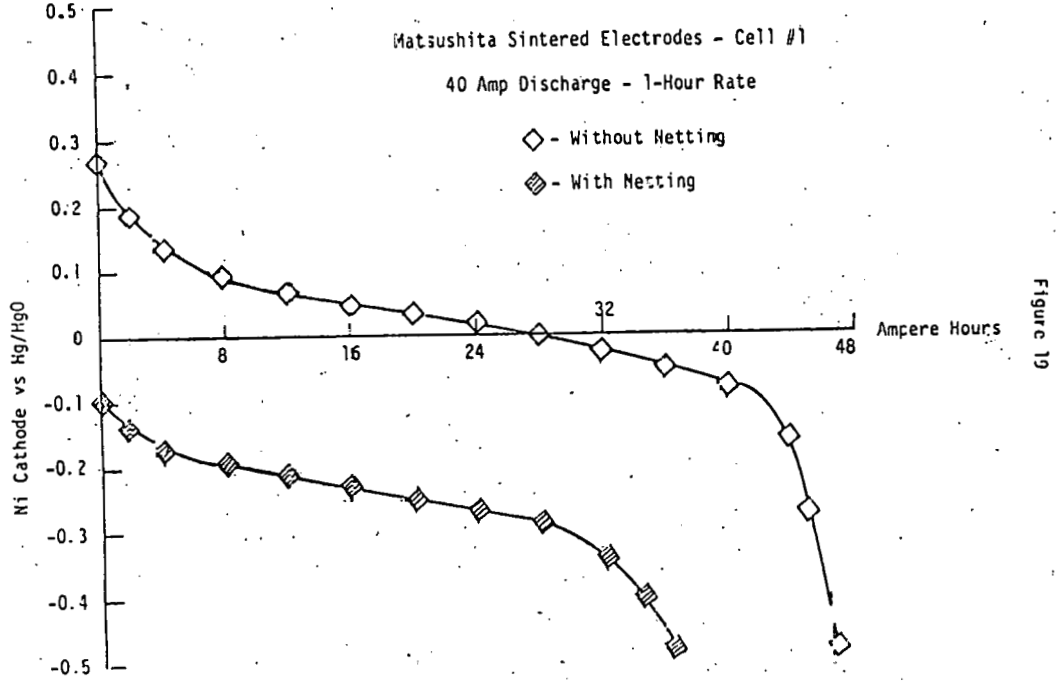
Matsushita Sintered Electrodes - Cell #1
40 Amp Discharge - 1-Hour Rate
◇ - Without Netting
▨ - With Netting
Ni Cathode vs Hg/HgO
0.5
0.4
0.3
0.2
0.1
0
-0.1
-0.2
-0.3
-0.4
-0.5
8
16
24
32
40
48
Ampere Hours

Figure 19

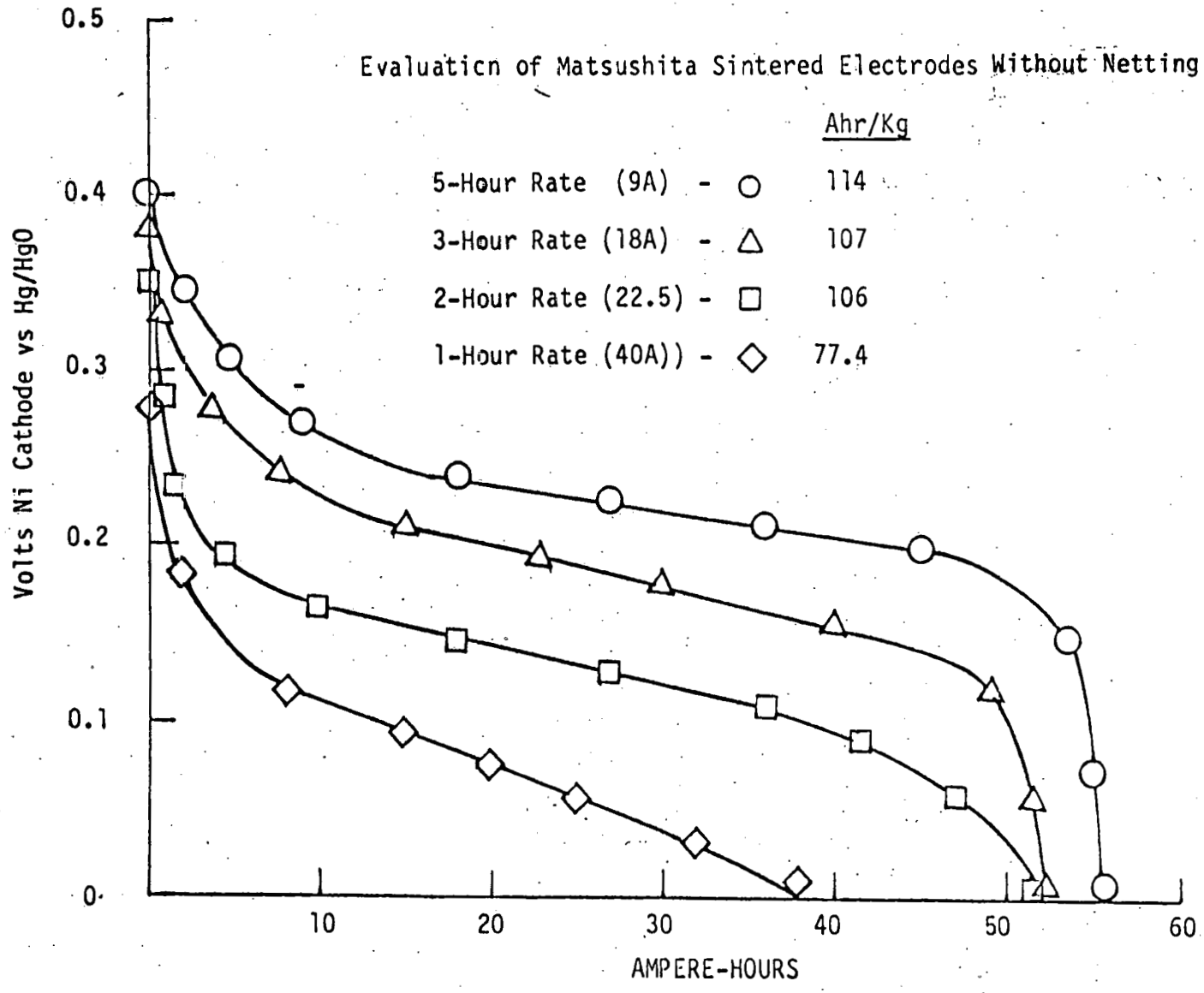
Evaluaticn of Matsushita Sintered Electrodes Without Netting
Ahr/Kg
5-Hour Rate (9A) - 114
3-Hour Rate (18A) - 107
2-Hour Rate (22.5) - 106
1-Hour Rate (40A)) - 77.4
Volts Ni Cathode vs Hg/HgO
0.5
0.4
0.3
0.2
0.1
0
10
20
30
40
50
60
AMPERE-HOURS

Figure 20

Evaluation of Matsushita Sintered Electrodes
with Vexar Matting (546 V360 PA NL) Polypropylene

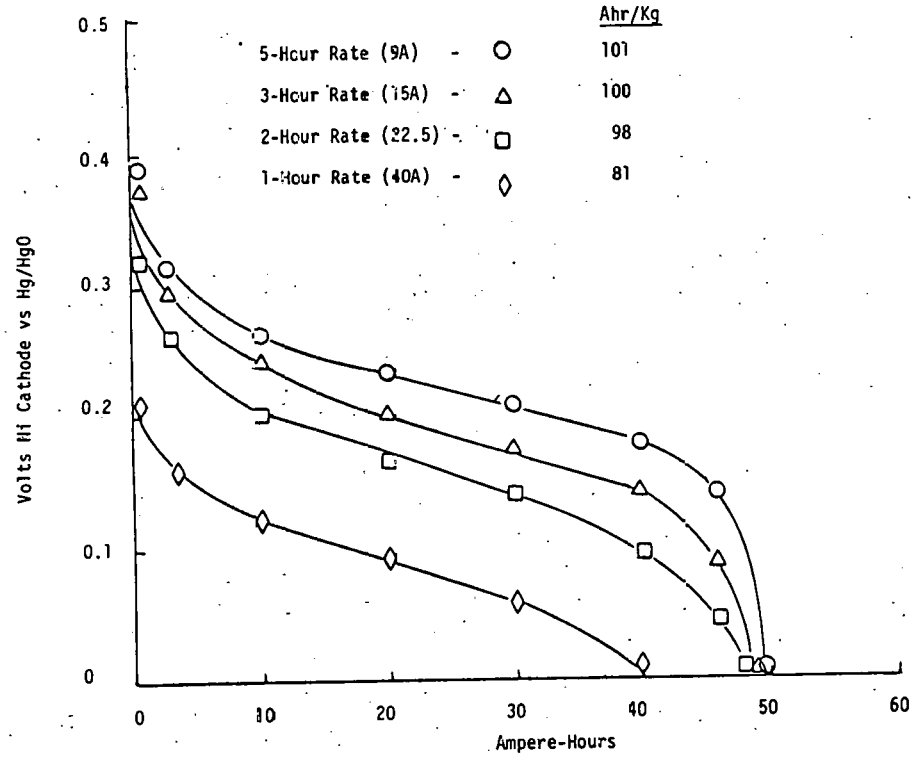

Figure 21

Evaluation of Matsushita Sintered Electrodes-
with Conwed Netting (XN3730) Polypropylene

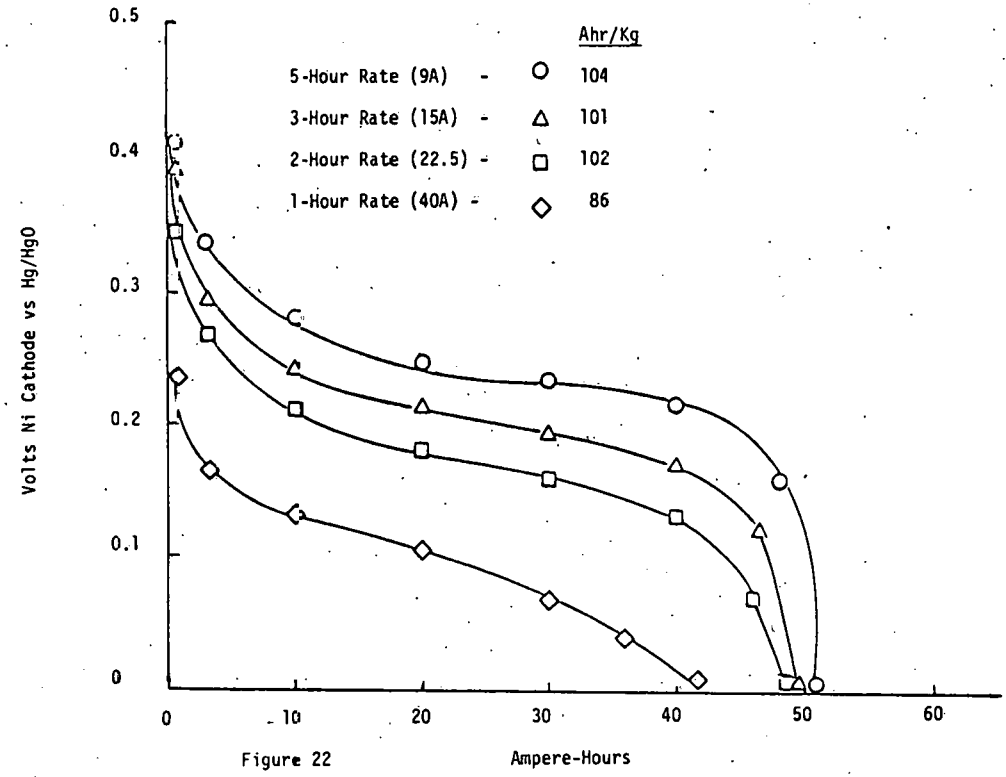

Figure 22

Charge/Discharge Efficiency

During the characterization of the candidate electrodes at various discharge rates, the charge has always been - charge at 5 hr rate - 100% overcharge. The primary reason for this type of charging regime is to determine if the "free standing" electrodes will accept the overcharge without warping, delaminating or sloughing off active material. Part of the electrode characterization studies is to determine what percent overcharge is required to maintain rated capacity.

The test scheme for determining charge/discharge efficiency was as follows:

Charge - 5 hour rate (9 amps) for periods of 1.5, 3.0, 4.5, 6.0, 7.5, 9.0 and 10 hrs.

Stand - 1/4 hr.

Discharge - 5 hour rate (9 amps) to 0 Volts Hg/HgO reference after each of the above charge periods.

The turn-around efficiencies are shown in Table 10. Results indicate the initial part of each charge is very efficient but as we approach full charge, the charging efficiency falls off. The ampere-hour input and ampere-output figures are plotted in Figure 23. These results indicate the Matsushita electrodes require a 35-40 percent overcharge to maintain rated capacity. A slight increase in capacity can be achieved by overcharging by 60 or 70 percent.

E) Jungner NIFE-Pocket Type Nickel Electrode

The Jungner cathodes received for evaluation measured 7.1 in. W x 8.9 in. H x .20 in. T, had an average weight of 495 grams and a rated capacity of 34 Ah. Eight plates were tank-formed as prescribed by the manufacturer.

Charge - 8 hr rate for 8 hrs + 100% overcharge

Discharge - 8 hr rate to 0 Volts vs Hg/HgO reference

At the end of five formation cycles, the cathodes were delivering 36 Ah. These cells were assembled using individual free standing Jungner electrodes (without netting) and two nickel sheet anodes for each cell assembly. Electrode performance was determined by the following test regime:

TABLE 10

CHARGE/DISCHARGE EFFICIENCIES
MATSUSHITA ELECTRODES

Period	Charge Hrs @ 9 Amps	Ah Input	Ah Output	Turnaround Efficiency	Percent Overcharge
1	1.5	13.5	12.9	96%	4%
2	3.0	27.0	26.5	98%	2%
3	4.5	40.5	38.1	94%	6%
4	6.0	54.0	46.1	85%	18%
5	7.5	67.5	49.0	72%	39%
6	9.0	81.0	52.6	65%	54%
7	10.0	90.0	53.3	59%	70%

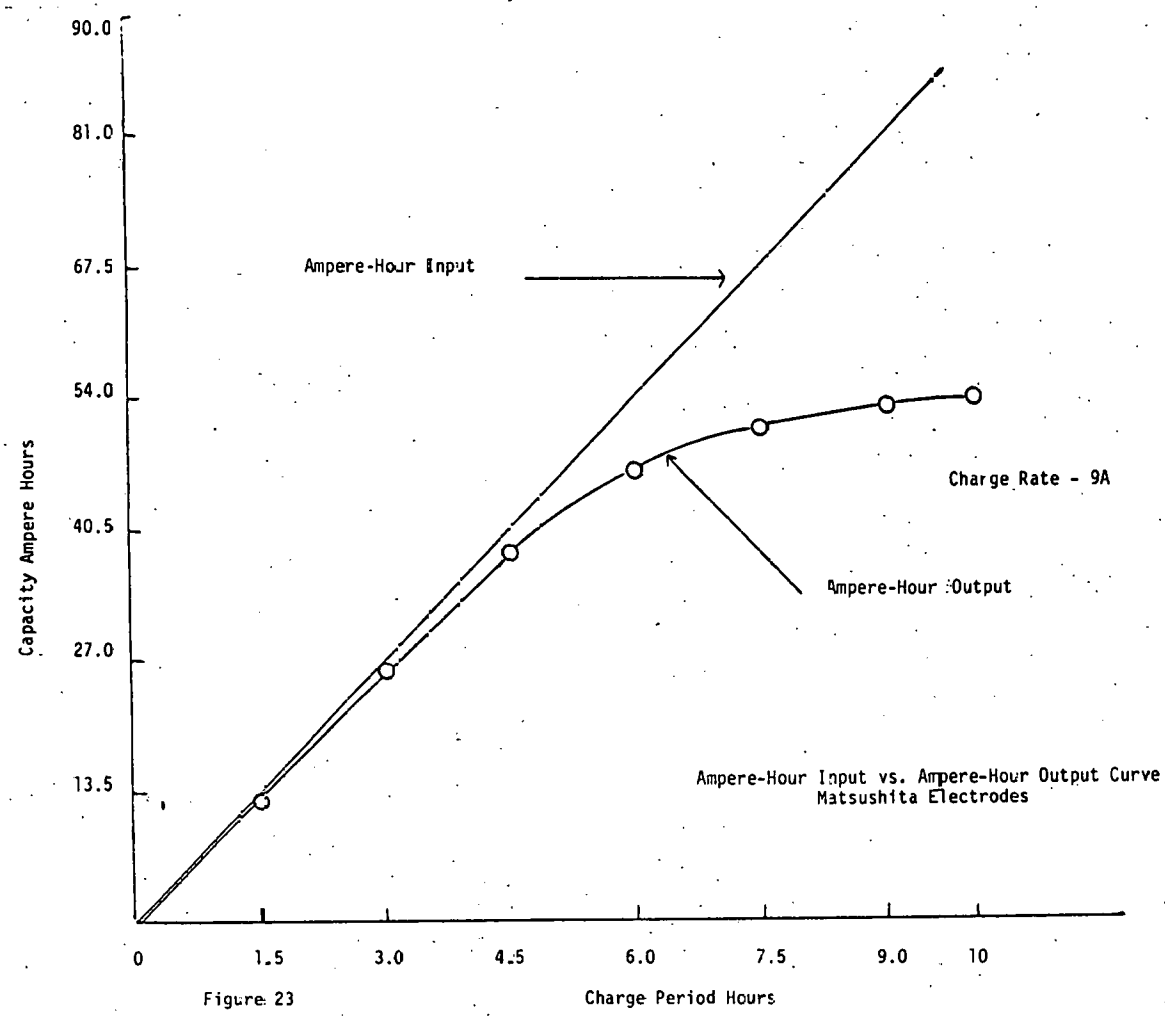
90.0
81.0
67.5
54.0
40.5
27.0
13.5
Capacity Ampere Hours
Ampere-Hour Input
Charge Rate - 9A
Ampere-Hour Output
Ampere-Hour Input vs. Ampere-Hour Output Curve
Matsushita Electrodes
0
1.5
3.0
4.5
6.0
7.5
9.0
10
Charge Period Hours

Figure 23

Charge - 7 amps for 10 hours (5 Ah rate + 100% overcharge)

Stand - 1/4 hour

Discharge - C/5, C/3, C/2 + C/1 rates to 0 Volts vs Hg/HgO reference.

The test results are shown in Figure 24. At the C/5, C/3 and C/2 discharge rates, the electrodes delivered acceptable voltage levels and ampere-hour capacities . At the C/1 discharge rate, the performance fell off sharply. The heavier weights of the pocket type electrode produced Ah/kg. figures that are marginal for VIBROCEL™ applications.

Charge/Discharge Efficiencies Jungner-NIFE Pocket Electrodes

The test scheme for determining charge/discharge efficiencies was as follows:

Charge - 5 hour rate (7 amps) for periods of 1.5, 3.0, 4.5, 6.0, 7.5, 9.0 and 10 hours.

Stand - 1/4 hour

Discharge - 5 hour rate (7 amps) to 0 Volts vs Hg/HgO reference after each of the above charge periods.

The turnaround efficiencies and percent overcharge figures are shown in Table 11. Again, the results indicate the initial part of each charge is very efficient, but as we approach full charge, the efficiencies fall off. The ampere-input and ampere-hour figures are plotted in Figure 25. Results indicate the Jungner-NIFE pocket electrode also requires 35-40 percent overcharge to maintain rated capacity.

F) ESB Plastic Bonded Electrode

First experiments utilized the standard ESB plastic bonded active material formulation to fabricate sheets of active material. Nominal percentages of components were:

Nickel Hydrate	76.5%
$Co(OH)_2$	6.5%
Carbon (Graphite)	15.0%
TFE	2.0%
	100.0%

Evaluation of Jungner Nife Pocket-Type Nickel Cathodes

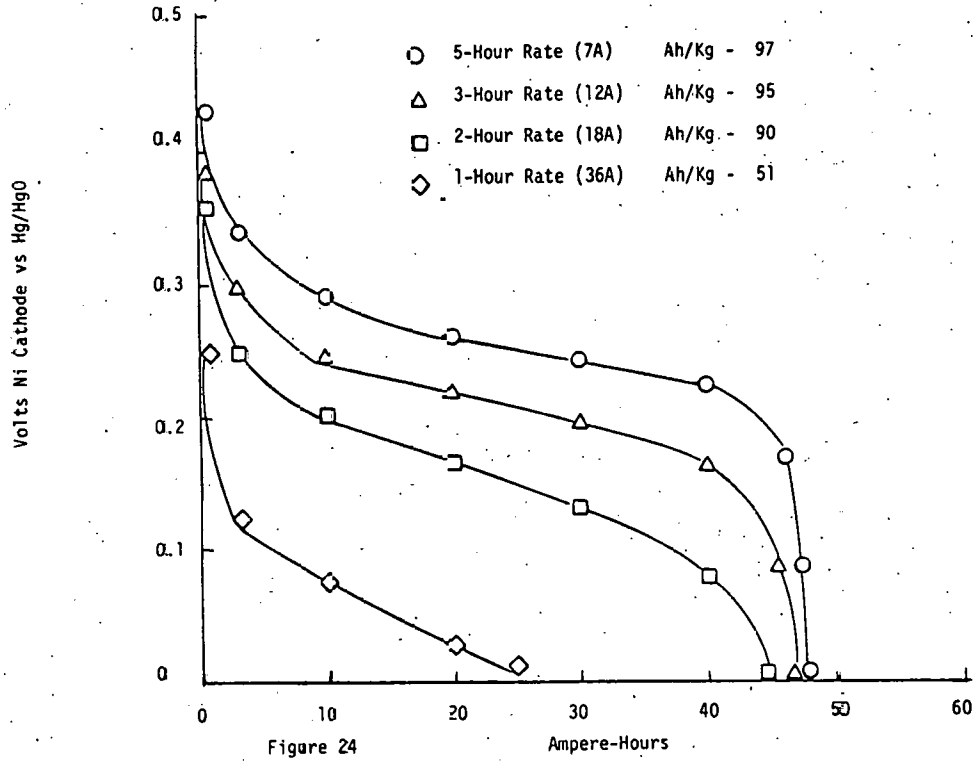

Figure 24

TABLE 11

CHARGE/DISCHARGE EFFICIENCIES
JUNGNER ELECTRODES

Period	Charge Hrs @ 7 Amps	Ah Input	Ah Output	Turnaround Efficiency	Percent Overcharge
1	1.5	10.5	10.3	98%	2%
2	3.0	21.0	20.6	98%	2%
3	4.5	31.5	29.0	92%	9%
4	6.0	42.0	37.3	89%	12%
5	7.5	52.5	43.3	82%	22%
6	9.0	63.0	46.9	74%	35%
7	10.0	70.0	47.5	68%	47%

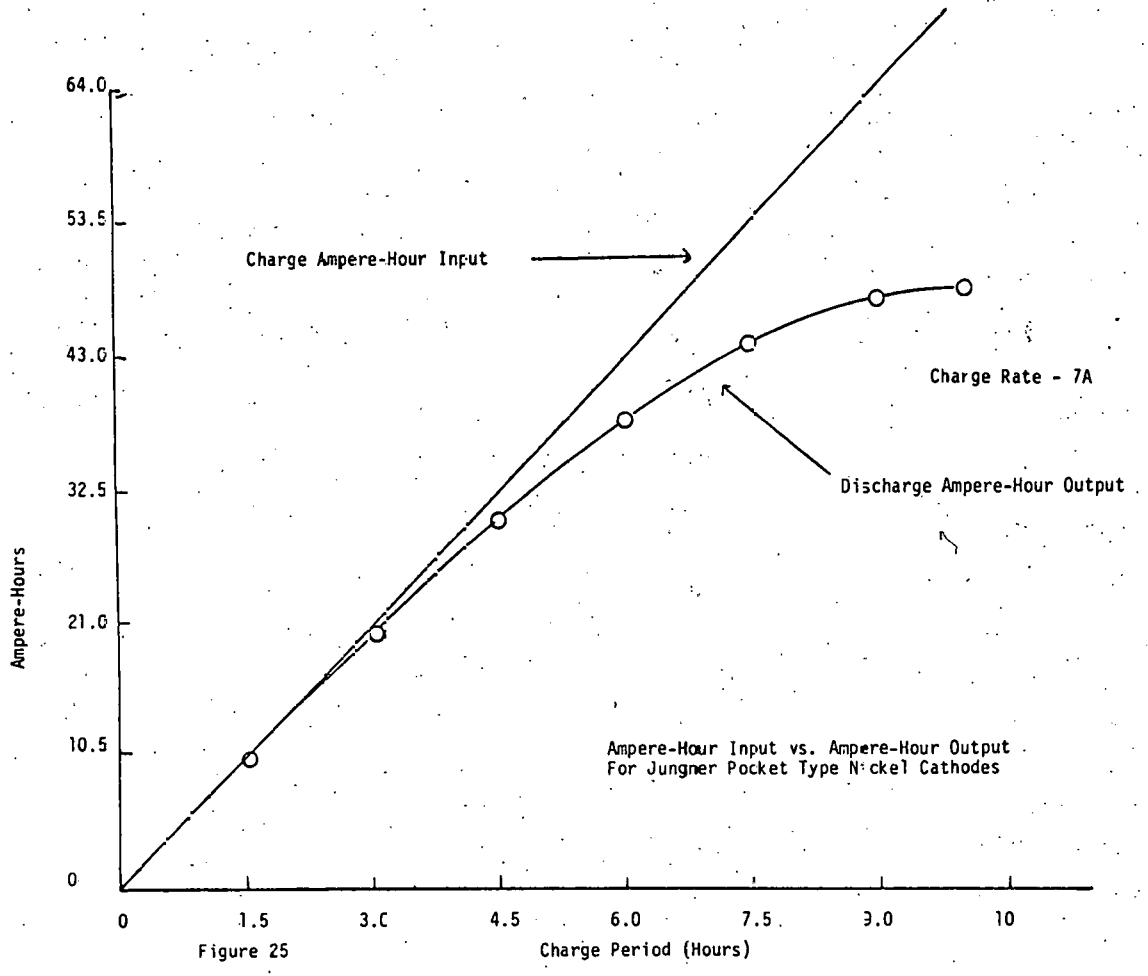
64.0
53.5
43.0
32.5
21.0
10.5
0
Ampere-Hours
Charge Ampere-Hour Input
Charge Rate - 7A
Discharge Ampere-Hour Output
Ampere-Hour Input vs. Ampere-Hour Output
For Jungner Pocket Type Nickel Cathodes
0
1.5
3.0
4.5
6.0
7.5
9.0
10
Charge Period (Hours)

Figure 25

Two types of electrodes were fabricated, i.e. a two-grid construction (1MNP2) utilizing a single thick sheet of active material pressed between two expanded nickel grids, and a three-grid construction (1MNP1) consisting of two half thickness sheets of active material with a center grid combined with the two outside grids. Electrode design details were as follows:

1 MNP 1 - 3 Grids (5 Ni 17 3/0 Distex)

Theoretical Capacity - 20 Ah

Dimensions - 8 in. H x 6.2 in. W x .127 in. T

Total Electrode Wt = 202 gms; Active Material Wt = 135.0 gms

Grid Positioning - Ni Distex
Active Mat'l
Ni Distex
Active Mat'l
Ni Distex
Compressed to .127 in. T

(Grids spot welded in pattern for strength)

1 MNP 2 - 2 Grids (5 Ni 17 3/0 Distex)

Theoretical Capacity - 32 Ah

Dimensions - 8.7 in. H x 6.2 in. W x .115 in. T

Total Electrode Wt - 194 gms; Active Material Wt = 142.5 gms

Grid Positioning - Ni Distex
Active Mat'l
Ni Distex
Compressed to .115 in. T

(Grids spot welded in pattern for strength)

The experimental electrodes were assembled in three plate cells, using nickel sheet anodes with excess 6M KOH. Electrodes were free standing with no physical support (similar to VIBROCEL™) conditions. Cells were charged and discharged at a nominal rate of C/5. Test results are shown in Figure 26 and Figure 27. Maximum capacity densities obtained were 141 Ah/kg for the 3 grid electrode (Cycle 6) and 121 Ah/kg for the two grid electrode. Voltage performance of the 3 grid design was higher, but both electrodes declined appreciably in voltage over a short test cycle regime (10-15 cycles). Disassembly of the test cells indicated that in both cases the active material had swelled and expanded through the grid structure to a total thickness of about .250 in. This type of unsupported construction evidently results in loss of electrical contact of the grid with the active material, with an accompanying high electrode polarization.

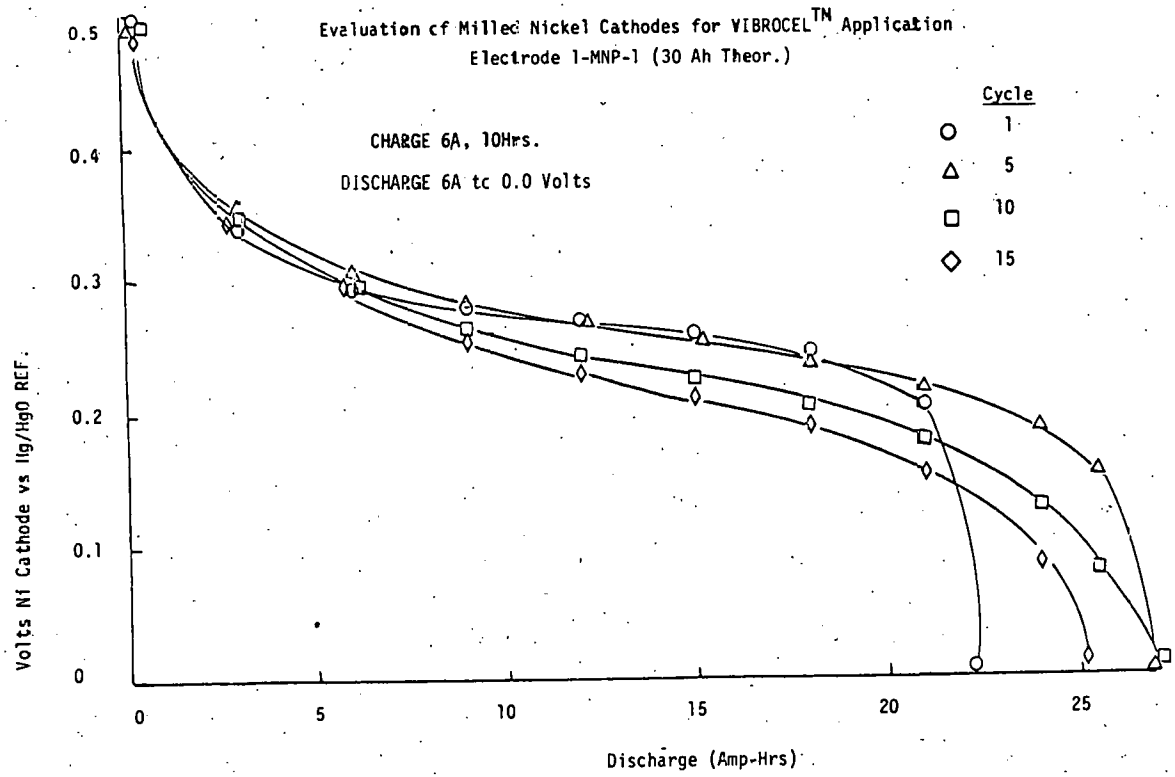
Evaluation of Milled Nickel Cathodes for VIBROCEL™ Application
Electrode 1-MNP-1 (30 Ah Theor.)
CHARGE 6A, 10Hrs.
DISCHARGE 6A to 0.0 Volts
Cycle
1
5
10
15
Volts Ni Cathode vs Hg/HgO REF.
0.5
0.4
0.3
0.2
0.1
0
0
5
10
15
20
25
Discharge (Amp-Hrs)

Figure 26

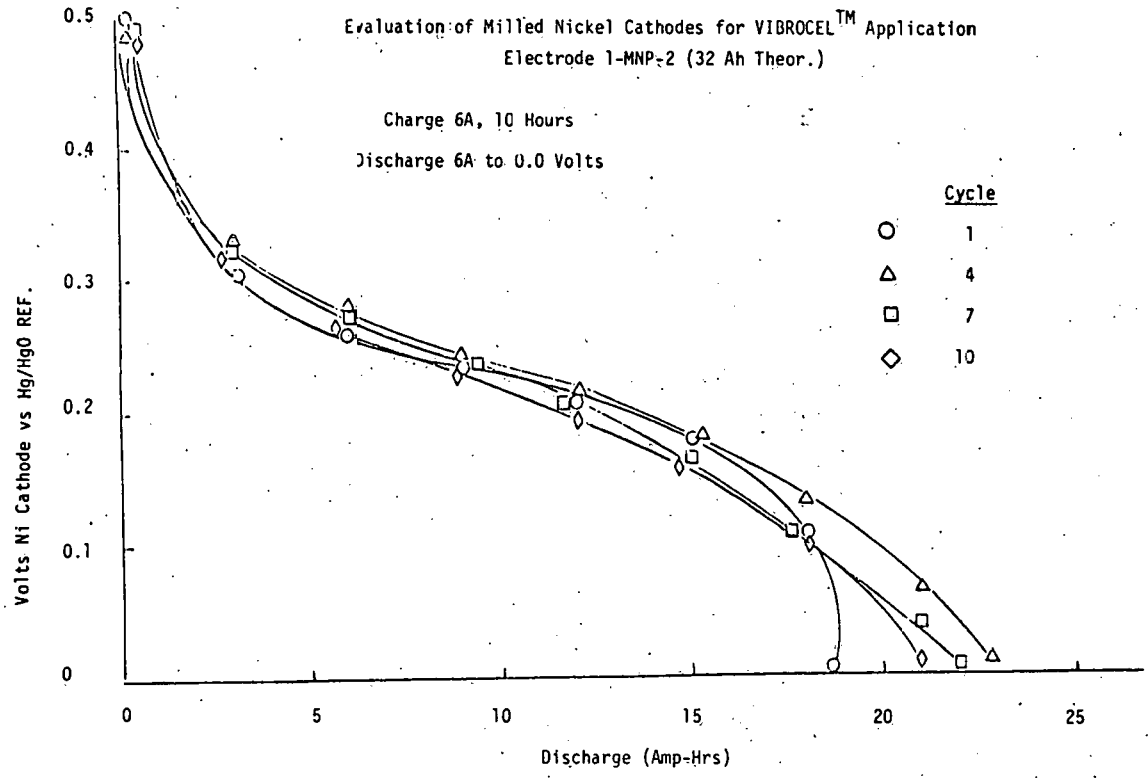
Evaluation of Milled Nickel Cathodes for VIBROCEL™ Application
Electrode 1-MNP-2 (32 Ah Theor.)
Charge 6A, 10 Hours
Discharge 6A to 0.0 Volts
Cycle
1
4
7
10
Volts Ni Cathode vs Hg/HgO REF.
0.5
0.4
0.3
0.2
0.1
0
0
5
10
15
20
25
Discharge (Amp-Hrs)

Figure 27

In order to minimize expansion of the active mass, an inert expander (TiO_2-Rutile grade) was added to the active material formulation. The active material formulation was:

Nickel Hydrate	76%
$Co(OH)_2$	3%
Carbon (Graphite)	15%
TFE	1%
TiO_2 (Rutile Grade)	5%
	100%

An electrode (2MNP1) measuring 8.7 in. H x 6.2 in. W x .124 in. T was fabricated using the 3 grid welded construction similar to electrode 1MNP1. Theoretical capacity of this electrode was 30.5 Ah. Again, the electrode was assembled in a 3 plate cell and tested in excess 6M KOH unsupported. Results are shown in Figure 28. The use of expander shows no improvement, and in fact, after 9 cycles, the electrode was removed from the cell and its thickness measured at .215 in.

Fabrication of plastic-bonded nickel electrodes must prevent this expansion in order to perform well in VIBROCEL™.

Evaluation of Milled Nickel Electrode 2-MNP-1
Active Material with 5% TiO_2 (Rutile)

CHARGE 6A, 10 Hours
DISCHARGE 6A to 0.0 Volts -vs- Hg/HgO

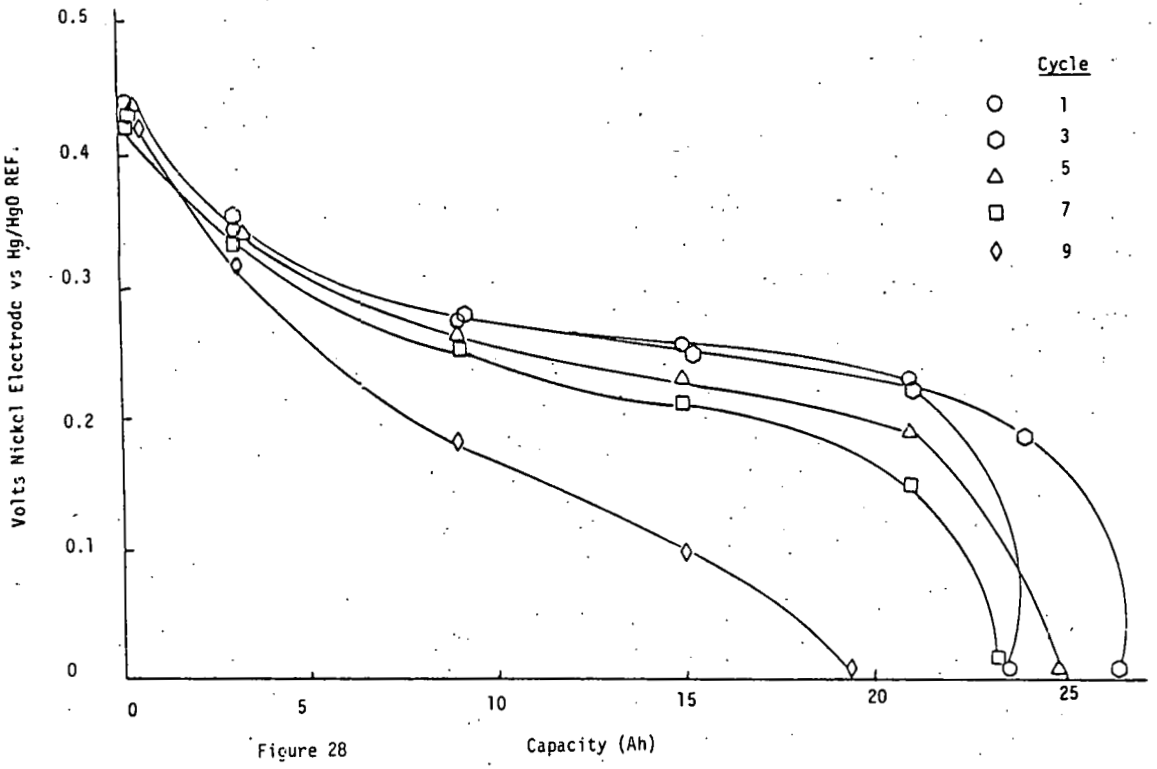

Figure 28

2.3 Basic Electrochemistry

Electrochemical studies in the VIBROCEL™ program are directed toward the improvement of Zn-electrode performance. Vibration of the Zn electrode eliminates dendrite formation, the main disadvantage of the Zn electrode in traditional Ni-Zn batteries. Problems which remain are the corrosion of active zinc (and the resultant loss in capacity) as well as the shedding of active zinc during charge under the influence of mechanical vibration. Electrochemical studies of the zinc electrode in VIBROCEL™ were in two main areas. These were:

- Corrosion of active zinc, and
- Electrodeposition of active zinc.

A) Corrosion and Self-Discharge of Zinc

Zn, deposited from alkaline solutions, is a very active material and tends to dissolve (or corrode). Investigation of corrosion of active zinc in KOH solutions indicates a dependence of the rate of dissolution of zinc on concentration of zincate.

Figure 29 depicts data of such measurements. It is evident that KOH solutions with extremely high concentration of zincate decreases the corrosion rate to a minimum (10 cm^3 of H_2 per gram of active zinc in 14 days at room temperature).

A second corrosion process which occurs is galvanic corrosion, i.e. the galvanic dissolution of zinc in contact with different substrate materials.

The rate of corrosion depends on the electrochemical difference between Zn and the more noble metals of the substrate. The ideal substrate would be one with a reversible potential close to zinc and with a high hydrogen overpotential.

Figure 30 depicts capacity losses for some substrate materials during 14 days of storage at room temperature. The performance of four different substrates is presented, with the lowest corrosion rate obtained being about 1 percent per day. It should be noted that for alloy 2 and alloy 3, the corrosion rate increased as cycling progressed, probably due to the deterioration of the plating used on these alloys.

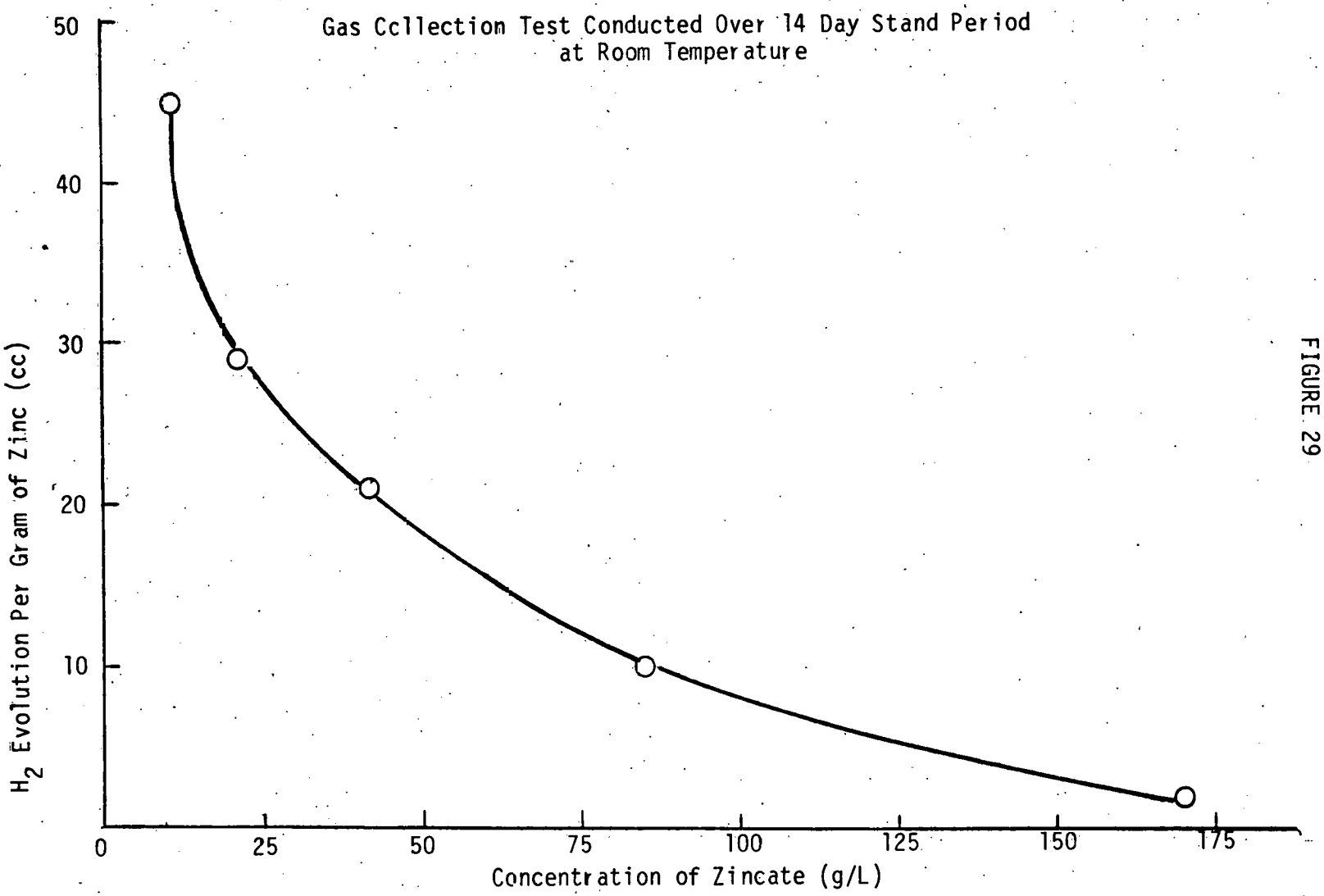
Gas Cclliection Test Conducted Over 14 Day Stand Period
at Room Temperature
H_2 Evolution Per Gram of Zinc (cc)
50
40
30
20
10
0
25
50
75
100
125
150
175
Concentration of Zincate (g/L)

FIGURE 29

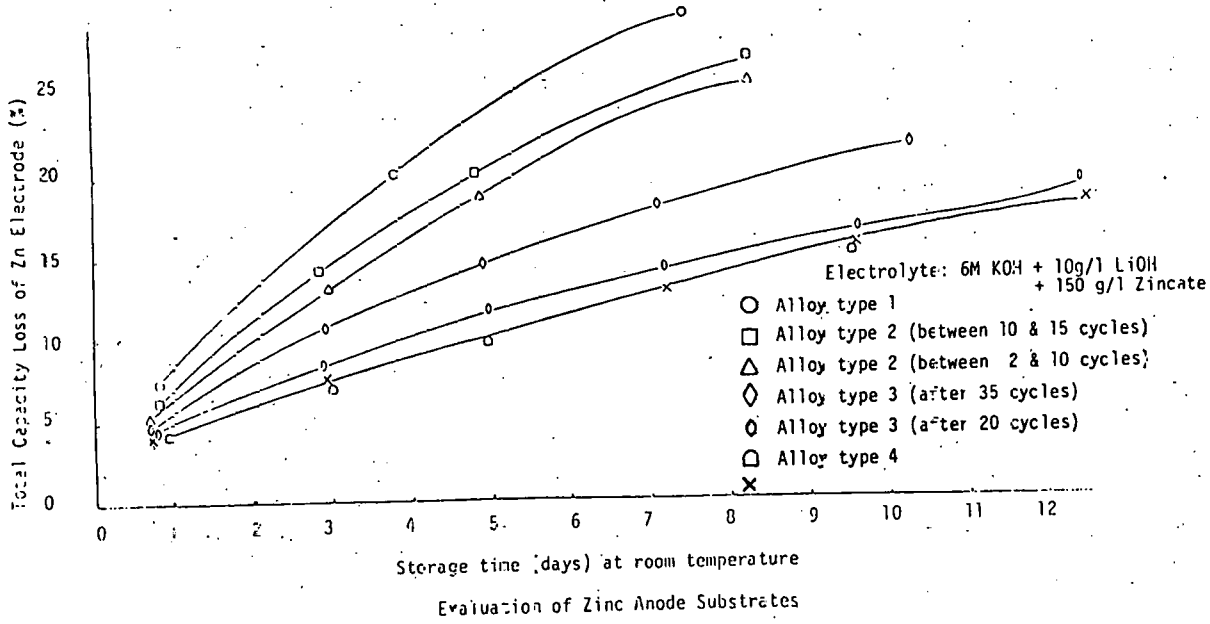

Evaluation of Zinc Anode Substrates

Figure 30

A further investigation was carried out on several other substrate materials, which exhibit hydrogen overpotentials close to the value of zinc when measured galvanostatically. Figure 31 illustrates the corrosion rate of one commonly available alloy, with, and without plating. Best results were obtained with plating type 2, however, it is interesting to note that the unplated material (alloy type 5) gave better results than with plating type 1. Some additional improvements were seen when alloy type 5 was used in the form of an expanded metal. Figure 32 depicts the performance of alloy type 5 as compared to some of the special alloys shown in Figure 30. The data indicates that alloy type 5, shows low corrosion rates, as in general is comparable in performance to some of the special alloys (ref Figure 30) tested.

B) Electrodeposition of Zn

Electrodeposition of zinc from alkaline solutions has been extensively studied in various aspects both from a fundamental interest in this complex system, and for the purpose of using Zn as a rechargeable electrode. In the latter case, the following was investigated:

1. Mechanism of dendrite formation,

2. Formation of slurry and porous deposits.

3. Mechanism of shape change.

4. Passivation of zinc-electrode.

The VIBROCEL™ is different from other secondary batteries in that it utilizes a completely soluble zinc electrode. Vibrating the zinc substrate in such a cell actually prevents dendrite formation, however, electrodeposition of zinc (without separators) from highly concentrated zincate solutions lead to very porous, mossy deposits. Such deposits are very active and tend to have higher rates of self-dissolution.

These mossy deposits also create the problem of shedding of zinc from the substrate surface (during vibration) and accumulation of zinc on the bottom of the cell. Accumulation of zinc can be avoided by galvanic dissolution with any number of materials (covering the bottom of the cell); for example, Ni, Cu, C, etc.

Zinc Capacity Loss on Alloy type 5 Substrate
(with and without plating)

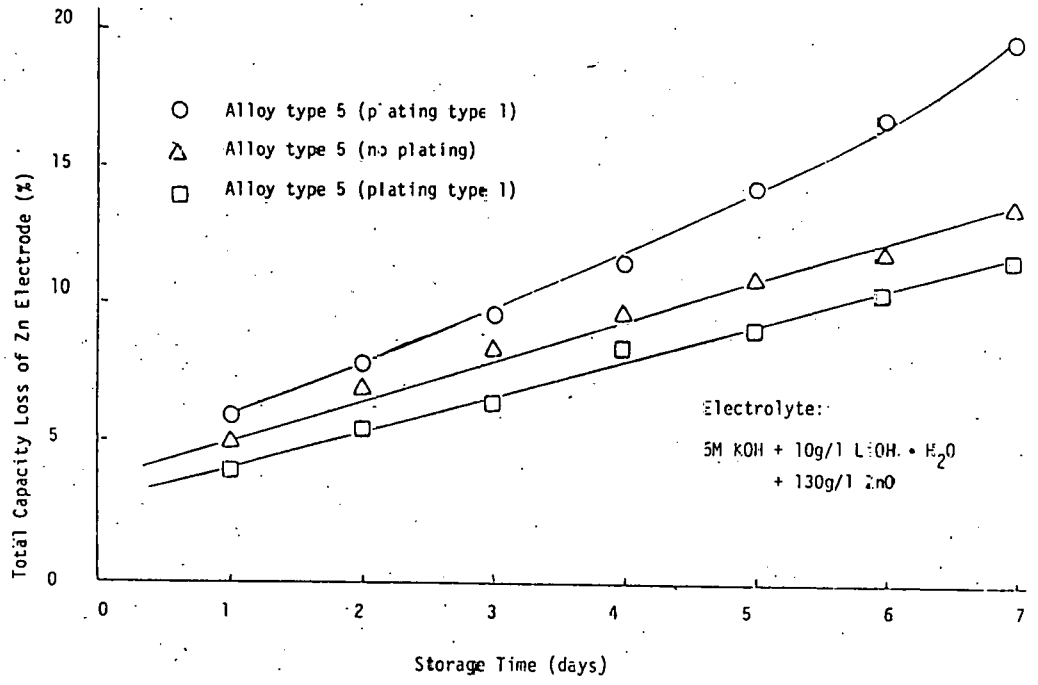

Figure 31

Effect of Substrate Materials on Zinc Capacity Loss

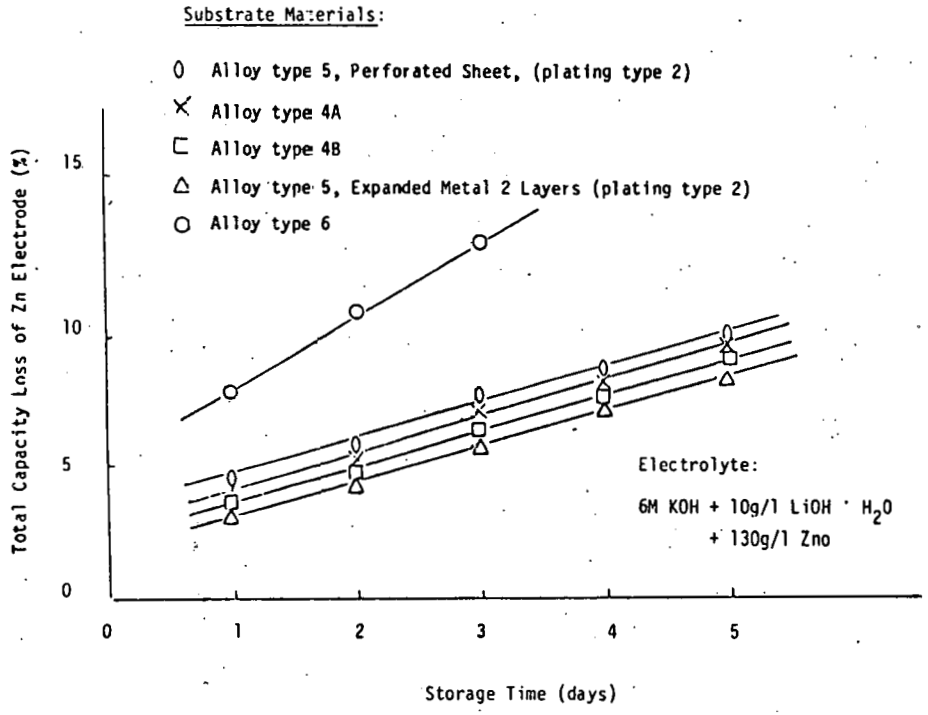

Figure 32

During cell operation, zinc concentration gradients may develop resulting in a ΔE from top to bottom of the electrode as follows:

$$\Delta E = E_2 - E_1 = \frac{RT}{2F} \ln A_2 - \frac{RT}{2F} \ln A_1$$

With certain assumptions, ΔE becomes about 10 mV for a 15-20 cm high electrode. This ΔE causes zinc to dissolve at the top and redeposit at the bottom, until $A_2 = A_1$. This condition is progressive, and after a number of cycles, a zinc "shape change" occurs. The calculations of this migration of zinc from the top to the bottom of the electrode were confirmed by experimental testing.

It is obvious that shape-change and its adverse effect on capacity are to be avoided. Various methods for improvement of the quality of zinc electrodeposition are suggested in the literature. One of these is the variation of plating current density. Experiments were run varying the plating current density, and it was found that improved quality zinc was deposited at certain current densities as compared to others. Other areas of improvement involve the use of special charging techniques as opposed to constant current D.C. charging. Here again, certain optimum conditions were found, which resulted in improved quality of plated zinc. This is illustrated in Figure 33, 34, 35 and 36. Figure 33 depicts a mossy type deposit often encountered when constant current D.C. charging is employed. Figure 34 on the other hand shows the same electrode when plated using one of the specialized charging techniques. Here the deposit is smooth, dense and crystalline in nature. Electrodes deposited with zinc, using these special techniques, occupy a much smaller volume and are approximately 80 percent of theoretical density. Figure 35 is a photograph of the surface of the electrode of Figure 34 with 50X magnification, showing the close packed, fine crystalline structure. As a comparison, the surface of the electrode of Figure 33 at 50X magnification is shown in Figure 36, illustrating the mossy non-crystalline nature of this surface.

We have also noticed a difference in performance of the densely deposited zinc as compared to the mossy type. This is shown in Figure 37 where curve No. 2 is the voltage of a 3-plate nickel zinc VIBROCEL™ using constant current D.C. charging, and a discharge current density of 14 ma/cm^2. The interelectrode spacing of this cell was fixed, so that a maximum of 5 Ah of zinc could only be deposited using constant current D.C. When the special charging technqiue was used, 7.5 to 8.0 Ah of zinc could be deposited, and cell polarization during discharge was reduced. Curve No. 1 shows the discharge of the cell at 14 ma/cm^2 (the same as curve No. 2), but with a higher capacity and voltage (than curve No. 2), with the denser zinc deposit. When the denser zinc was discharged at 21 ma/cm^2, cell voltage was at approximately the same level as the mossy zinc at 14 ma/cm^2, but again with an increased capacity. The denser zinc offers a possible increase in specific energy and volumetric energy if the same benefits are fully attainable in scaled-up cell and battery designs.

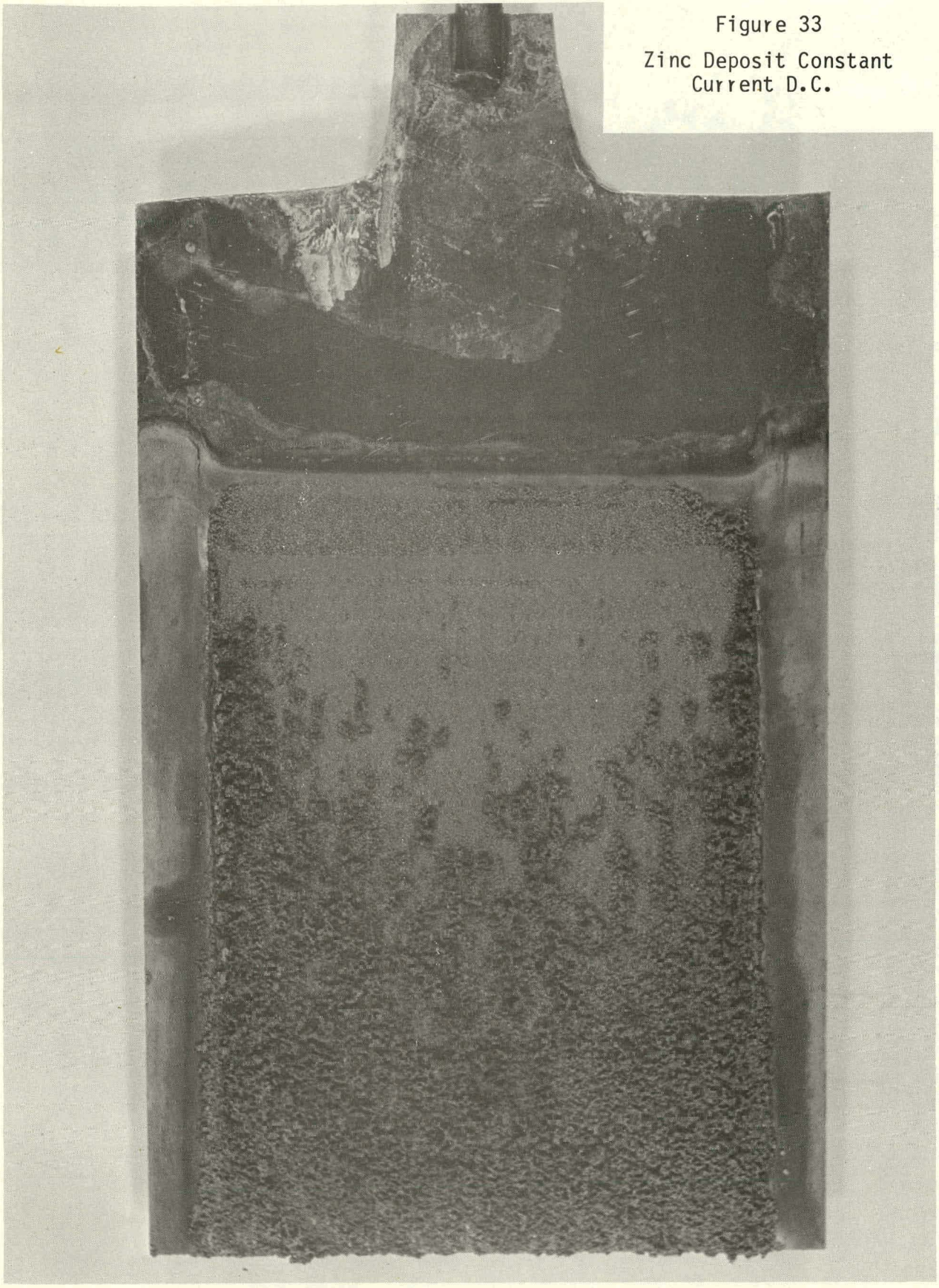

Figure 33

Zinc Deposit Constant
Current D.C.

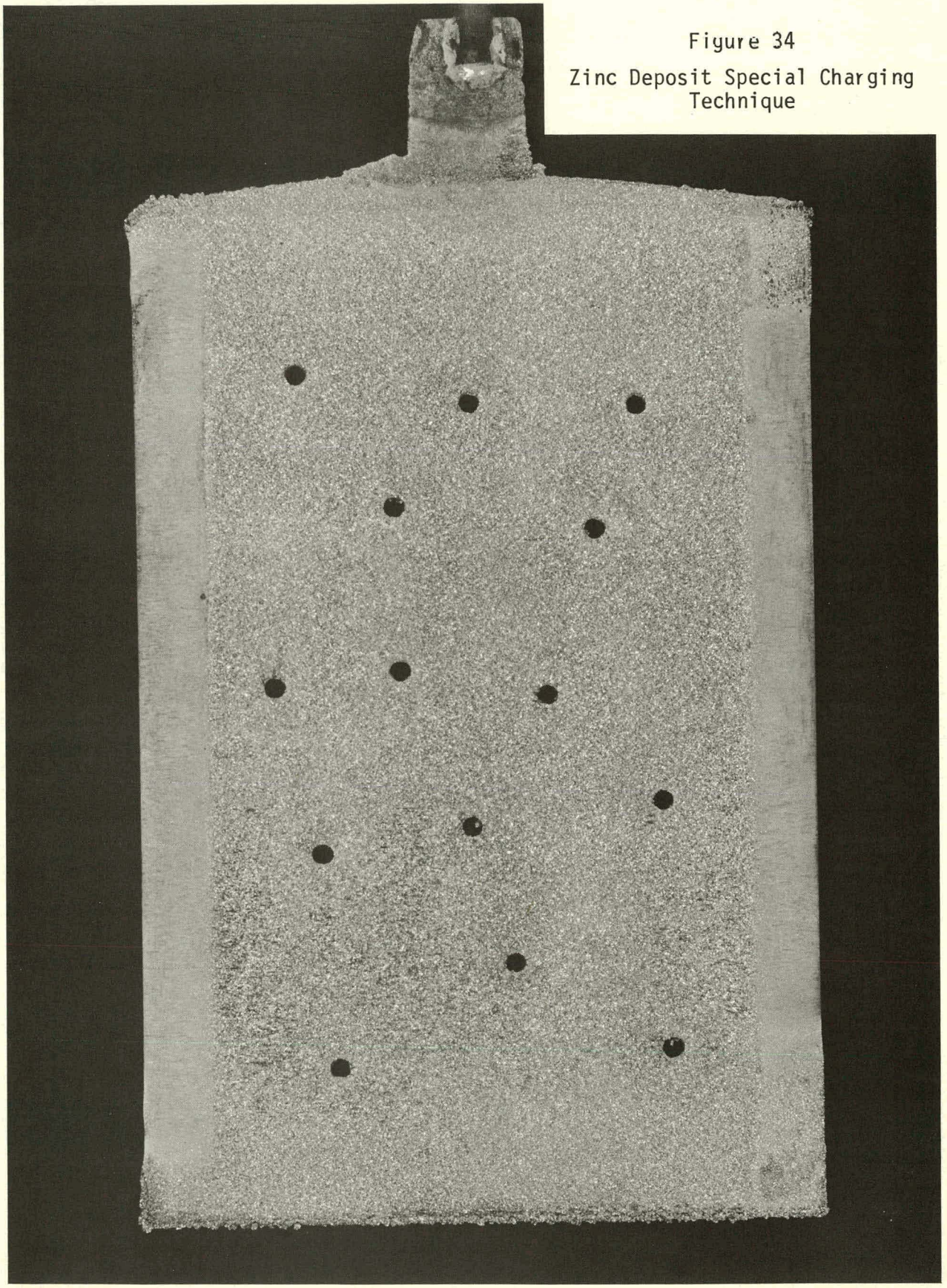

Figure 34

Zinc Deposit Special Charging Technique

Figure 35

Zinc Deposit 50X
Special Charging Technique

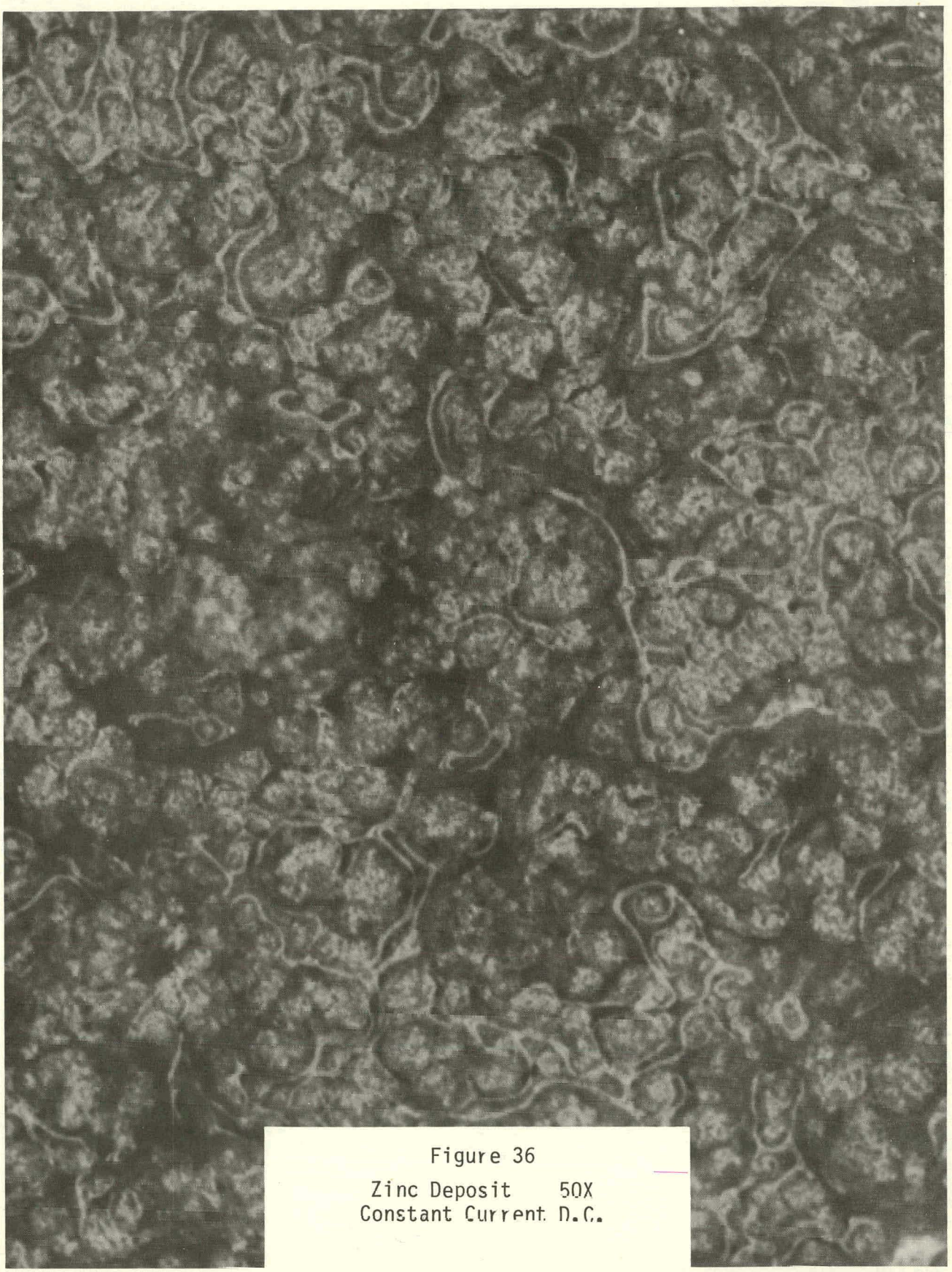

Figure 36

Zinc Deposit 50X
Constant Current D.C.

Performance of VIBROCEL™ with Specially Charged Zinc Electrodes

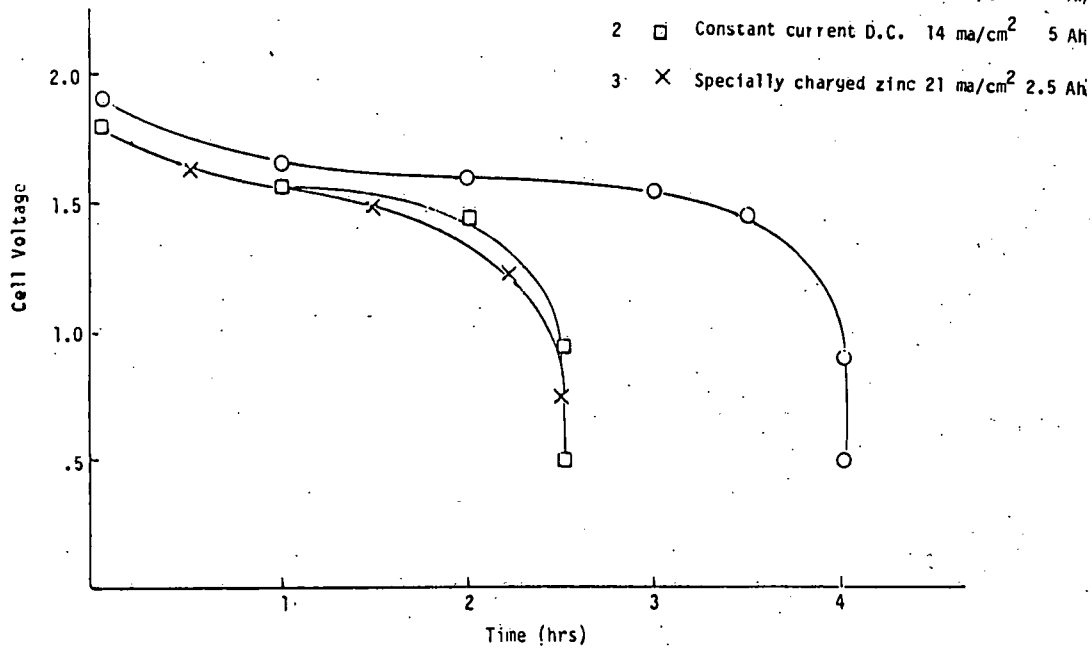

Figure 37

2.4 Reporting

Monthly reports have been prepared giving an update of technical progress for the periods:

April 15-May 31, 1979	No. 1
June 1-June 30, 1979	No. 2
July 1-July 31, 1979	No. 3

In addition, the Milestone Schedule and Status Report (DOE Form 535), the Manpower Management Report (DOE Form 534M), and Cost Management Report (DOE Form 533M) have been prepared for each of the first three reporting periods as well as the period Aug. 1-Aug. 31, 1979. This, "First Annual Report," provides a summary of technical progress for the three reporting periods above, as well as the period Aug. 1-Aug. 31, 1979.

APPENDIX A

DETAILED VIBROCEL™ DRAWINGS

DETAILED VIBROCEL™ DRAWINGS

Drawing No.	
EC-15588	VIBROCEL™ Test Cell 7-Plate
EC-15593	Cell Test Station for VIBROCEL™
EB-15569	Anode Electrode MS Size
EC-15567	VIBROCEL™ Container MS Size
EB-15568	Covers for VIBROCEL™ Test Cells
EB-15571	Double Plate Cathode for VIBROCEL™ 44-Ah
EA-15572	Netting for Double Plate Cathode "VIBROCEL™"
EB-15586	VIBROCEL™ Guide Rails
EB-15574	Negative Connector
EA-15575	Actuator
EA-15576	Shuttle
EA-15585	Eccentric Shaft
EA-15573	Positive Connector
EA-15578	Intercell Connector
EA-15579	Jam Nut
EA-15581	Stud
EA-15582	Spacer
EA-15583	Nut
EA-15584	Nut
EA-15580	Cover Clamp for VIBROCEL™ Cells
EA-15589	Cover Gasket for VIBROCEL™ Test Cells
EA-15587	Zinc Getter for VIBROCEL™
EA-15577	Vent Tube and Cap VIBROCEL™
EA-15570	Single Plate Cathode for VIBROCEL™ 22-Ah

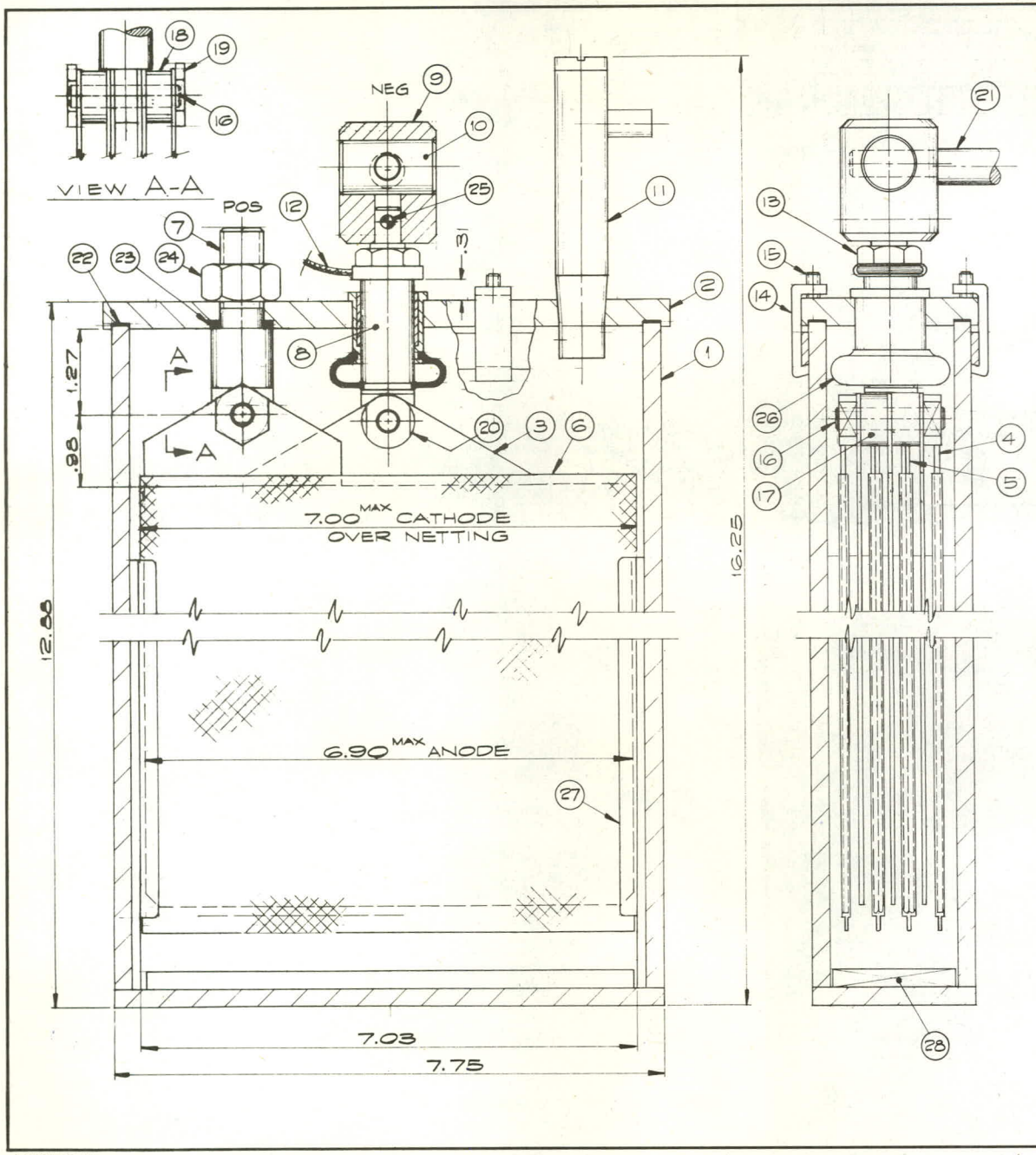

NO.	QTY	DESCRIPTION	DWG NO.	MATL
1	1	CONTAINER FIG.2	EC-15567	ACRYLIC
2	1	COVER FIG.2	EB-15568	"
3	3	ANODE	EB-15569	
4	2	SINGLE PL CATHODE	EA-15570	
5	2	DOUBLE PL CATHODE	EB-15571	
6	4	NETTING	EA-15572	POLYPROPYLENE
7	1	POS CONNECTOR FIG 2	EA-15573	CRS,NP
8	1	NEG CONNECTOR	EB-15574	"
9	1	ACTUATOR	EA-15575	ACRYLIC
10	1	SHUTTLE	EA-15576	RULON
11	1	VENT TUBE	EA-15577	ACRYLIC
12	1	INTERCELL CONN	EA-15578	COPPER
13	1	JAM NUT 5/8-18	EA-15579	CRS,NP
14	8	COVER CLAMP	EA-15580	"
15	8	SKT SET SCR #10-32x3/8,CUP PT		STL
16	2	STUD	EA-15581 FIG.2	CRS,NP
17	1	SPACER	EA-15582 FIG.2	"
18	2	SPACER	EA-15582 FIG.5	"
19	2	NUT	EA-15583	"
20	2	NUT	EA-15584 FIG.2	"
21	1	ECCENTRIC SHAFT	EA-15585 FIG.2	STL
22	1	GASKET	EA-15589 FIG.5	NEOPRENE
23	1	GASKET		"
24	1	HEX NUT 5/8-18		ST.
25	1	PIN .19 DIAx1.25		"
26	1	BELLOWS SEAL		NEOPRENE
27	2	GUIDE RAILS	EB-15586 FIG.1	ACRYLIC
28	1	ZINC GETTER	EA-15587	CARBON

EC-15588

INSPECTION SPECIFICATION

SEE EC-5593 FOR TEST STAND

THIS DWG SHOWS ASSY FOR 2.5MM PLATE GAP

REV.	DATE	ALTERATION	BY	APP.
A		REVISED & REDRAWN	JFL	

TITLE: "VIBROCEL" TEST CELL 7 PLATE ASSEMBLY

MATERIAL:

EXIDE INDUSTRIAL BATTERY DIVISION ESB INCORPORATED — Exide

ENGINEERING DEPT. - DESIGN DIVISION
HORSHAM, PA 19044

SCALE FULL DATE

DRAWN J.L.M.K.S CHKD. APPD.

THIS DWG. SUPERSEDES YARDLEY 6280-1000

EC-15588

MADE IN U. S. A.

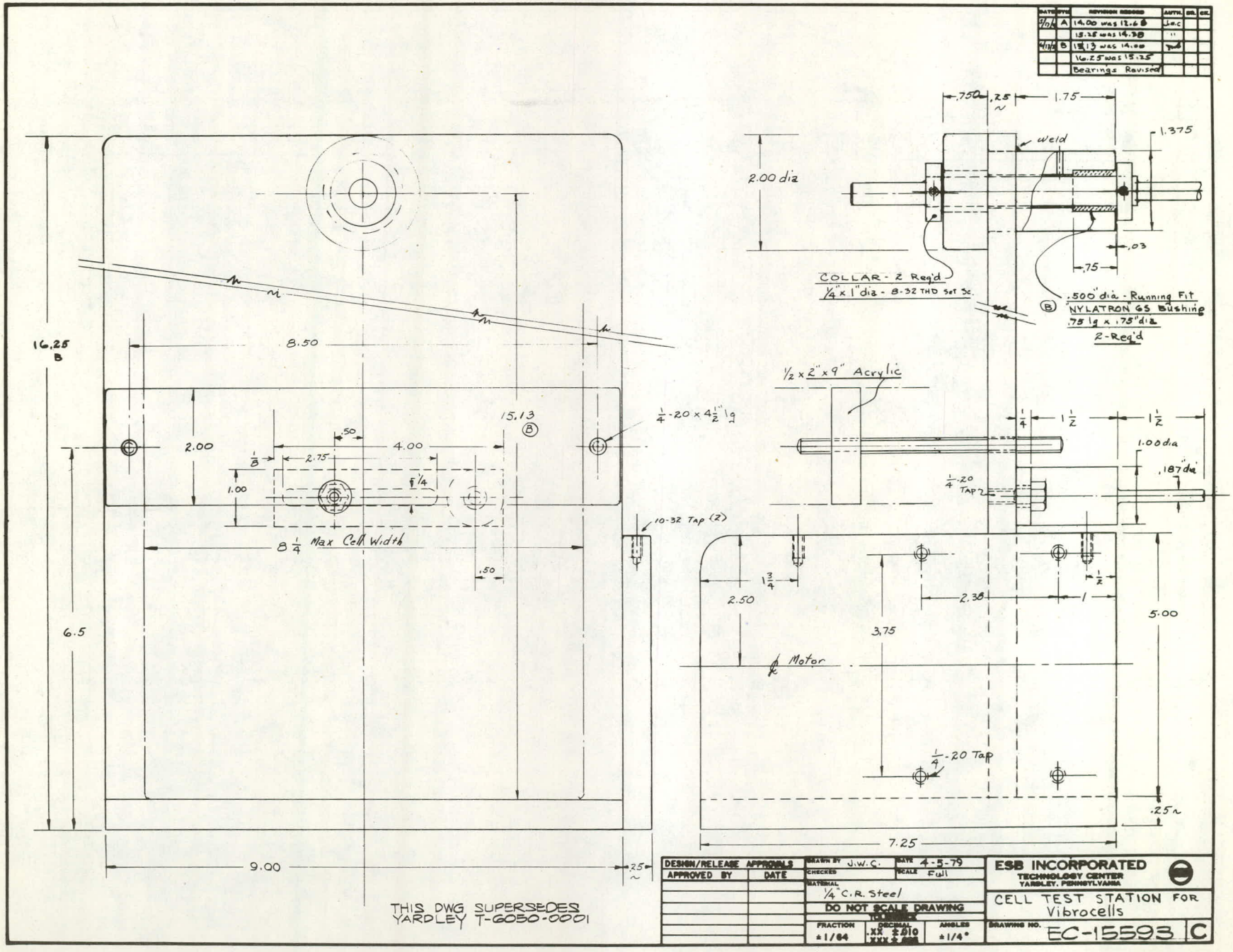
REVISION RECORD
A 14.00 was 12.68
15.25 was 14.38
B 15.13 was 14.00
16.25 was 15.25
Bearings Revised
16.25 B
8.50
2.00
.50
4.00
15.13 B
2.75
1.00
8 1/4 Max Cell Width
.50
6.5
9.00
.25
THIS DWG SUPERSEDES YARDLEY T-6050-0001
1/4-20 x 4 1/2" lg
10-32 Tap (2)
.750
.25
1.75
Weld
1.375
2.00 dia
.03
.75
COLLAR - 2 Req'd
1/4" x 1" dia - 8-32 THD Set Sc.
B .500" dia - Running Fit
NYLATRON GS Bushing
.75 lg x .175" dia
2-Req'd
1/2 x 2" x 9" Acrylic
1/4
1 1/2
1 1/2
1.00 dia
.187" dia
1/4-20 Tap 2
2.50
1 3/4
2.38
1
1/2
3.75
5.00
Motor
1/4-20 Tap
.25
7.25
DESIGN/RELEASE APPROVALS
APPROVED BY
DATE
DRAWN BY J.W.C.
DATE 4-5-79
CHECKED
SCALE Full
MATERIAL 1/4" C.R. Steel
DO NOT SCALE DRAWING
TOLERANCE
FRACTION ±1/64
DECIMAL .XX ±.010 .XXX ±.005
ANGLES ±1/4°
ESB INCORPORATED
TECHNOLOGY CENTER
YARDLEY, PENNSYLVANIA
CELL TEST STATION FOR Vibrocells
DRAWING NO. EC-15593 C

DATE	SYM	REVISION RECORD	AUTH.	DR.	CK.
3/6/80	A	ADDED TOL. TO 9.75 DIM.			

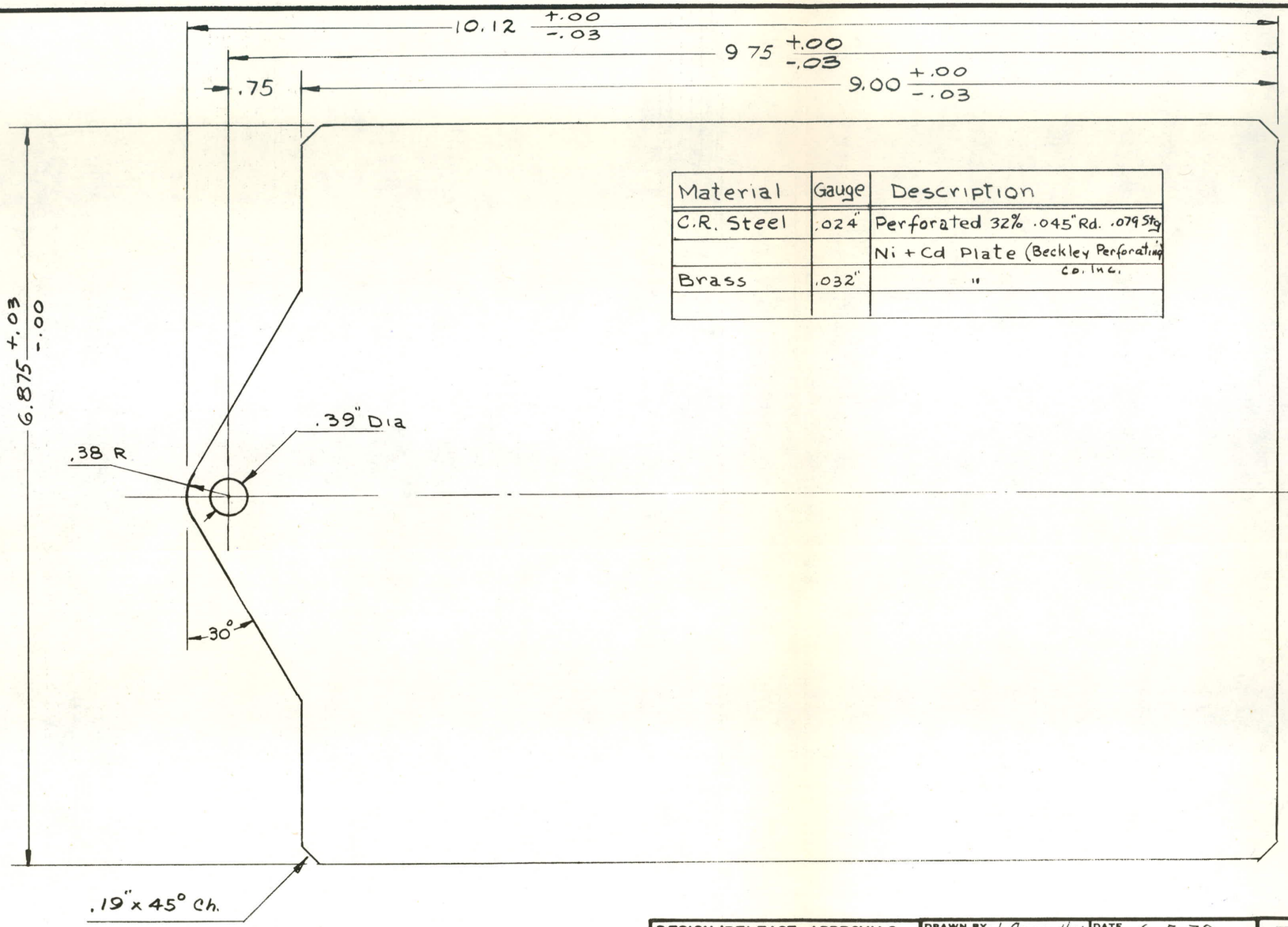

Material	Gauge	Description
C.R. Steel	.024"	Perforated 32% .045" Rd. .079 Stg
		Ni + Cd Plate (Beckley Perforating Co. Inc.
Brass	.032"	"

THIS DWG SUPERSEDES YARDLEY 6050-0101

DESIGN/RELEASE APPROVALS	
APPROVED BY	DATE

DRAWN BY J. Consolloy DATE 6-5-79
CHECKED SCALE Full
MATERIAL AS NOTED
DO NOT SCALE DRAWING
TOLERANCE

FRACTION	DECIMAL	ANGLES
±1/64	.XX ±.010 .XXX ±.005	±1/4°

ESB INCORPORATED
TECHNOLOGY CENTER
YARDLEY, PENNSYLVANIA

ANODE ELECTRODE
M·S SIZE

DRAWING NO. EB-15569 B

DATE	SYM	REVISION RECORD	AUTH.	DR.	CK.

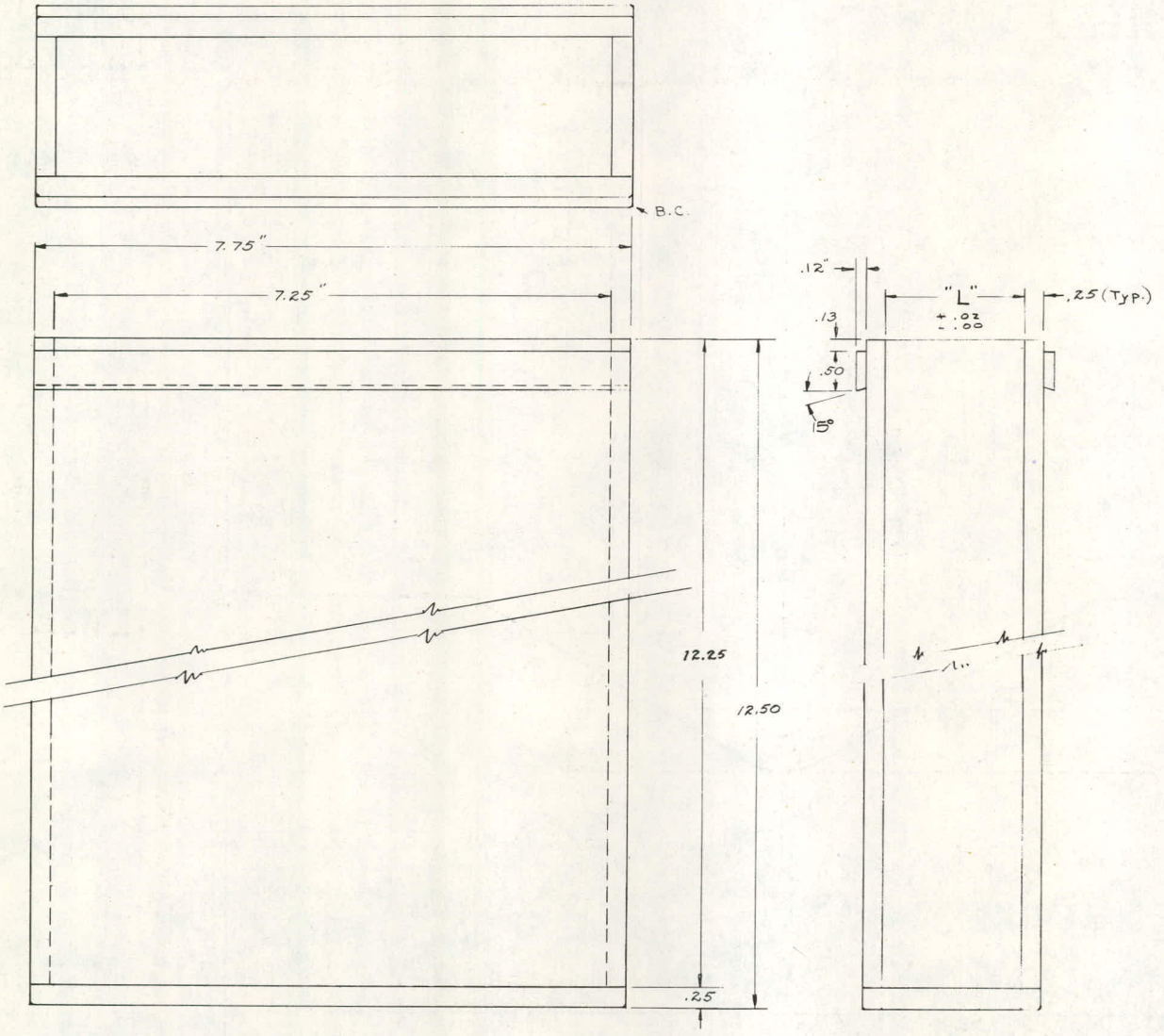

FIG	L +.02 -.00	NO. OF PLATES AND GAP, (MM)
1	1.32	7 (1.5)
2	1.56	7 (2.5)
3	1.79	7 (3.5)
4	3.34	15 (2.5)

THIS DWG SUPERSEDES YARDLEY 6050-0102

DESIGN/RELEASE APPROVALS	
APPROVED BY	DATE

DRAWN BY J.W.C. DATE 6/5/79
CHECKED SCALE —
MATERIAL Acrylic Sheet
DO NOT SCALE DRAWING
TOLERANCE
FRACTION ±1/64 DECIMAL .XX ±.010 .XXX ±.005 ANGLES ±1/4°

ESB INCORPORATED
TECHNOLOGY CENTER
YARDLEY, PENNSYLVANIA

VIBROCEL CONTAINER
M-S SIZE

DRAWING NO. EC-15567 C

DATE	SYM	REVISION RECORD	AUTH.	DR.	CK.
8/6/80	A	GENERAL REVISIONS	JFL		

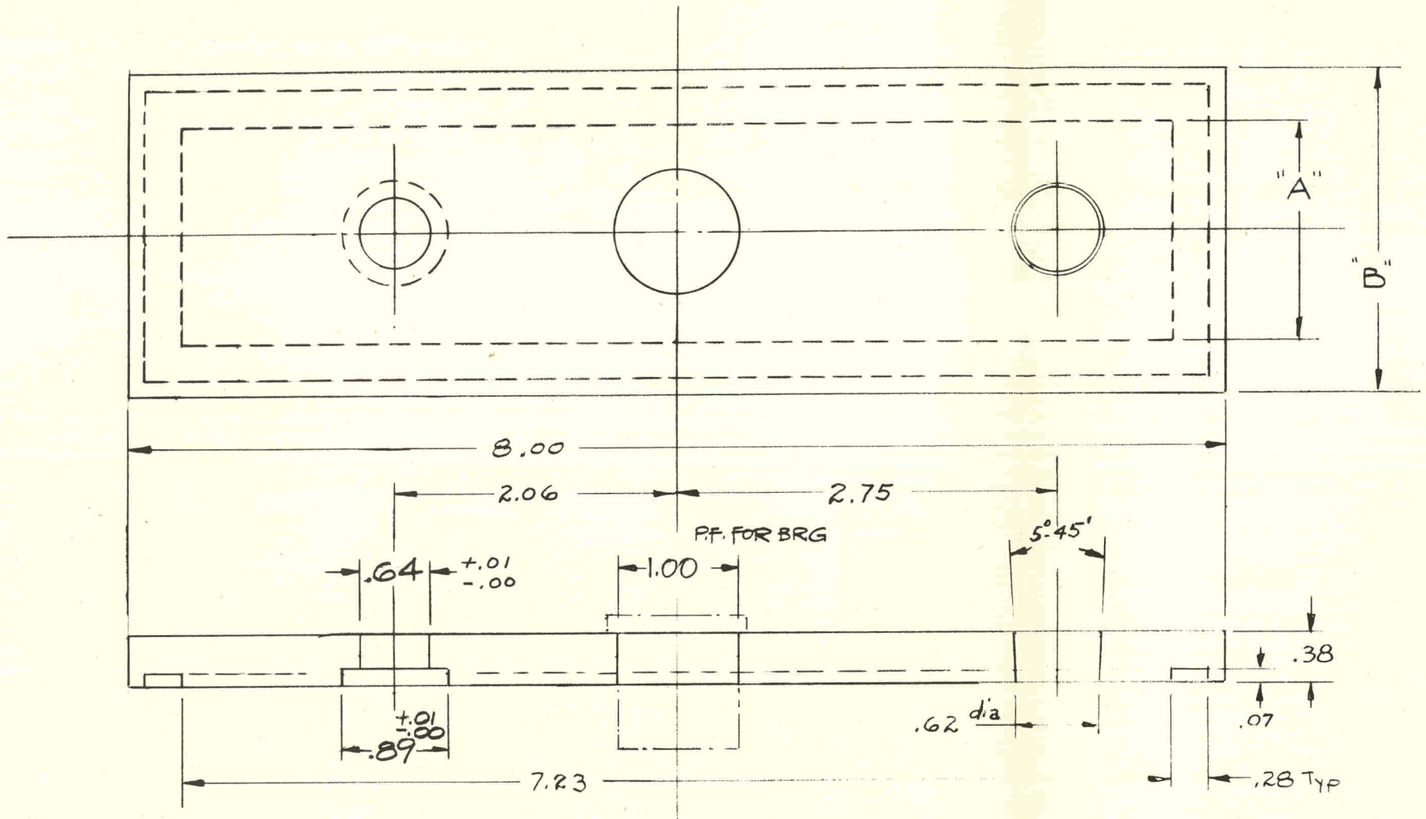

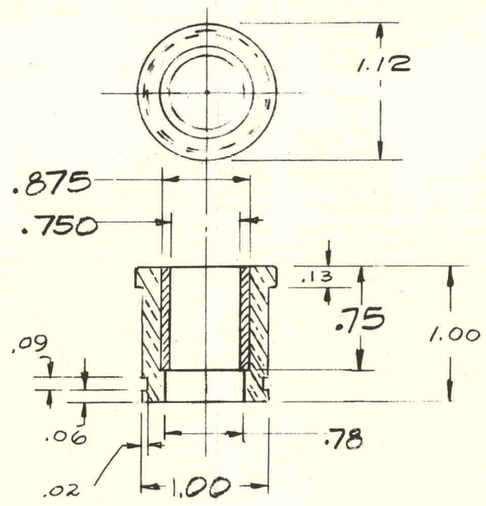

LINEAR BEARING

Mat.- Bearing - TFE or Nyloil

Bushing Holder - Acrylic

Cement to Cover

FIG	NO. OF PLATES AND GAP, (MM)	A	B
1	7 (1.5)	1.30	2.09
2	7 (2.5)	1.53	2.30
3	7 (3.5)	1.77	2.54
4	15 (2.5)	3.32	4.09

THIS DWG SUPERSEDES
YARDLEY 6050-0103

DESIGN/RELEASE APPROVALS	
APPROVED BY	DATE

DRAWN BY J.W.C. DATE 6-12-79

CHECKED SCALE Full

MATERIAL Acrylic

DO NOT SCALE DRAWING

TOLERANCE

FRACTION	DECIMAL	ANGLES
±1/64	.XX ±.010 .XXX ±.005	±1/4°

ESB INCORPORATED
TECHNOLOGY CENTER
YARDLEY, PENNSYLVANIA

COVERS FOR "VIBROCEL" TEST CELLS

DRAWING NO. 6[illegible] EB-15568 B

DATE	SYM	REVISION RECORD	AUTH.	DR.	CK.
12/4	A	WAS CONWED	V.S	J.C	
		15x15 Strands/inch			
		.030 thk - 50-60 lbs/sq in			
3/3/80	B	MATL WAS VEXAR, ADDED		JPL	
		(2) RIVETS @ TAB			

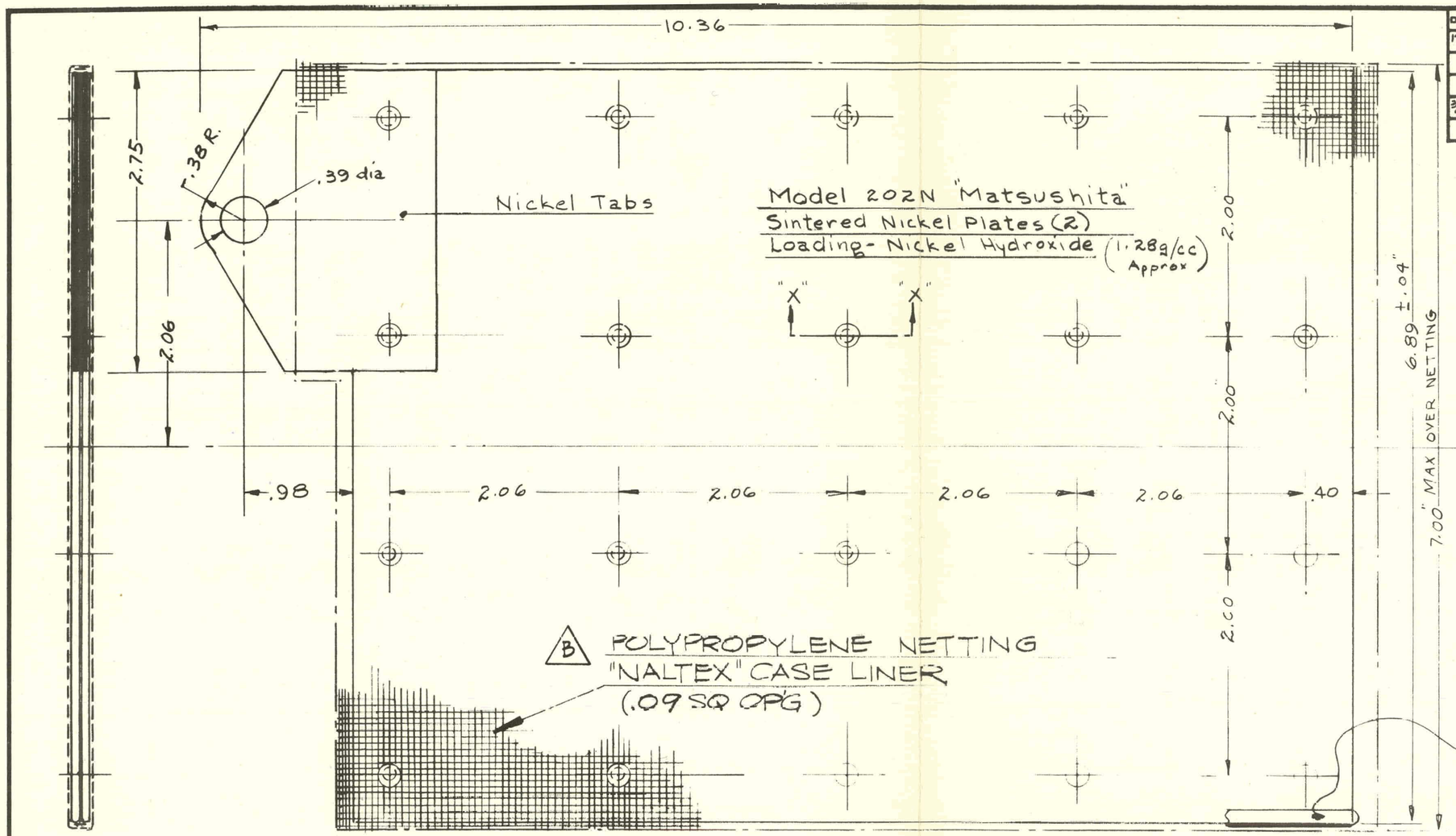

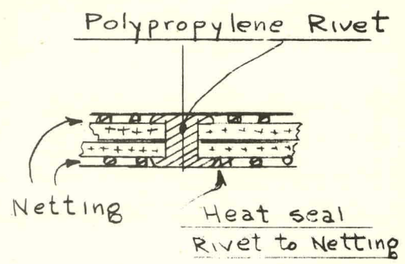

SECTION "XX"

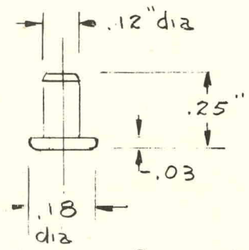

Rivet 20 Req'd

Mat.- Polypropylene

Option - TFE Tape ½" wide with silicone adhesive as aid in putting net & sleeve over double plates.

THIS DWG SUPERSEDES YARDLEY 6050-0104

DESIGN/RELEASE APPROVALS	
APPROVED BY	DATE

DRAWN BY J. Consolley	DATE 7-13-79
CHECKED	SCALE Full
MATERIAL As Specified	
DO NOT SCALE DRAWING	
TOLERANCE	

FRACTION	DECIMAL	ANGLES
±1/64	.XX ±.010 .XXX ±.005	±1/4°

ESB INCORPORATED
TECHNOLOGY CENTER
YARDLEY, PENNSYLVANIA

DOUBLE PLATE CATHODE (4)
FOR VIBROCEL 44AH

DRAWING NO. EB-15571 B

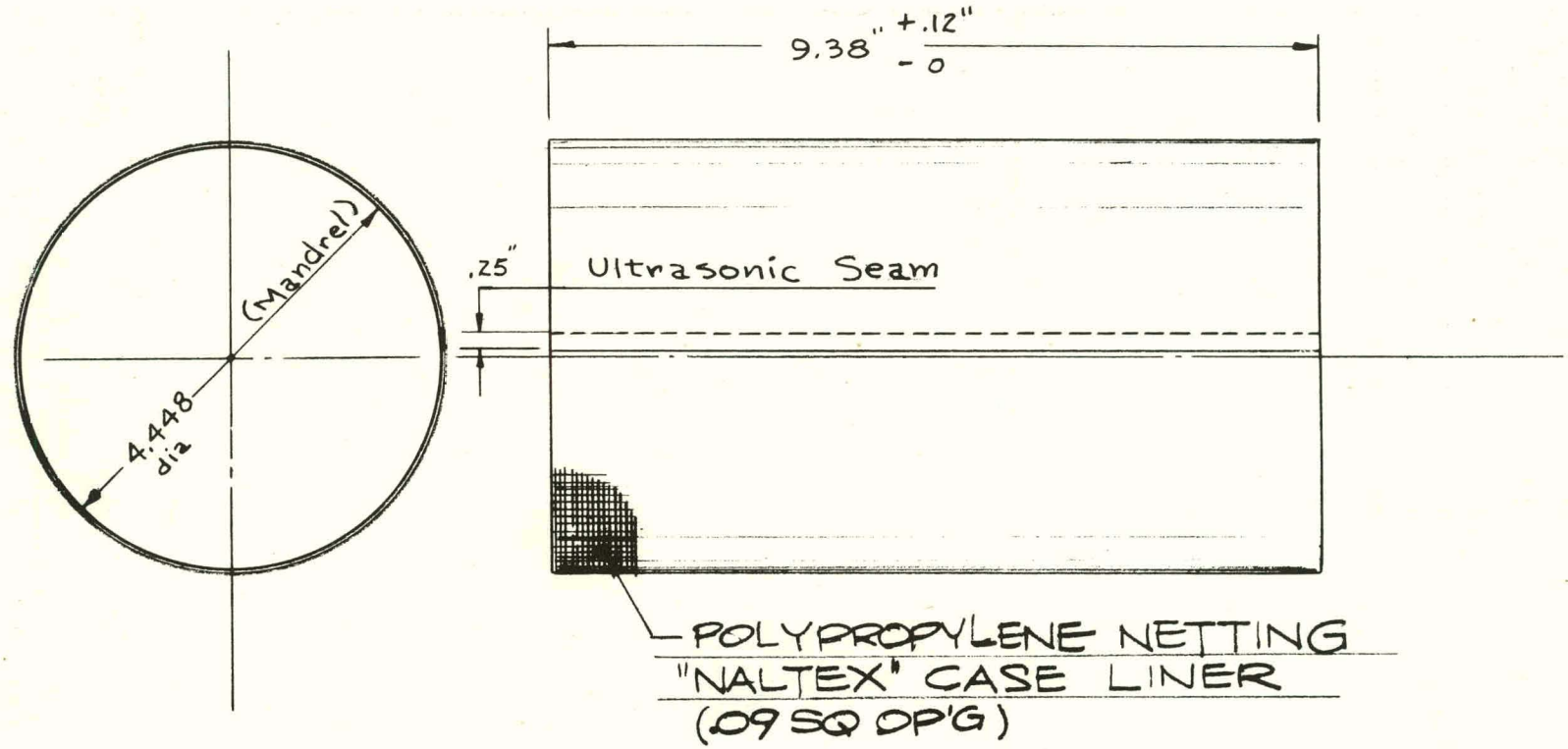

THIS DWG SUPERSEDES YARDLEY G050-0105

SYM	DATE	REVISION	CK
A	12/4/79	was Conwed Netting	V.S
	Jan 80	18x18/in - Polypropylene	
		Wt - 50-60#/MSF	
B	3/3/80	MATL WAS VEXAR	JFL

DRAWN BY J.W.C | DATE 7-13-79
CHECKED | SCALE ~
MATERIAL: As Noted
DO NOT SCALE DRAWING
TOLERANCE

FRACTION	DECIMAL	ANGLES
±1/64	.XX ±.010 .XXX ±.005	±1/4°

ESB INCORPORATED
TECHNOLOGY CENTER
YARDLEY, PENNSYLVANIA

NETTING FOR DOUBLE PLATE CATHODE "VIBROCEL" (5)

DRAWING NO. EA-15572 A

DATE	SYM.	REVISION RECORD	AUTH.	DR.	CK.
8/20/79	A	.230 was .206"	J.W.C		
		.086 was .098			

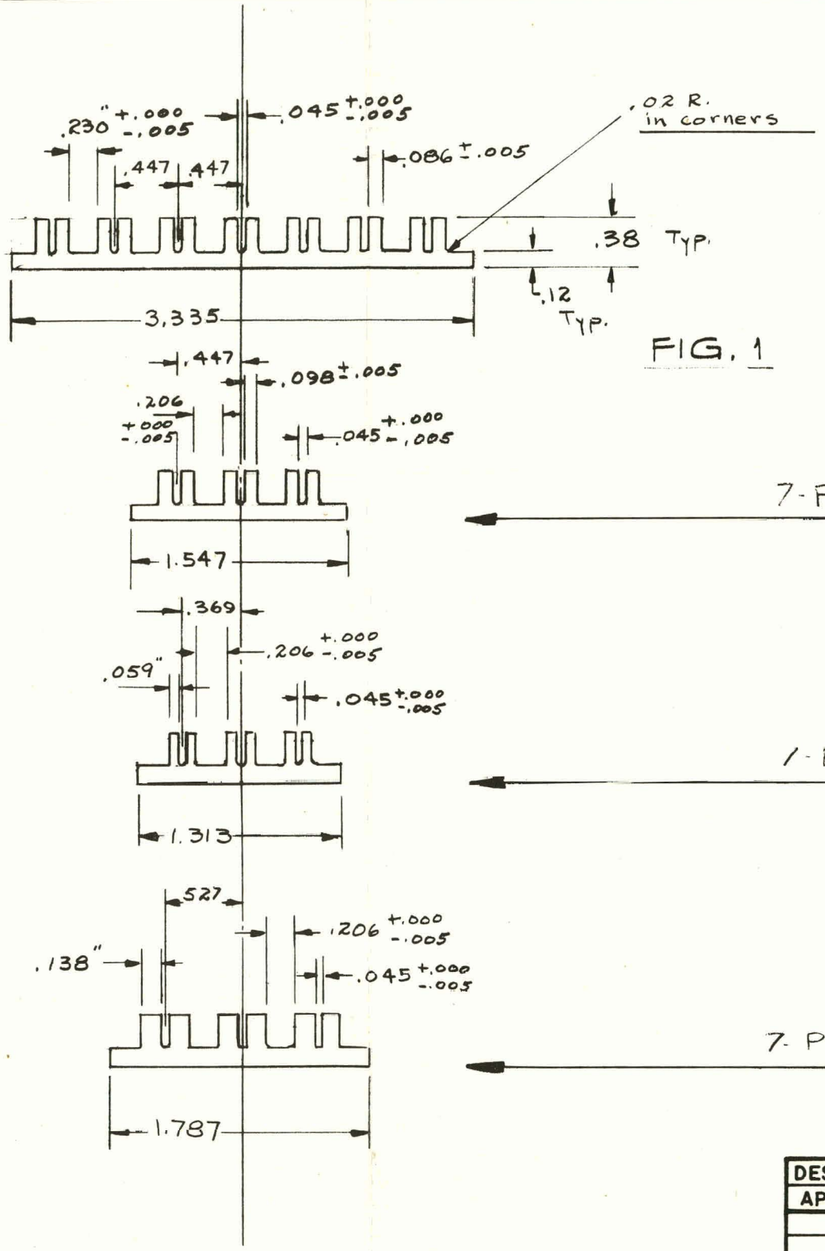

FIG. 1

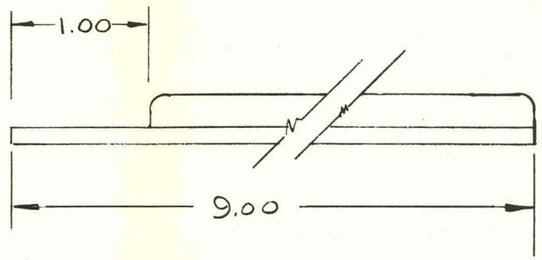

TYP SIDE VIEW
ALL FIG.

15 Plate 2.5mm Spacing
2-Req'd/Set

7-Plate 2.5mm Spacing

FIG. 2

7-Plate 1.5mm Spacing

FIG. 3

7-Plate 3.5mm Spacing

FIG. 4

THIS DWG SUPERSEDES
YARDLEY 6050-0106

DESIGN/RELEASE APPROVALS	
APPROVED BY	DATE

DRAWN BY J.W.C	DATE 6-8-79
CHECKED	SCALE Full
MATERIAL: AS SPECIFIED	
DO NOT SCALE DRAWING	
TOLERANCE	
FRACTION ±1/64	DECIMAL .XX ±.010 .XXX ±.005
	ANGLES ±1/4°

ESB INCORPORATED
TECHNOLOGY CENTER
YARDLEY, PENNSYLVANIA

VIBROCEL GUIDE RAILS

DRAWING NO. EB-15586 B

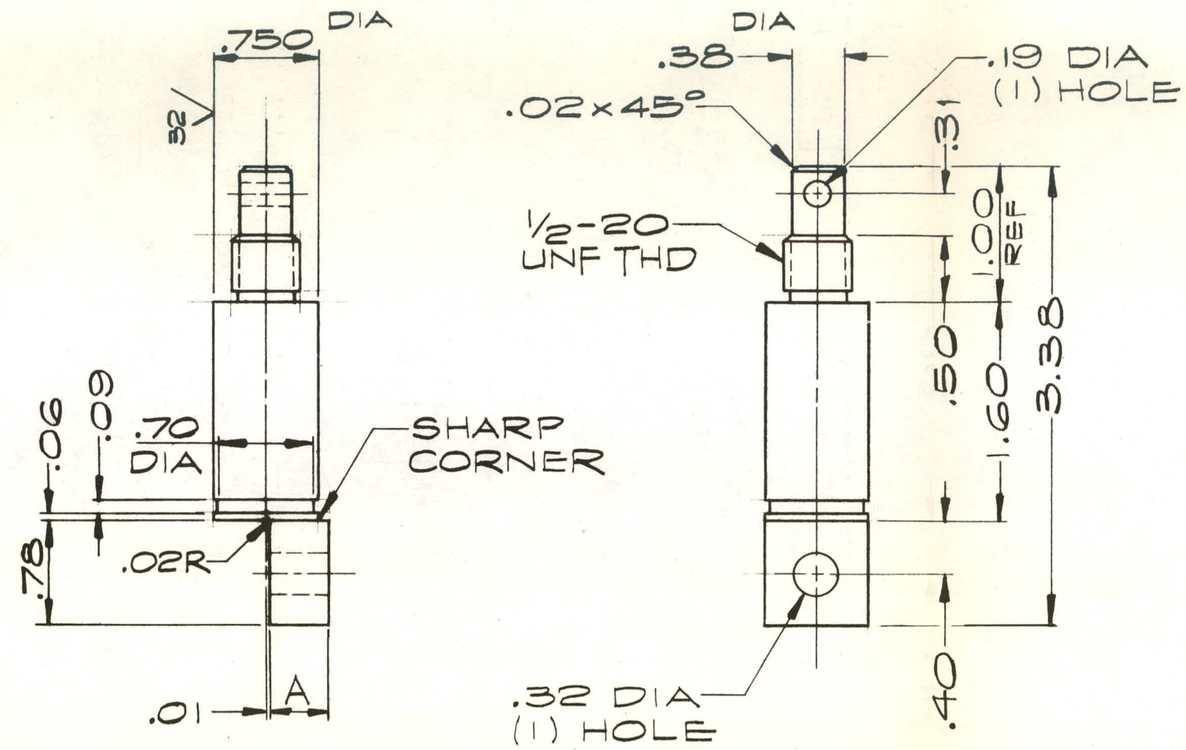

FIG NO.	PLATE GAP, MM	A ±.005
1	1.5	.344
2	2.5	.422
3	3.5	.502

INSPECTION SPECIFICATION

MATL: C.R.S.

FINISH: NICKEL PLATE

TOLERANCE

.XX	±.01
.XXX	±.005

REV.	DATE	ALTERATION	BY	APP.

TITLE: NEGATIVE CONNECTOR

MATERIAL: AS NOTED

EXIDE POWER SYSTEMS DIVISION
ESB INCORPORATED
ENGINEERING DEPT. – DESIGN DIVISION
HORSHAM, PA. 19044

SCALE FULL DATE

DRAWN J.L.M.K.S CHKD. APPD.

THIS DWG. SUPERSEDES

EB-15574

MADE IN U. S. A.

TOLERANCE
±.01 UNLESS NOTED OTHERWISE

EA-15575

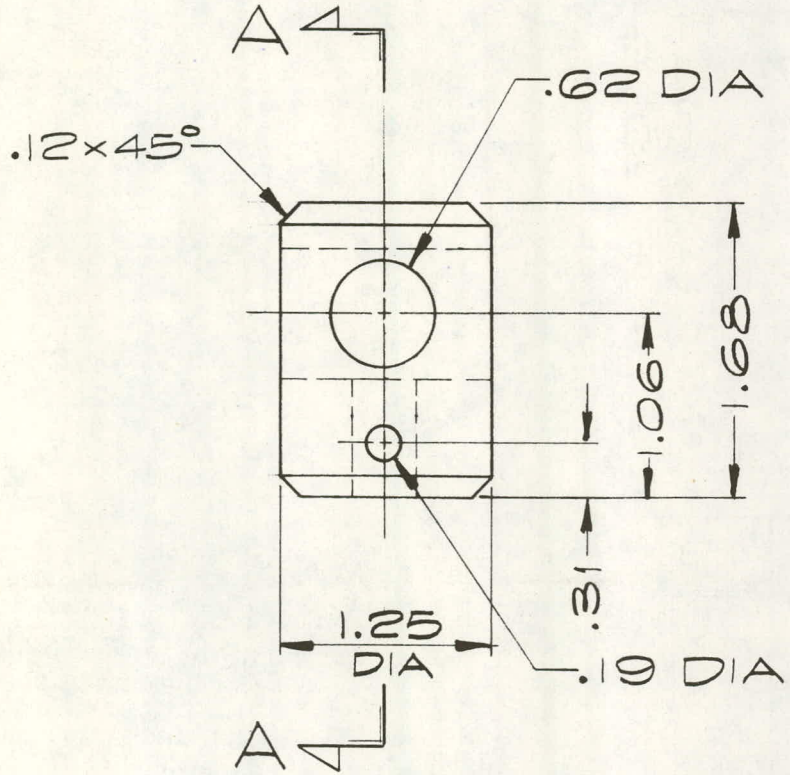

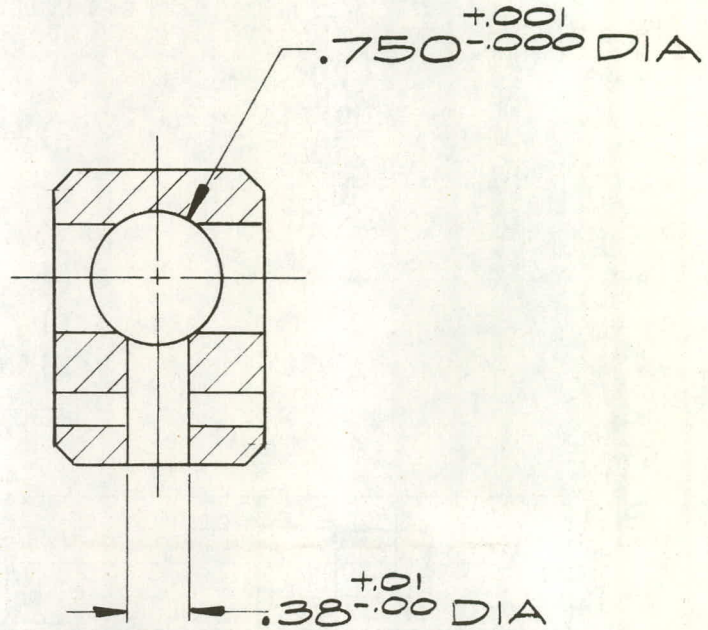

SECTION A-A

MATL: ACRYLIC

ACTUATOR

EXIDE POWER SYSTEMS DIVISION
ESB INCORPORATED
ENGINEERING DEPT.– DESIGN DIVISION
PHILADELPHIA, PA. 19120
SCALE FULL DATE
DRAWN J.LMKS CHKD. APPD.

REV.	DATE	ALTERATION	BY	APP.

THIS DWG. SUPERSEDES
EA-15575
MADE IN U. S. A.

S. & M. H. 1-77

EA-15576

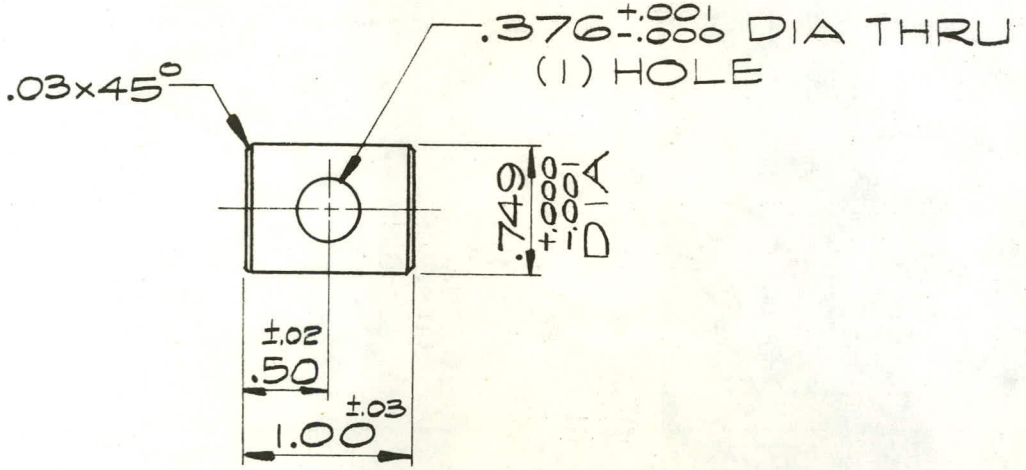

MATL : NYLON OR TEFLON

SHUTTLE

EXIDE POWER SYSTEMS DIVISION
ESB INCORPORATED
ENGINEERING DEPT. – DESIGN DIVISION
PHILADELPHIA, PA. 19120

SCALE FULL DATE

DRAWN J.LMKS CHKD. APPD.

REV.	DATE	ALTERATION	BY	APP.

THIS DWG. SUPERSEDES

EA-15576

MADE IN U. S. A.

S. & M. H. 1-77

EA-15585

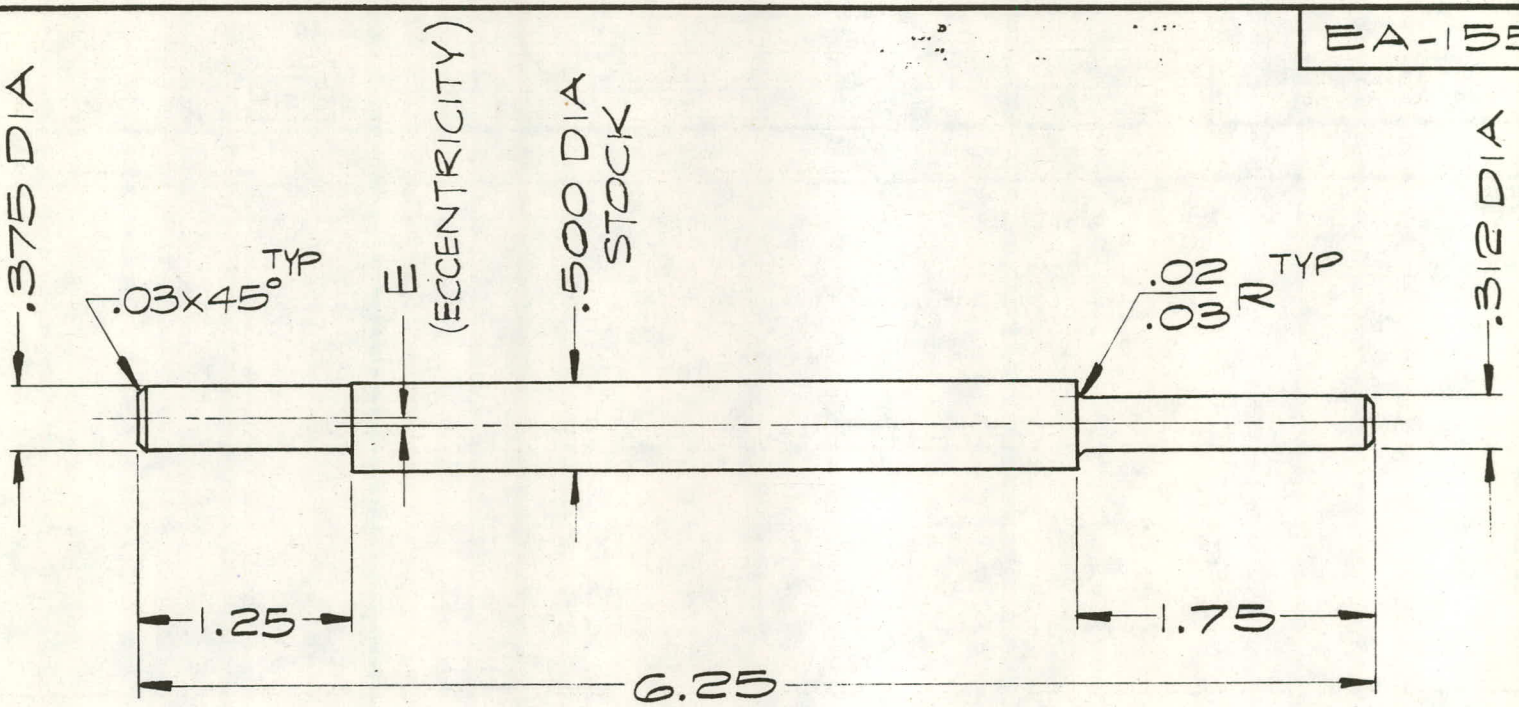

MATL: 1025 OR 1045
T.I.G & P STOCK

FIG. NO.	E ±.005
1	.035
2	.045
3	.060

TOLERANCE

.XX	±.02
.XXX	±.005

ECCENTRIC SHAFT

EXIDE POWER SYSTEMS DIVISION
ESB INCORPORATED
ENGINEERING DEPT. – DESIGN DIVISION
PHILADELPHIA, PA. 19120

SCALE DATE

DRAWN CHKD. APPD.

REV.	DATE	ALTERATION	BY	APP.

THIS DWG. SUPERSEDES

EA-15585

MADE IN U. S. A.

*, O. & M. H. 1-77

EA-15573

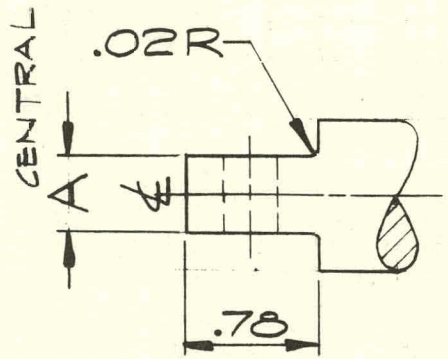

FIG NO.	PLATE GAP, MM	$A^{\pm.005}$
1	1.5	.344
2	2.5	.422
3	3.5	.502

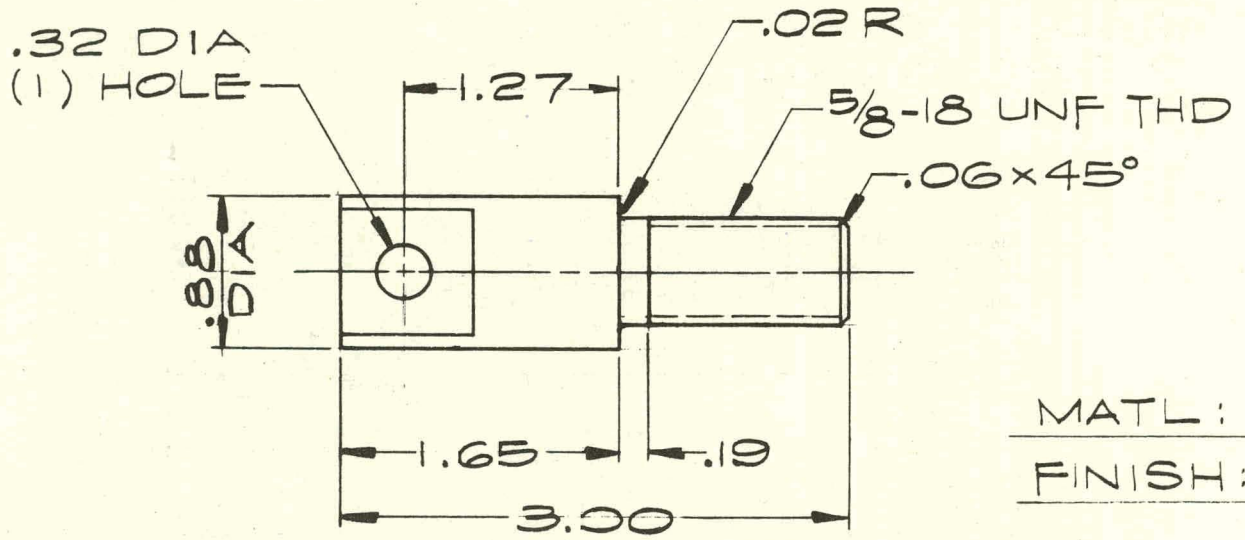

MATL: C.R.S.

FINISH: NKL PL

TOLERANCE

±.01 UNLESS NOTED OTHERWISE

POSITIVE CONNECTOR

EXIDE POWER SYSTEMS DIVISION
ESB INCORPORATED
ENGINEERING DEPT. – DESIGN DIVISION
PHILADELPHIA, PA. 19120

SCALE FULL DATE

DRAWN J.LMKS CHKD. APPD.

REV.	DATE	ALTERATION	BY	APP.

THIS DWG. SUPERSEDES

EA-15573

MADE IN U. S. A.

S. & M. H. 1-77

EA-15578

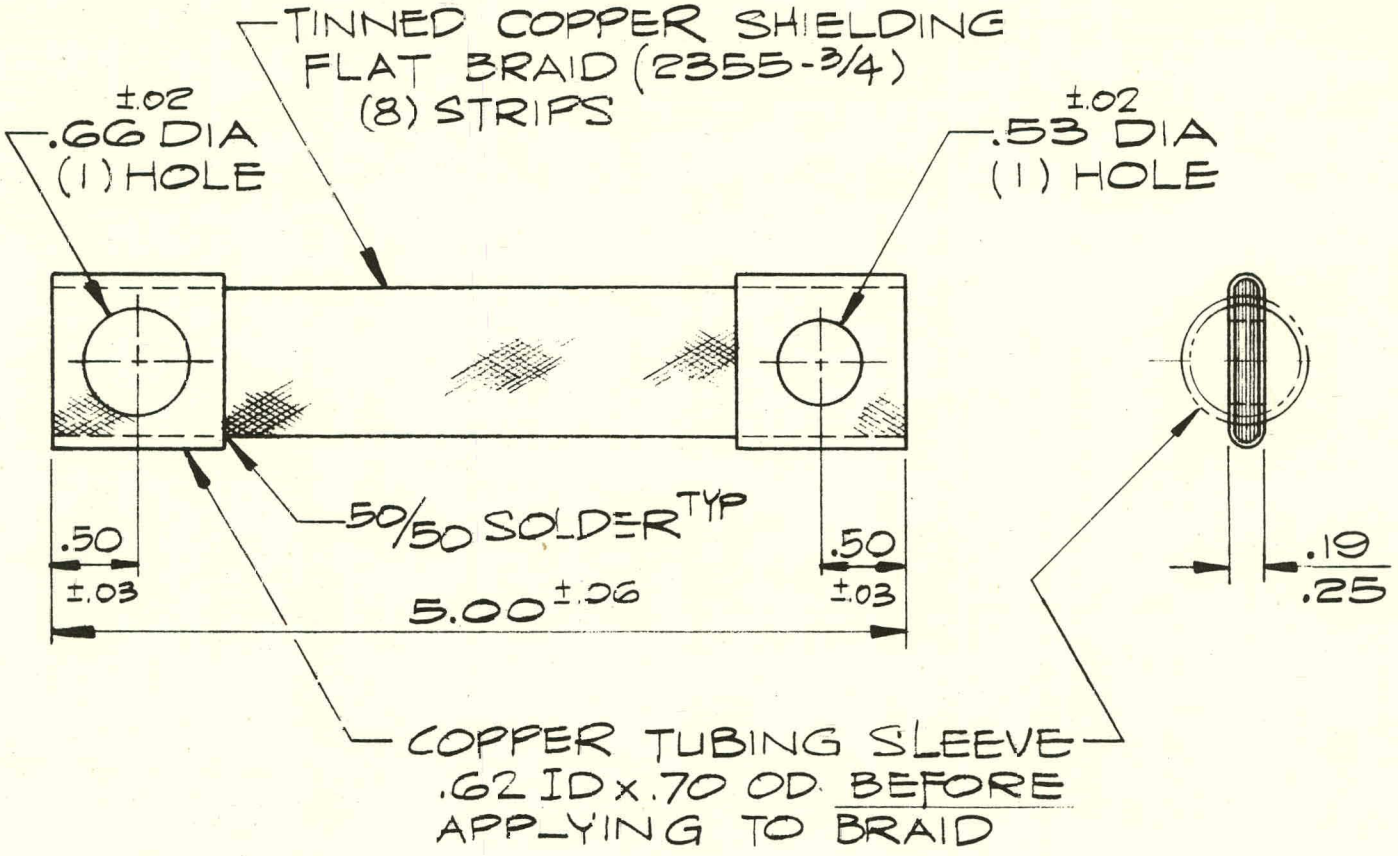

INTERCELL CONNECTOR

EXIDE POWER SYSTEMS DIVISION
ESB INCORPORATED
ENGINEERING DEPT. – DESIGN DIVISION
PHILADELPHIA, PA. 19120

SCALE FULL DATE

DWN J.LMKS CHKD. APPD.

REV.	DATE	ALTERATION	BY	APP.

THIS DWG. SUPERSEDES

EA-15578

MADE IN U. S. A.

S. a M. H. 1-77

EA-15579

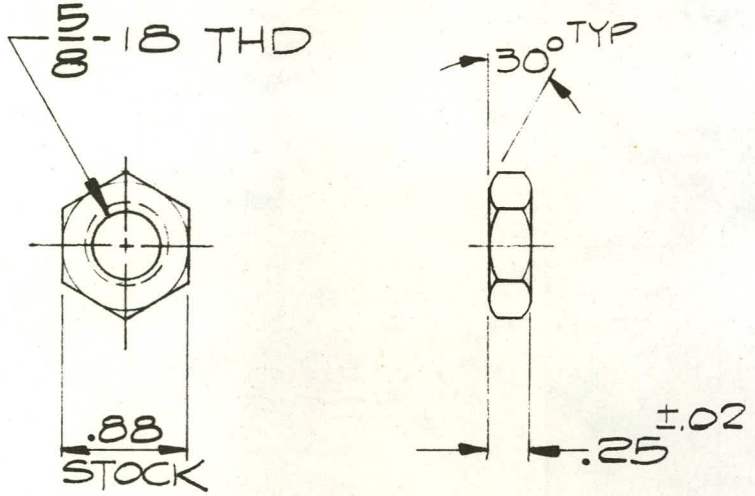

MAT'L: C.R.S.

FINISH: NICKEL PLATE

JAM NUT

EXIDE POWER SYSTEMS DIVISION
ESB INCORPORATED
ENGINEERING DEPT.—DESIGN DIVISION
PHILADELPHIA, PA. 19120

SCALE FULL DATE

DRAWN J.L.M. CHKD. K.S. APPD.

REV.	DATE	ALTERATION	BY	APP.

THIS DWG. SUPERSEDES

EA-15579

MADE IN U. S. A.

S. & M. H. 1-77

EA-15581

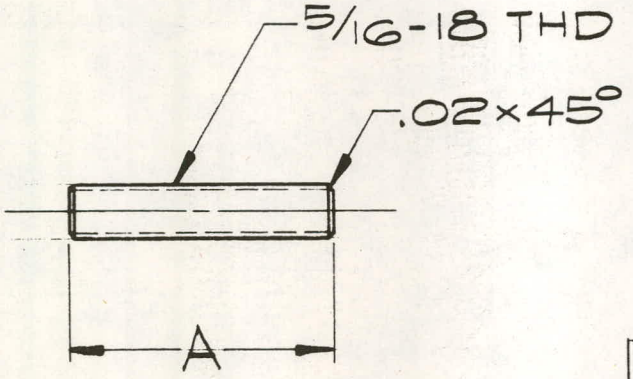

FIG. NO.	PLATE GAP, MM	A ±.01
1	1.5	1.30
2	2.5	1.55
3	2.5	3.27
4	3.5	1.78

MATL: C.R.S.

FINISH: NICKEL PLATE

STUD

EXIDE POWER SYSTEMS DIVISION
ESB INCORPORATED
ENGINEERING DEPT. – DESIGN DIVISION
PHILADELPHIA, PA. 19120

SCALE FULL DATE

W.J. LMKS CHKD. APPD.

REV.	DATE	ALTERATION	BY	APP.

THIS DWG. SUPERSEDES

EA-15581

MADE IN U. S. A.

S. & M. H. 1-77

EA-15582

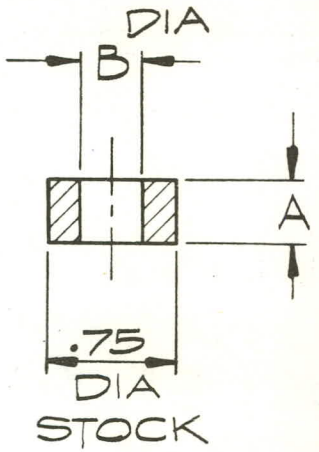

FIG. NO.	PLATE GAP, MM	A ±.005	B
1	1.5	.344	.32 .33
2	2.5	.422	
3	3.5	.502	
4	1.5	.344	.38 .39
5	2.5	.422	
6	3.5	.502	

MATL: C.R.S.

FINISH: NICKEL PLATE

SPACER

EXIDE POWER SYSTEMS DIVISION
ESB INCORPORATED
ENGINEERING DEPT. – DESIGN DIVISION
PHILADELPHIA, PA. 19120
SCALE FULL DATE
DRAWN J.LMKS CHKD. APPD.

REV.	DATE	ALTERATION	BY	APP.

THIS DWG. SUPERSEDES

EA-15582

MADE IN U. S. A.

S. & M. H. 1-77

EA-15583

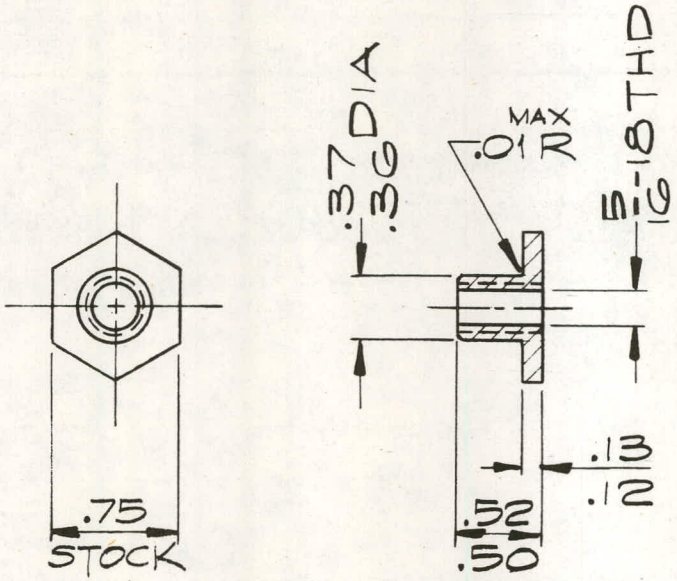

MATL: C.R.S.

FINISH: NICKEL PLATE

NUT

EXIDE POWER SYSTEMS DIVISION
ESB INCORPORATED
ENGINEERING DEPT. – DESIGN DIVISION
PHILADELPHIA, PA. 19120
SCALE FULL DATE
DRAWN J.L.M. CHKD. APPD.

REV.	DATE	ALTERATION	BY	APP.

THIS DWG. SUPERSEDES
EA-15583
MADE IN U. S. A.

M. H. 1-77

EA-15584

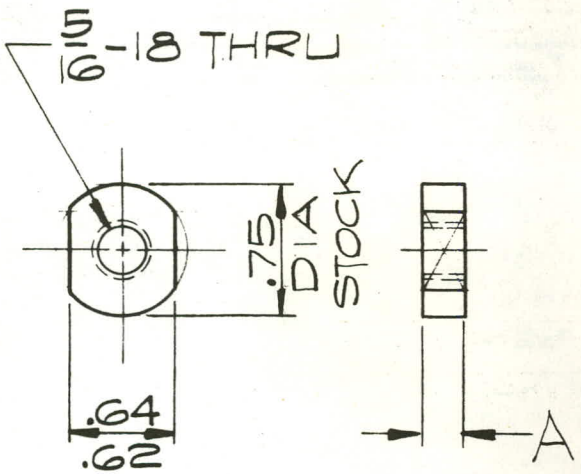

FIG. NO.	PLATE GAP, MM	A ±.01
1	1.5	.187
2	2.5	.250
3	3.5	.312

MATL: C.R.S.

FINISH: NICKEL PLATE

NUT

EXIDE POWER SYSTEMS DIVISION
ESB INCORPORATED
ENGINEERING DEPT. – DESIGN DIVISION
PHILADELPHIA, PA. 19120
SCALE FULL DATE
DRAWN J.L.M. K'S CHKD. APPD.

REV.	DATE	ALTERATION	BY	APP.

THIS DWG. SUPERSEDES
EA-15584
MADE IN U. S. A.

S. & M. H. 1-77

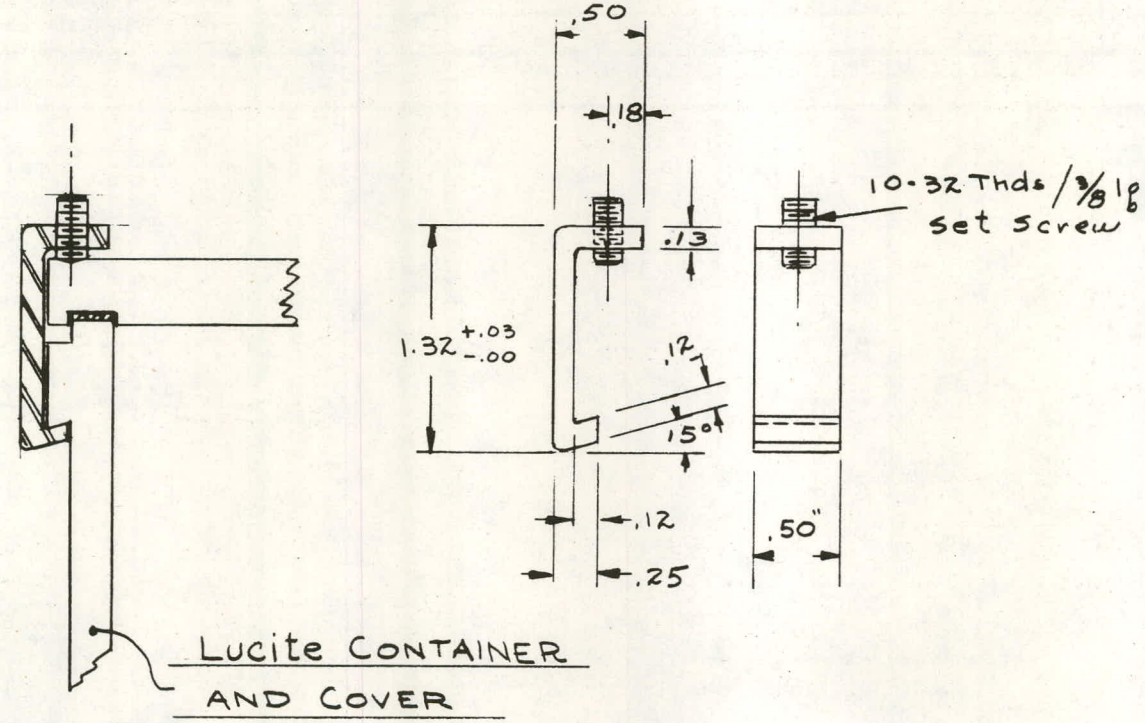

APPLIED

THIS DWG SUPERSEDES YARDLEY 6050-0109

SYM.	DATE	REVISION	CK.

DRAWN BY J.W.C. DATE 6/21/79
CHECKED SCALE Full
MATERIAL Ni Plated C.R. Steel
DO NOT SCALE DRAWING
TOLERANCE

FRACTION	DECIMAL	ANGLES
±1/64	.XX ±.010 .XXX ±.005	±1/4°

ESB INCORPORATED
TECHNOLOGY CENTER
YARDLEY, PENNSYLVANIA

(20) COVER CLAMP FOR "VIBROCEL" CELLS

DRAWING NO. EA-15580 A

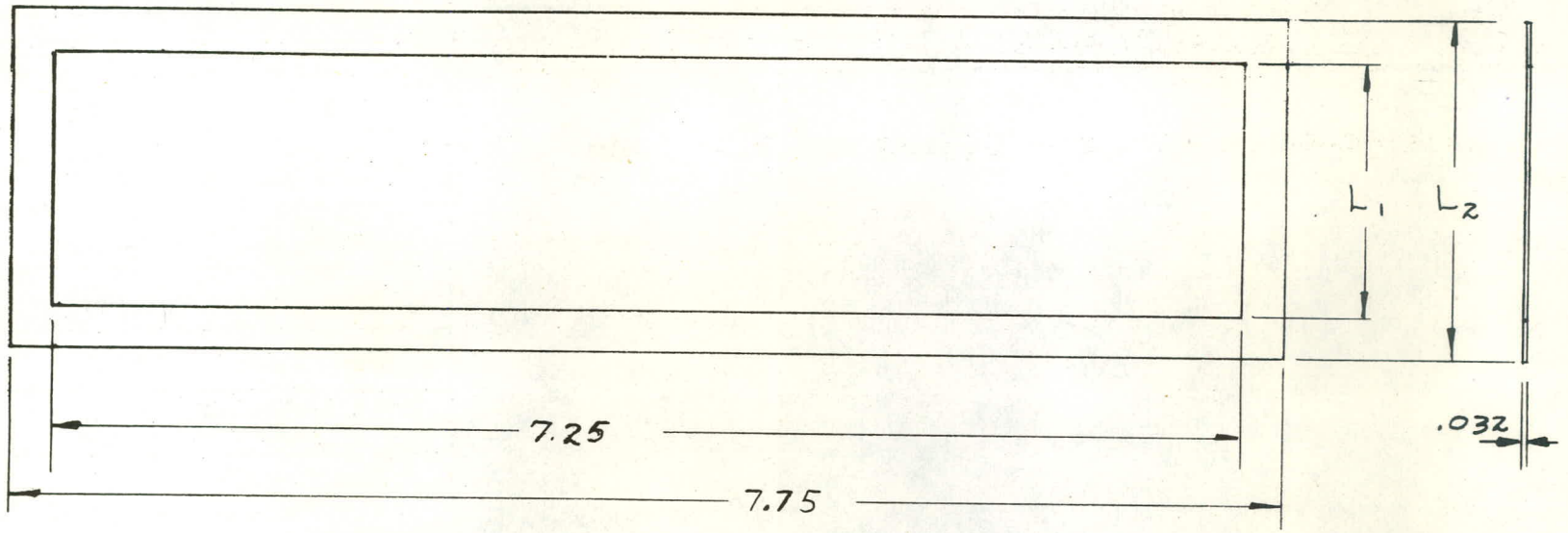

FIG	L_1	L_2	NO. OF PL & GAP. (MM)
1	1.32	1.82	7(1.5)
2	1.55	2.05	7(2.5)
3	1.79	2.29	7(3.5)
4	3.34	3.84	15(2.5)

THIS DWG SUPERSEDES
YARDLEY 6050-0110

SYM.	DATE	REVISION	CK.

DRAWN BY J.W.C. DATE 6-21-79
CHECKED SCALE Full
MATERIAL Butyl Rubber
DO NOT SCALE DRAWING
TOLERANCE

FRACTION	DECIMAL	ANGLES
± 1/64	.XX ±.010 .XXX ±.005	± 1/4°

ESB INCORPORATED
TECHNOLOGY CENTER
YARDLEY, PENNSYLVANIA

COVER GASKET FOR "Vibrocel" TEST CELLS (25)

DRAWING NO. EA-15589 A

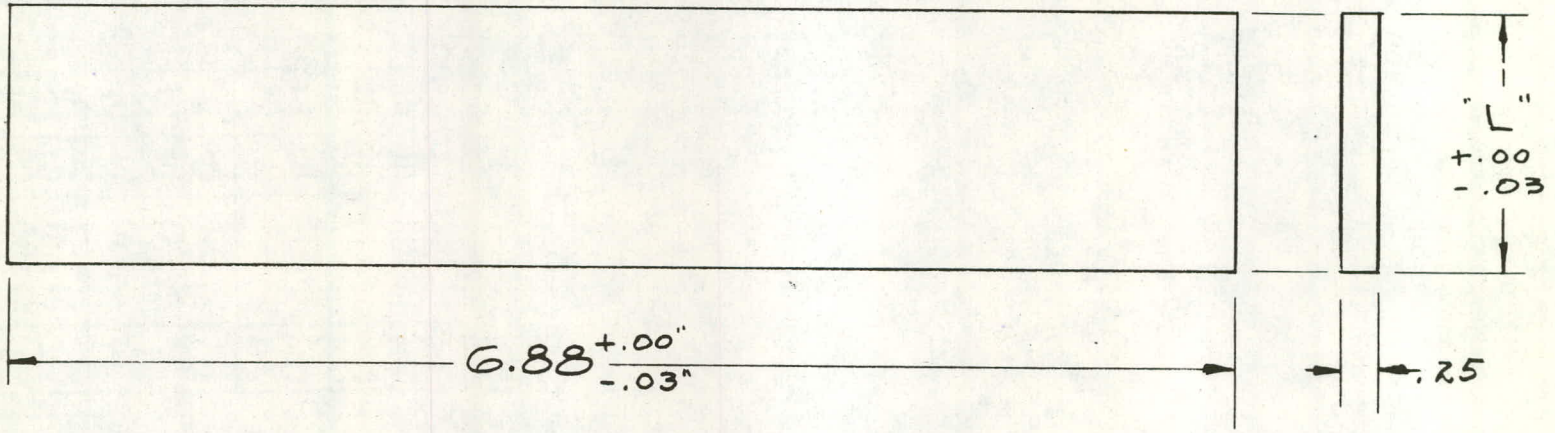

FIG	L +.00 -.03	NO. OF PLATES AND GAP, (MM)
1	1.29	7 (1.5)
2	1.50	7 (2.5)
3	1.75	7 (3.5)
4	3.30	15 (2.5)

THIS DWG SUPERSEDES YARDLEY 6050-0111

SYM.	DATE	REVISION	CK.

DRAWN BY J. Consolloy | DATE 7-10-79
CHECKED | SCALE Full
MATERIAL "Pure Carbon" POROUS FC-13
DO NOT SCALE DRAWING
TOLERANCE

FRACTION	DECIMAL	ANGLES
±1/64	.XX ±.010 .XXX ±.005	±1/4°

ESB INCORPORATED
TECHNOLOGY CENTER
YARDLEY, PENNSYLVANIA

ZINC GETTER FOR "VIBROCEL"

DRAWING NO. EA-15587 A

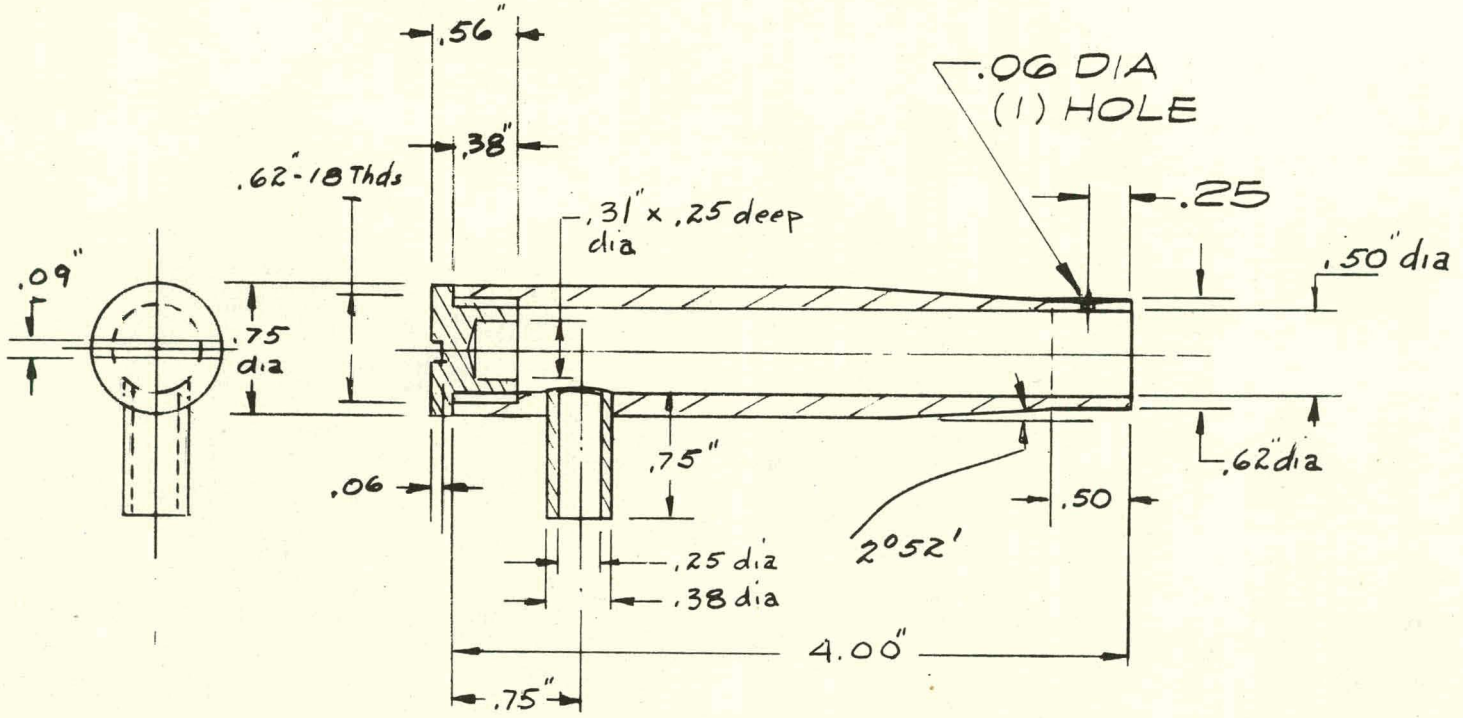

THIS DWG SUPERSEDES YARDLEY 6050-0112

SYM.	DATE	REVISION	CK.
	10/3/80	ADDED .06 DIA HOLE	

DRAWN BY J. Consolloy | DATE 7-10-79
CHECKED | SCALE Full
MATERIAL Acrylic
DO NOT SCALE DRAWING
TOLERANCE

FRACTION	DECIMAL	ANGLES
±1/64	.XX ±.010 .XXX ±.005	±1/4°

ESB INCORPORATED
TECHNOLOGY CENTER
YARDLEY, PENNSYLVANIA

VENT TUBE & CAP
"VIBROCEL"

DRAWING NO. EA-15577 | A

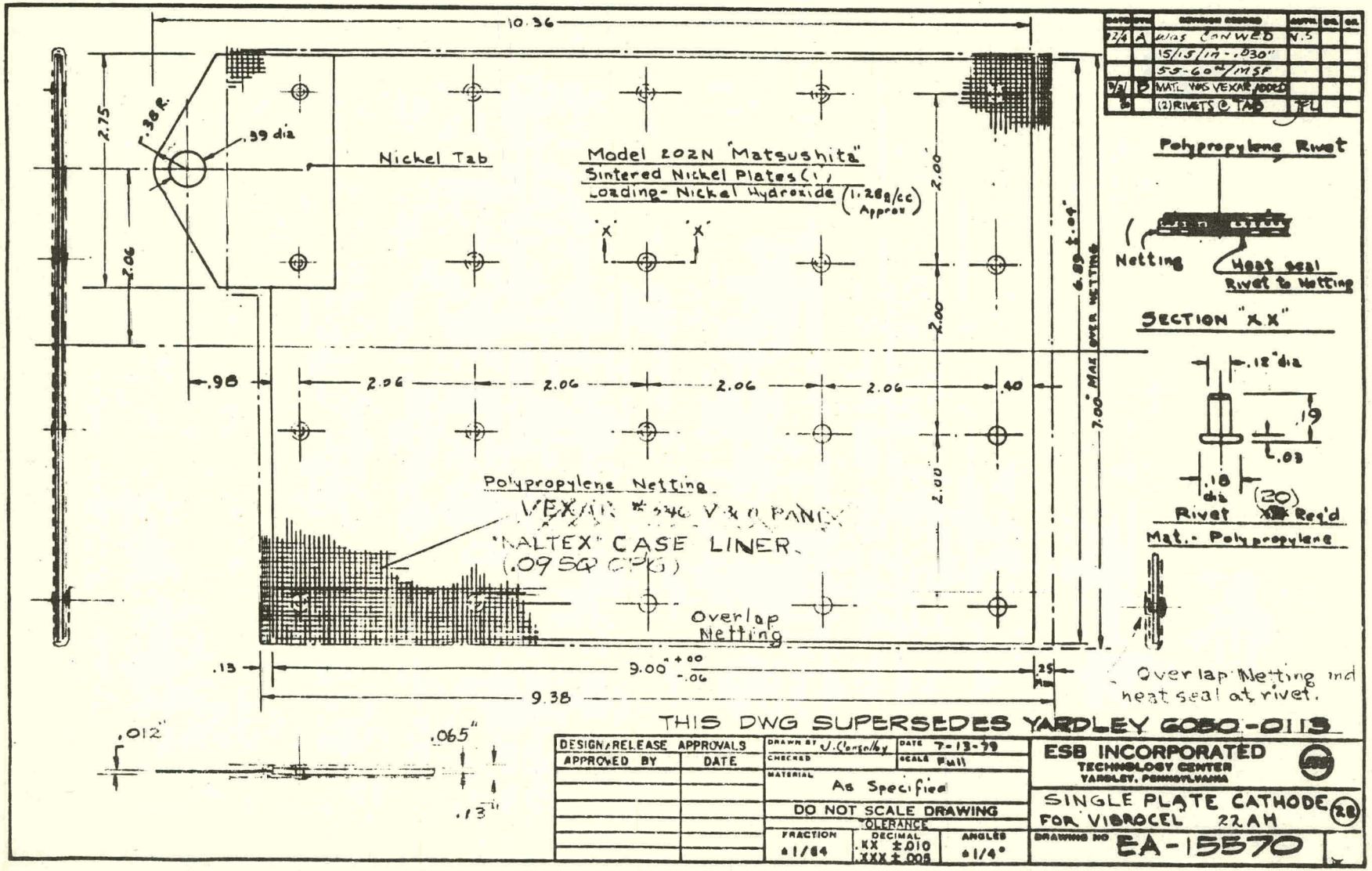

DATE	BY	REVISION RECORD	APPR.	CK.	QC.
7/4	A	was CANWED	V.S		
		15/1.5/in - .030"			
		55-60 g/MSF			
9/1	B	MATL WAS VEXAR ADDED			
9/6		(2) RIVETS & TAB	TPL		

THIS DWG SUPERSEDES YARDLEY 6080-0113

DESIGN/RELEASE APPROVALS	
APPROVED BY	DATE

DRAWN BY J. Connolly — DATE 7-13-79
CHECKED — SCALE Full
MATERIAL As Specified
DO NOT SCALE DRAWING
TOLERANCE
FRACTION ±1/64 — DECIMAL .XX ±.010 .XXX ±.005 — ANGLES ±1/4°

ESB INCORPORATED
TECHNOLOGY CENTER
YARDLEY, PENNSYLVANIA

SINGLE PLATE CATHODE FOR VIBROCEL 22AH (28)

DRAWING NO EA-15570

Distribution for ANL/OEPM-79-12

Internal:

J. J. Barghusen
D. Barney
C. Bean
E. C. Berrill
R. Biwer
A. Brown
L. Burris
G. Chapman
A. A. Chilenskas
C. C. Christianson
G. Cook
D. Corp
E. Creamer
S. A. Davis
W. DeLuca
R. C. Elliott
M. Farahat
P. R. Fields
F. Foster
D. Fredrickson
B. R. T. Frost
E. C. Gay
J. Geller
M. Genger
F. Hornstra
C. C. Hsu
J. Klinger
V. Kremesec
A. B. Krisciunas
M. Kronenberg
W. W. Lark
T. S. Lee
M. Liu
R. Loutfy
W. Massey
J. Miller
W. Miller
P. A. Nelson
M. V. Nevitt
E. G. Pewitt
D. Poa
J. Rajanwitt
J. J. Roberts
M. F. Roche
H. Shimotake
R. K. Steunenberg
C. Swoboda
Z. Tomczuk
A. Tummillo
R. Varma
P. D. Vashishta
D. R. Vissers
D. S. Webster
N. P. Yao (44)
ANL Contract File
ANL Libraries
TIS Files (6)

External:

DOE-TIC, for distribution per UC-94ca (318)
Manager, Chicago Operations and Regional Office, DOE
Chief, Office of Patent Counsel, DOE-CORO
V. Hummel, DOE-CORO
J. Purcell, DOE-CORO
Argonne Universities Association
President
C. B. Alcock, U. of Toronto
W. L. Worrell, U. of Pennsylvania
W. Ahmad, KW Battery, Skokie, IL
R. Alkire, University of Illinois, Urbana
M. Allen, Mechanical Technology Inc., Latham, NY
E. T. Ames, TRW Systems, Redondo Beach, CA
L. Andrews, Electric Vehicle Council, Washington, DC
S. J. Angelovich, Mallory Battery Co., Tarrytown, NY
C. M. Arcand, Idaho State University, Pocatello, ID
R. Aronson, Electric Field Propulsion Corp., Troy, MI
G. N. Ault, NASA-Lewis Research Center, Cleveland
J. D. Baker, Stewart Warner Corp., Chicago
W. Bales, Jet Industries, Inc., Austin
H. Balzan, Chattanooga, TN
K. F. Barber, DOE, Office of Transportation Programs, Washington
T. Barber, Jet Propulsion Laboratory, Pasadena

R. J. Barkley, Compass Industries, Inc., Hermosa Beach, CA
J. W. Barlass, Westinghouse Electric Corp., Skokie, IL
T. M. Barlow, Lawrence Livermore Lab.
D. Barron, Delco-Remy Div., GMC, Anderson, IN
R. Bassett, Sandia Labs, Albuquerque
W. Bauer, KW Battery, Skokie, IL
E. Baumann, LILCO, Mineola, NY
W. C. Beasley, Union Carbide Corporation, New York, NY
H. Bell, Arizona Public Service Co., Phoenix
J. Bellack, Cleveland Electric Illuminating Co., Cleveland
L. Belove, Marathon Battery Corp., Waco, TX
C. Berlsterling, C. Franklin Institute, Philadelphia
W. R. Benn, Great Lakes Carbon Corporation, New York, NY
D. N. Bennion, Brigham Young University, Provo, UT
C. Berger, Electrochemical & Water Desal. Technology, Santa Ana, CA
D. Bergmann, GM Transportation Systems Center, Warren, MI
J. Birk, Electric Power Research Institute, Palo Alto
W. S. Bishop, Air Force Acro Propulsion Lab, Wright Patterson AFB
K. Blurton, Institute of Gas Technology, Chicago
D. P. Boden, C&D Batteries, Plymouth Meeting, PA
J. Bolger, University of California, Berkeley
D. Borello, Die Mesh Corp., Pelham, NY
A. Borucka, Borucka Research Co., Livingston, NJ
P. Bowen, C & D Batteries, Plymouth Meeting, PA
D. Bowman, United States Postal Service, Washington
J. C. Boylan, Electric Dynamics Corp., Plainwell, MI
B. J. Bragg, Bell Laboratories, Murray Hill, NJ
J. Brennand, General Research Corp., Santa Barbara
A. F. Brewer, Malibu, CA
D. C. Briggs, Philco-Ford Corp., Palo Alto
P. Bro, J. R. Mallory & Co., Inc., Burlington, MA
J. Broadhead, Bell Laboratories, Murray Hill, NJ
R. Brodd, Union Carbide Corp., Cleveland
E. P. Broglio, Eagle-Picher Industries, Joplin, MO
A. D. Brown, EVE Electric Motor Car, Inc., East Lansing, MI
P. J. Brown, DOE, Office of Transportation Programs, Washington
R. A. Brown, Eagle-Picher Industries, Joplin, MO
S. B. Brummer, EIC Corporation, Newton, MA
R. Buchholz, Honeywell Corp., Minneapolis
T. Burgess, Lucas Industries, N. A. Inc., Troy, MI
H. Burghart, Cleveland State University, Cleveland
D. Burns, Onan Corporation, Minneapolis
B. W. Burrows, Gould Inc., Rolling Meadows, IL
M. Burtgon, Delco Remy Div. of GMC, Anderson, IN
J. D. Busi, USA Foreign Science & Tech. Center, Charlottesville, VA
E. Buzzelli, Westinghouse Electric Corp., Pittsburgh
W. P. Cadogan, Emhart Corp., Hartford, CT
E. Cairns, Lawrence Berkeley Lab.
E. Campbell, Electric Vehicle Consultants, Inc., New York, NY
P. Campbell, University of Southern California, Los Angeles
J. Campbell, DOT/UMTA, Washington, DC
R. T. Carpenter, Kimberly Clark Corp. Neenah, WI
T. V. Carvey, Hughes Aircraft Corp., Culver City, CA
A. Charkey, Energy Research Corp., Danbury, CT

L. D. Christian, General Electric, Gainesville, FL
R. C. Chudacek, McGraw Edison Co., Bloomfield, NH
R. Clark, Sandia Labs., Albuquerque
J. E. Clifford, Battelle Memorial Institute, Columbus
J. A. Consiglio, Solva-Tek Associates, Topsfield, MA
A. R. Cook, ILZRO Inc., New York,
J. E. Cooper, Aero Propulsion Laboratory, Wright-Patterson AFB
K. E. Cooper, Trojan Battery Co., Santa Fe Springs, CA
G. Coraor, E. I. Du Pont de Nemours & Co., Inc., Wilmington, DE
R. E. Corbett, Lockhead Missiles & Space Co., Sunnyvale
K. E. Cox, University of New Mexico, Albuquerque
W. W. Craig, Edward Harding and Co., Chicago,
D. Crane, United States Postal Service, Washington
R. A. Crawford, PPG Industries, Barberton, OH
H. H. Crist, AM General Corp., Wayne, MI
R. H. Dare, Battronic Truck Corp., Boyertown, PA
D. Davis, Lawrence Livermore Lab.
R. J. Dawson, ESB Inc., Madison, WI
J. Devitt, Denver, CO
A. N. Dey, P. R. Mallory & Co. Inc., Burlington, MA
G. A. DiBari, INCO, Suffern, NY
W. J. Dippold, DOE, Office of Transportation Programs, Washington
T. P. Dirske, Calvin College, Grand Rapids, MI
D. DiVirgillo, Lockhead Missiles and Space Co., Inc., Sunnyvale, CA
D. Douglas, Electric Power Research Institute, Palo Alto
D. Dow, Detroit, MI
D. Dunoye, Reston, VA
T. Dwyer, Corning Glass Works, Corning, NY
E. F. Echolds, AiResearch Manufacturing Co., Torrance, CA
M. Eisenberg, Electrochimica Corp., Mountain View, CA
D. B. Eisenhaure, Charles Stark Draper Lab Inc., Cambridge, MA
T. Eissenberg, Oak Ridge National Lab., Oak Ridge, TN
M. W. Ellison, Hughes Aircraft Corp., El Segundo
D. Elson, Black and Decker Inc., Towson, MD
R. English, General Battery Co., Reading, PA
B. Enserik, Dynamic Science, Phoenix
R. Enters, McCraw Edison Co., Bloomfield, NJ
H. Espig, Gould Inc., Rolling Meadows, IL
A. Ewing, DOE, Office of Transportation Programs, Washington
G. Farbman, Westinghouse Electric Corp., Pittsburgh
F. Fedor, Bell Laboratories, Murray Hill, NJ
R. Fedora, Gould Inc., Rolling Meadows, IL
W. Feduska, Westinghouse Electric Corp., Pittsburgh
W. H. Fengler, Meteor Research Limited, Roseville, MI
F. Feres, KW Battery Company, Skokie, IL
R. Ferraro, Electric Power Research Institute
D. T. Ferrell, Exide Corporation, Yardley, PA
E. Fiss, Duke Power Company, Charlotte, NC
A. Fleischer, Orange, NJ
C. W. Fleischmann, C&D Batteries, Plymouth Meeting, PA
R. F. Fogle, North American Rockwell, Anaheim
R. T. Foley, American University, Washington, DC
J. S. Fordyce, NASA-Lewis Research Center, Cleveland
H. A. Fuggiti, Exide Management and Technology Co., Yardley, PA

T. Fujita, Pasadena, CA
B. Ganji, KW Battery Co., Skokie, IL
G. Gelb, Advanced Ground Systems, Long Beach, CA
J. H. B. George, Arthur D. Little, Inc., Concord, MA
S. Geppert, Eaton Corporation, Southfield, MI
L. J. Gerlach, United States Postal Service, Rockville, MD
J. A. Gilchrist, Chloride America, Tampa
W. Gillespie, Structural Plastics Inc., Tulsa
C. Glassman, Transportation Research Center, East Liberty, OH
H. Glixon, Chevy Chase, MD
M. Globerman, General Services Administration, Washington
W. Goldman, Electric Vehicle Engineering, Lexington, MA
G. Goodman, Globe-Union Inc., Milwaukee
R. E. Goodson, Purdue University
J. Gould, Unique Mobility Inc., Englewood, CO
L. B. Gratt, IWG Corp., San Diego
H. Grepke, TurElec Inc., Bradenton, FL
D. Griter, Solar Centra, Mechanicsburg, OH
E. E. Grough, Lucas Industries Inc., Troy, MI
R. Guess, General Electric Research Lab, Schenectady
R. G. Gunther, General Motors Research Labs, Warren, MI
M. Hadden, Billing Energy Corp., Provo, UT
G. Hagey, DOE, Division of Technology Overview, Washington
N. Halterm, Chrysler Corporation, Detroit
H. Hamilton, University of Pittsburgh
R. Hamilton, Institute for Defense Analysis, Arlington, VA
W. Hamilton, General Research Corp., Santa Barbara
B. Hamlen, Exxon Enterprises Inc., Florham Park, NJ
D. Hanify, Fiat, Chicago
K. L. Hanson, Genearl Electric Co., Philadelphia
W. Harhay, Electric Vehicle Associates, Cleveland
J. H. Harrison, Naval Ship R&D Center, Annapolis, MD
G. Hartman, Exide Management and Technology Co., Yardley, PA
J. Hartman, General Motors Research Labs, Warren, MI
E. A. Heintz, Airso Speer Carbon Graphite, Niagara Falls, NY
E. V. Hellman, Gould Inc., Langhorne, PA
R. Heppenstall, Penn Jersey Suburu Inc., Pennsauken, NJ
A. Himy, Naval Sea Systems Command, Washington
V. Hlavin, NASA-Lewis Research Center
G. Hobbib, Exide Management and Technology Co., Cleveland
A. Hodgman, General Electric, Gainesville
R. Hoenburg, Mechanical Technology Inc., Latham, NY
R. Hudson, Eagle-Picher Industries, Joplin, MO
J. R. Huff, US Army Mobility Equipment R&D Command, Fort Belvoir, VA
H. L. Hughes, Oklahoma State University, Stillwater, OK
J. R. Hunt, International Nickel Co., Washington
H. R. Ivey, Wood-Ivey Systems Corp., Winter Park, FL
J. Jacus, Moore Haven, FL
M. A. Janse, Allegheny Power Service Corporation, Greensburg, PA
G. H. Jantz, Rensselaer Polytechnic Institute
A. W. Johnson, General Electric Co., Philadelphia
F. Johnson, Department of Industry, Trade and Commerce, Ottawa, Canada
L. Jokl, MERADCOM, Fort Belvoir, VA
K. R. Jones, Thiensville, WI

W. J. Jones, Westinghouse Electric Corp., Pittsburgh
R. E. Jordan, Omega Motors Corp., Garden Grove, CA
D. Kane, National Motors Corp., Lancaster, PA
E. Kanter, Gulton Battery Corp., Metuchen, NJ
N. Kaplan, Harry Diamond Laboratories, Washington
V. Kapur, Arco Solar Inc., Chatsworth, CA
R. Kaylor, Kaylor Energy Products, Menlo Park
J. Keith, Kamon Sciences, Colorado Springs, CO
H. C. Kelly, OTA, U.S. Congress, Washington
J. G. Kennard, NASA-Lewis Research Center
R. L. Kerr, Aero Propulsion Lab., Wright Patterson AFB
J. A. Kerrella, Delco-Remy Division/GMC, Anderson, IN
R. A. Keyes, Robert A. Keyes Associates, Martinsville, IN
R. A. Kingery, Oconomowoc, WI
R. S. Kirk, DOE, Office of Transportation Programs, Washington
M. Klein, Energy Research Corporation, Danbury, CT
G. B. Kliman, General Electric Co., Schenectady
G. B. Klinean, General Electric Co., Schenectady
R. C. Knechtli, Malibu, CA
R. A. Knight, AMF Inc., Stamford, CT
O. R. Kozak, American Battery Corp., Long Beach, NY
J. G. Krisilas, Aerospace Corporation, El Segundo, CA
P. E. Krouse, Exide Management & Technology Co., Yardley, PA
R. R. Kubalek, St. Joe Lead Co., Clayton, MD
L. Kulin, Whirlpool Corp. Benton Harbor, MI
C. M. Langkau, Union Carbide Co., Cleveland
H. Lauve, Electric Auto Corporation, Troy, MI
J. Lee, RAI Research Corp., Hauppauge, NY
I. J. Levine, Consolidated Edison, New York
K. Levine, St. Joe Minerals Corp., Pittsburgh
H. Lim, Hughes Research Lab., Malibu, CA
D. Linden, Little Silver, NJ
E. L. Littauer, Lockhead Palo Alto Research Laboratory
A. Long, Zeonics Corp., Fairfax, VA
E. Long, St. Joe Minerals Corp., Monaca, PA
M. Lugash, Maxon Industries, Huntington Park, CA
J. T. Lundquist, W. R. Grace & Co., Columbia, MD
T. Lynch, Fiber Materials, Inc., Biddeford, ME
E. N. Mabuce, Union Electric Co., St. Louis
J. MacDougall, AT&T, Basking Ridge, NJ
D. E. Mains, Naval Weapons Support Center, Crane, IN
J. Maisel, Cleveland State University, Cleveland
J. S. Makulowich, Electric Vehicle Council, Washington
V. Manson, National Aeronautics and Space Adm., Washington
L. S. Marcoux, Hughes Aircraft Company, Los Angeles
K. Marshall, KW Battery Company, Skokie, IL
T. W. Martin, United States Postal Service, San Bruno, CA
A. Masters, Packaged Promotions Inc., Chicago
S. Matsuda, Thermo Electron Corp., Waltham, MA
C. E. May, NASA-Lewis Research Center, Cleveland
E. Meeks, Derl Manufacturing Co., Compton, CA
N. Merriman, Army Picatinny Arsenal, Dover, NJ
S. Meschkow, Franklin Research Institute, Philadelphia
J. D. Meiggs, Kaman Sciences Corp., Colorado Springs

P. Mighdoll, Booz-Allen & Hamilton, Cleveland
R. P. Mikkelson, General Dynamics, San Diego
D. G. Miley, U.S. Naval Ammunition Depot, Crane, IN
H. Miller, Department of Transportation, Cambridge, MA
D. K. Miner, Copper Development Associates, Birmingham, MD
L. J. Minnick, Industrial Research Consultant, Plymouth Meeting, PA
L. G. Morin, Tarrytown, NY
F. Morse, University of Maryland, College Park
A. Moss, Leesona Moos Laboratories, Warwick, RI
R. Mueller, University of California, Berkeley
J. H. Muir, Dimension V Inc., Indialantic, FL
J. P. Mullin, National Aeronautics & Space Administration, Washington
G. Murphy, Northwestern University
B. McCormick, Los Alamos Scientific Lab.
L. R. McCoy, Energy Systems Group, Canoga Park
R. McKee, McKee Engineering, Palatine, IL
F. McLarnon, Lawrence Berkeley Lab.
P. McRay, ILC Technology, Sunnyvale
W. J. Nagle, NASA-Lewis Research Center, Cleveland
H. V. Nadham, Bogue Batteries, El Segundo
L. Nalley, Creative Research Co., Roebuck, SC
J. Newman, Univ. of California, Berkeley
J. S. Newton, Newton Engineering Co., Glen Ellyn, IL
M. M. Nickolson, Atomics International Division, Canoga Park
A. O. Nilsson, NIFE Incorporated, Lincoln, RI
J. Norberg, Exide Management & Technology Co., Philadelphia
A. C. Occhipinti, Kenner, LA
L. G. O'Connell, Lawrence Livermore Lab.
G. Odom, Georgia Power Company, Atlanta, GA
R. Oglesby, GM Transportation Systems Ctr., Warren, MI
L. Omohundro, Kingery Research & Development, Wake Forest, NC
E. I. Onstott, Los Alamos Scientific Lab
R. Osteryoung, Colorado State University, Fort Collins
B. N. Otzinger, North American Aviation, Downey, CA
J. P. Overman, Hammond Lead Products Inc., Hammond, IN
J. E. Oxley, Gould Inc., Rolling Meadows, IL
E. Papandreas, REI, Lake Worth, FL
J. S. Parkinson, Johns-Manville R&D Center, Manville, NJ
J. M. Parry, Arthur D. Little Inc., Cambridge, MA
E. Patagalia, General Services Administration, Washington
S. Pauling, Naperville, IL
J. E. Pavolsky, NASA/Lyndon B. Johnson Space Ctr., Houston
C. Pax, DOE, Office of Transportation Programs, Washington
E. Pearlman, Exide Management and Technology Co., Yardley, PA
G. F. Pezdirtz, DOE, Energy Storage Systems, Washington
A. G. Plunckett, General Electric R&D Center, Schenectady
R. A. Powers, Union Carbide Corp., Cleveland
V. J. Puglisi, Yardney Electric Corp., Pawcatuck, CT
E. Ramirez, Amectran, Dallas
E. Raskin, USAF Cambridge Research Laboratory, Bedford, MA
A. D. Raynard, AiResearch Manufacturing Co., Torrance, CA
E. C. Read, Exxon Enterprises, Linden, NJ
H. L. Recht, Atomics International Division, Canoga Park
N. Richie, KW Battery Co., Skokie, IL

C. Ridgway, Walt Disney World Co., Lake Buena Vista, FL
E. Rizkalla, DOE, Office of Controller, Washington
R. A. Rizzo, Globe-Union Inc., Milwaukee
R. Robert, The MITRE Corporation, McLean, VA
F. T. Rooney, Bureau of Automotive Maintenance, Norfolk, VA
L. Rosenblum, NASA-Lewis Research Center, Cleveland
N. Rosenburg, Department of Transportation, Cambridge, MA
R. Rosey, Westinghouse Electric Corp., Pittsburgh
J. Rossmon, Cornell University
G. Rowland, General Electric, Schenectady
J. Rubenzer, NASA-Ames Research Center, Moffett Field
P. H. Rubie, Electric Passenger Cars, Inc., San Diego
H. E. Ruskie, Naval Intelligence Support Center, Washington
A. J. Salkind, Exide Management & Technology Co., Yardley, PA
R. Schmidt, Volkswagen of America Inc., Englewood Cliffs, NJ
R. T. Schneider, RTS Laboratories, Gainesville, FL
L. W. Schopen, NASA-Lewis Research Center, Cleveland
H. J. Schwartz, NASA-Lewis Research Center, Cleveland
W. R. Scott, TRW Systems Inc., Redondo Beach
H. Seigel, South Coast Technology Inc., Santa Barbara
H. Seiger, Harvey Seiger Associates, Waterford, CT
J. Seliber, Fluid Drive Engineering Co., Wilmette, IL
E. Seo, Gates Energy Products, Denver, CO
L. Shahnasarian, Elcar Corp., Elkhart, IN
R. C. Shair, CENTREC Corporation, Fort Lauderdale
H. Shalit, ARCO Chemical Corp., Glendolden, PA
D. W. Sheibley, NASA-Lewis Research Center, Cleveland
E. Small, Amectran Corporation, Washington
G. A. Smith, Englehard Industries, Iselin, NJ
S. Smith, St. Joe Minerals Corp., Monaca, PA
V. Smith, Delco-Remy Div. GMC, Anderson, IN
J. Smits, Nevada Operations Office, Las Vegas, NV
I. J. Soloman, IIT Research Institute, Chicago
W. C. Spindler, Electric Power Research Institute, Palo Alto
J. S. Stanley, Dept. of the Army, U.S. Army Foreign Sci. & Tech. Center, Charlottesville, VA
E. J. Steeve, Commonwealth Edison Co., Chicago
I. Stein, Jet Propulsion Laboratory, Pasadena
T. A. Stoneham, Marathon Battery Company, Waco, TX
R. Strauss, Communications Satellite Corp., Clarksburg, MD
W. E. Strawbridge, Caterpiller Tractor Co., Peoria, IL
R. L. Strombotne, Transportation Systems Center, Cambridge, MA
S. Sudar, Rockwell International, Canoga Park
P. C. Symons, Energy Development Associates, Madison Heights, MI
F. Tepper, Catalyst Research Corp., Baltimore
R. Thacker, General Motors Research Labs, Warren, MI
C. E. Thomas, Chrysler Corp., New Orleans, LA
F. Thomas, Grumman Aerospace Corp., Bethpage, NY
G. M. Thur, DOE, Office of Transportation Programs, Washington
W. H. Tiedemann, Globe-Union Inc. Milwaukee, WI
C. W. Tobias, University of California, Berkeley
M. Thorpe, Towson, MD
A. Topouzian, Ford Motor Co., Dearborn, MI
W. Toth, Society of Automotive Engineers, Inc., Warrendale, PA

H. Toulmin, Bloomfield, MI
I. Trachtenberg, Texas Instruments, Dallas
G. W. Tuffnell, The International Nickel Co., Troy, MI
D. Turford, Western Mining Corp., Pittsburgh
G. H. Turney, Western Research Industries, Las Vegas, NV
E. A. Ulrich, Creative Automotive Research, Whittier, CA
R. L. Ulrich, General Services Administration, Washington
T. Ulrich, McGraw-Edison Co., Bloomfield, NJ
G. Underhill, A. D. Little, Cambridge, MA
H. B. Urbach, Naval Ship R&D Center, Annapolis, MD
H. Vaidyanathan, Energy Research Corp., Danbury, CT
C. J. Venuto, C&D Batteries, Plymouth Meeting, PA
S. W. Vreeland, General Dynamics, Convair Division, San Diego
A. Waddell, EBCO Battery Co., Columbus, GA
E. H. Wakefield, Linear Alpha Inc., Evanston, IL
R. Walker, University of Florida, Gainesville
C. H. Waterman, C. H. Waterman Industries, Althol, MA
G. Way, Troy, MI
W. Webster, DOE, Divison of Energy Storage Systems, Washington
R. D. Wehrle, Sandia Labs, Albuquerque, NM
C. Weinlein, Globe-Union Inc., Milwaukee
S. A. Weinter, Ford Motor Co., Detroit, MI
M. Weinreb, Consolidated Edison, New York
E. Y. Weissman, GASF Wynadotte Corp., Wynadotte, MI
I. Wender, Bureau of Mines, Pittsburgh, PA
H. B. West, McGraw-Edison Company, Bloomfield, NJ
M. E. Wilke, Burgess Battery Company, Freeport, IL
R. Wilks, Lavelle Aircraft Co., Newton, PA
C. F. Williams, Teledyne Isotopes, Timonium, MD
H. R. Williams, Detroit Edison Co., Detroit
J. M. Williams, E. I. DuPont De Nemours & Co., Wilmington, DE
E. Willhnganz, C&D Batteries, Plymouth Meeting, PA
N. L. Willmann, Delco-Remy Div. of GMC, Anderson, IN
J. F. Wing, Booz-Allen & Hamilton Inc., Bethesda, MD
K. Winters, Chrysler Corp., New Orleans, LA
T. J. Wissing, Eaton Corp., Southfield, MI
J. Wooldrige, Boeing Corp., Seattle
V. Wouk, Petro-Electric Motor Ltd., New York
R. A. Wynveen, Life Systems Inc., Cleveland
L. S. Yao, University of Illinois, Urbana
H. Yoder, Battronic Truck Corp., Boyertown, PA
M. Yontar, Jersey City, NJ
J. E. Zanks, NASA-Langley Research Center, Hampton, VA